# Seismic Background Noise of Puerto Rico


By

Rafael Andrés Pujols Guridy


A thesis submitted in partial fulfillment of the requirements for the degree of

MASTER OF SCIENCE

In

ELECTRICAL ENGINEERING

UNIVERSITY OF PUERTO

MAYAGÜEZ CAMPUS

2008

*Approved by:*

| | |
|---|---|
| *Rafael Rodríguez Solís, Ph.D.* | Date |
| *Member, Graduate Committee* | |
| *Víctor Huérfano Moreno, Ph.D.* | Date |
| Member, Graduate Committee | |
| *Henrick M. Ierkic, Ph.D.* | Date |
| President, Graduate Committee | |
| *José Martínez Cruzado, Ph.D.* | Date |
| Representative of Graduate Studies | |
| *Isidoro Couvertier, Ph.D.* | Date |
| Chairperson of the Department | |

# ABSTRACT

In this thesis, the seismic background noise in Puerto Rico was characterized using data from eleven broadband seismic stations for a period of three years from 2005 to 2007. Then the calibration files and data conversion were made for each seismic station to the Standard for Exchange of Earthquake Data (SEED) format, and then used the software PQLX to make noise analysis, which use power spectral density (PSD) and probability density function (PDF) with algorithms describe in McNamara and Buland (2004). The different noises that were characterized are: 1) Cultural noise, 2) Wind, water and geological noise, 3) Microseisms and 4) System artifact in the PDF noise field like data gaps and sensor glitches. This is very useful for seismic network quality control. In addition the diurnal, seasonal geographical variations of the seismic noise were made. In general, The Puerto Rico Seismic Network has a good performance in their broadband seismic station and need to improve their site for reducing cultural noise.

# RESUMEN

En esta tesis, se caracteriza el ruido sísmico de trasfondo en Puerto Rico usando los datos de onces estaciones sísmicas de banda ancha en un periodo de tres años, desde el 2005 hasta el 2007. Se realizaron los archivos de calibración y se convirtió la data de cada estación a el formato estándar para el intercambio de datos sísmicos (SEED). Luego se utilizó el software PQLX para hacer los análisis de ruidos. Este software utiliza la densidad espectral de potencia (PSD) y una función de densidad de probabilidad (PDF) cuyos algoritmos son explicados en Mcnamara and Buland (2004). Los diferentes ruidos que fueron caracterizados son: 1) ruido cultural, 2) ruidos del viento, del agua y geológico, 3) microsismo y 4) artefactos del sistema como son huecos de datos, interferencias del sensor, los cuales son muy útiles para el control de calidad de las redes sísmicas. Además, se realizó la variación diurna, estacional y geográfica del ruido sísmico. En general, observamos que la Red Sísmica de Puerto Rico tiene un buen comportamiento en sus estaciones banda ancha y necesita mejorar sus instalaciones para un mejor desenvolvimiento en el ruido cultural.

Dedicated to my family, especially to my wife Leticia

## ACKNOWLEDGMENTS

I would like to thank my advisor Dr. Mario Ierkic, President of my graduate committee, for his support and the advice given to me throughout the masters program and especially in this research work. I would also like to thank Dr. Rafael Rodriguez Solís for the advice and dedication during my days as a graduate student at the University of Puerto Rico at Mayagüez. Besides, I would like to thank Dr. Victor Huerfano Moreno for encouraging and help me during my work at The Puerto Rico Seismic Network (PRSN) as a graduate student.

I would like to give an especial acknowledgment to Professor Christa von Hillebrandt-Andrade for giving me the opportunity of getting a Master through being a graduate student in the PRSN.

I want to express my gratitude to the Staff of the PRSN, Gisela, Harold, Juan, Jose, Yamilette, and Jeanette.

I would like to thank Dr. Ramón Vásquez for motivating me to finish my graduate studies.

I would like to thank my friends during my days as a student in the Mayagüez Campus.

Finally, but not less important, I would like to thank to God for being with me everytime.

# TABLE OF CONTENTS

# TABLE LIST

# FIGURE LIST

# CHAPTER 1 INTRODUCTION

The Puerto Rico Seismic Network (PRSN) of the Department of Geology, University of Puerto Rico at Mayagüez (UPRM) is the institution responsible for seismic and tsunami monitoring in Puerto Rico, British and United States Virgin Islands. Its area of responsibility (AOR) is within latitudes 17ºN-20º N and longitudes 63.5ºW-69º W (Figure 1.1).

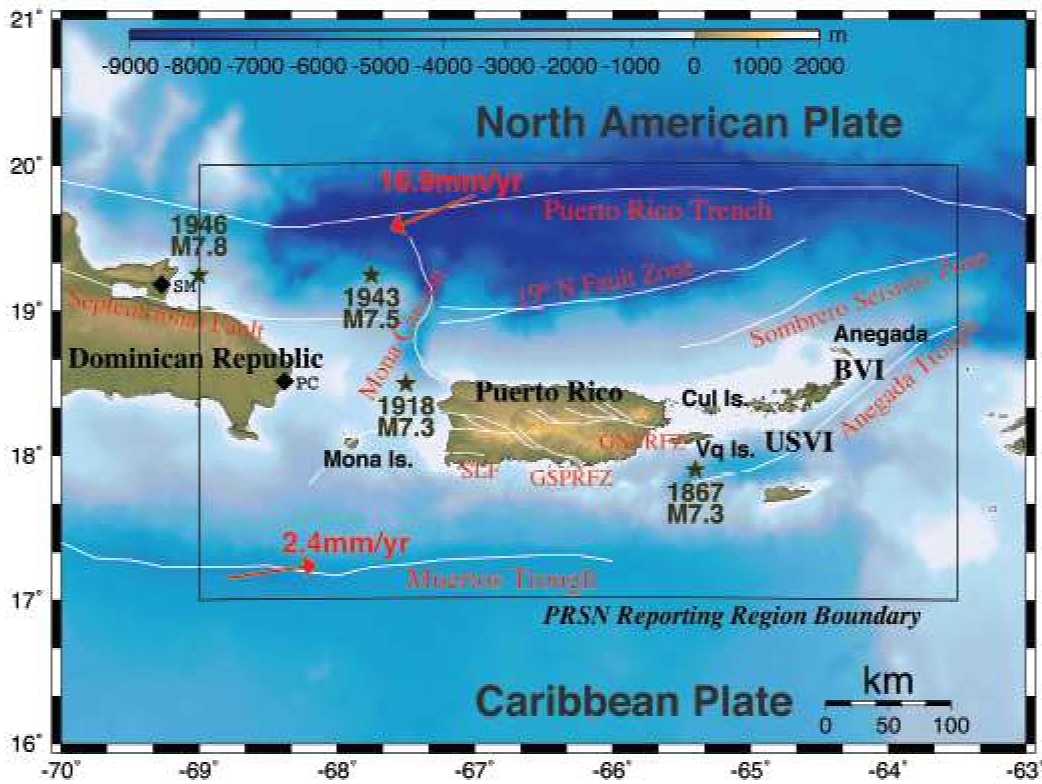


Figure 1.1 Area of Responsibility (AOR) of PRSN (Clinton et al, 2006)

Puerto Rico is located on a microplate sandwiched between the obliquely subducting North American and Caribbean plates (Figure 1.1). Puerto Rico accommodates approximately 16.9 mm/yr of deformation relative to North America and 2.4 mm/yr (Jansma et al 2000) relative to the Caribbean Plate, primarily by left-lateral strike-slip motion along east-west striking faults. The main sources of seismic activity in the region are at the supposed boundaries of the microplate: the subduction zone to the north (the Puerto Rico Trench) and south (the Muertos Trough), and zones of extension at the Anegada Trough to the east and the Mona Canyon region to the west (Figure 1.1). All these regions are capable of producing events greater than M7.0 (Clinton et al 2006).

The island of Puerto Rico has a long history of damaging earthquakes and tsunamis. The island is bounded on all sides by major tectonic fault lines (Figure 1.1). The most recent large event to cause widespread damage across the island occurred in the Mona Passage in 1918, with Ms 7.3.

To locate earthquakes, PRSN has a pool of seismic stations (broadband, short period and accelerometers) that are installed around Puerto Rico and adjacent islands of Mona, Vieques and Culebra, the British and United States Virgin Islands, and eastern Dominican Republic. Most of these stations have a sensitivity of 1500 volts over meter per second (V/m/s) in the frequency band from 0.01 to 50 Hertz (Hz) and are sampled at 40 samples per second (sps). These stations share the common goal of providing high quality data and information in response to needs of the emergency management, engineering, and scientific communities, as well as the general public (Clinton et al, 2006).

Using the data set recorded by eleven broadband seismic stations, it intends to characterize the background seismic noise of the main island of Puerto Rico. These seismic background noises are sometimes referred as ambient earth vibration (Brune et al 2006) and include: Cultural noise, wind, water, geological noise, microseisms, system electronic artifacts, diurnal, seasonal and geographical variations.

This is the first research on this topic in Puerto Rico, and the results will help to know the performance of existing broadband stations, detecting operational problems and to improve the installation of broadband stations. Result will also be used to calibrate the magnitude and real ground shaking scales used in the earthquake location programs.

## 1.1 Objectives and Contribution of the Thesis

In this research, the method for analysis of seismic noise using power spectral density (PSD) and probability density function (PDF) (McNamara et al 2004) was used to characterize the seismic noise at PRSN seismic stations.

The principal objective of this work is to characterize seismic noise due to ambient earth vibration in the frequency range from 0.01 to 16 Hz

Our major contributions are:

a) The dataless of the whole broadband PRSN station was done. This dataless is the database that has all the information of the sensor and digitizer used.
b) This is the first time that the seismic noise has been characterized at PRSN seismic stations.

## 1.2 Thesis Outline

This work presents some chapters that begin with Seismic Station Description, Seismic Noise Analysis, Seismic Noise Characterization, seismic station result and finally Conclusions, Recommendations and Future Works

# CHAPTER 2 LITERATURE REVIEW AND THEORETICAL BACKGROUND

## 2.1 Seismic Station Description

A typical seismic station is composed primarily by a seismometer (sensor), recorder, data communication channel, and power systems. It's time to describe the basis equipment of the system: telemetry, power supply, the seismometer and the recorder.

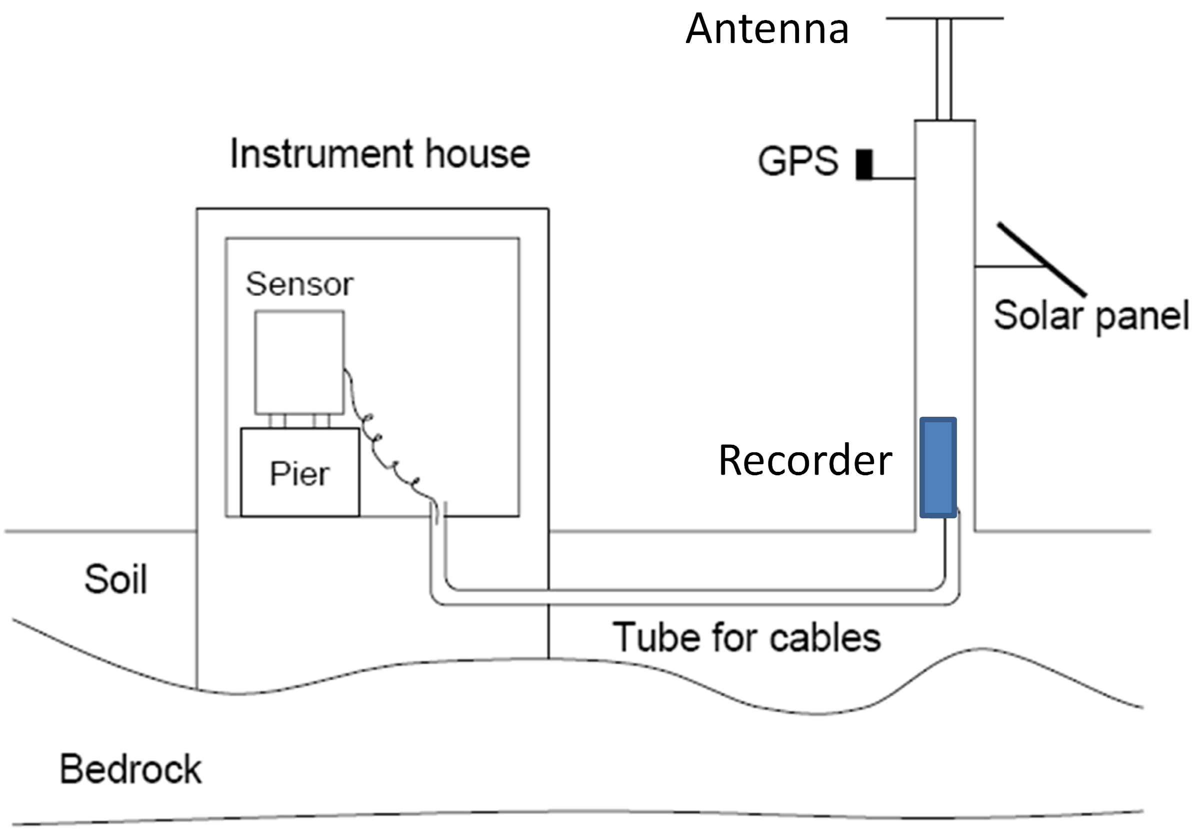


Figure 2.1 Typical seismic station (Havskov et al 2002).

Most of the seismic stations used in the Puerto Rico Seismic Network are based on digital telemetry and internet. For telemetry the PRSN use radio Willam in the frequency band of 2.5 GHz and the internet of the University of Puerto Rico and Electric Company.

The **power supply** uses solar panel and acid gel material (AGM) batteries. The solar panels are 75W module and the batteries are 115Ah.

A **seismometer** is a transducer that has as an input signal a velocity. Most of the time specified in m/s, and as an output signal a voltage in volts (V). Also, the seismometer has a frequency response specified as a Laplace transform which have poles, zeros and a normalization factor (Havskov et al 2002).

Sensor self noise: All electronic components as well as the sensor itself generate noise. Instrument self noise can be divided into two parts. (1) Brownian thermal motion of the seismometer mass spring system, which is inversely proportional to the mass and directly proportional to the damping. Unless the mass is very small, this noise is so small that it has no practical importance. Even for a seismometer with a mass of 23g, this noise is below the level of the New Low Noise Model.

Figure 2.2 show that the thermal noise is below the Low Noise Model so it does not have practical importance. The contribution from each element is shown and the Peterson noise curves are shown for reference. Thermal noise is the noise due to Brownian thermal motion of the mass, Johnson noise is caused by thermal fluctuation of the electrons within any dissipative element in the electronic circuit.

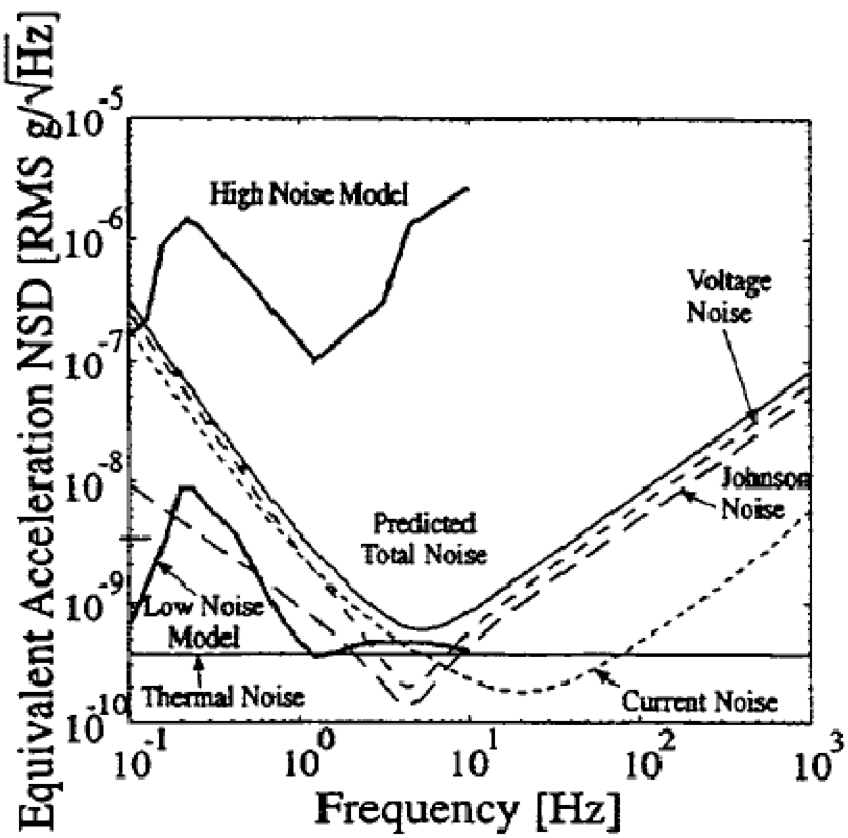


Figure 2.2 Predicted total noise equivalent acceleration of a standard electronic circuit with a 4.5Hz seismometer. Figure form Barzilai et al 1998.

Electronic Noise: This is caused by current flowing through different elements and semiconductor noise. The electronic noise (voltage and current noise) is thus the real limiting factor in seismograph sensitivity. This is particularly a problem at low frequencies because sensor output is low and semiconductors tend to have a higher noise at low frequencies.

Sensor parameters:

Frequency responses: sensors are described to have a flat velocity or acceleration response within a given frequency band and for velocity sensors, even for active sensors, the frequency response at the low end can be described with the usual response function. For example flat response within 0.01-50Hz.

Sensitivity: sensitivity is given as the gain of the instrument like 1000V/m/s.

Sensor dynamic range: is the ratio between the largest and smallest signal the sensor can record. For example, the guralp CMG-40T sensor has a dynamic range of 145dB

The **recorder** is an electronic equipment that has as an input signal a voltage in volts (V) and as an output signals counts. Most of the recorder used by PRSN has a resolution of 24 bit and has a frequency response specify as a Z transform whose specification meet the frequency response of the seismometer. The recorder use a time stamp mark given by a Global Positioning System (GPS).

The process of analog to digital conversion involves two steps: first the signal is sampled at discrete time intervals, and then each sample is evaluated in terms of a number.

Basic digitizer properties

Resolution: The smallest step that can be detected. Resolution is also labeled as a sensitivity. It is measured in V/number of bit.

Gain: The sensitivity expressed in Counts/V. Can be derived from resolution.

Sample rate: Number of samples acquired per second. For seismology the usual sample rate is 40sps.

Maximum input or full scale (FS): The maximum input for the Analog to Digital Converter (ADC). Typical values from +/-2.5 to +/- 20V.

**2. 2 General representation of the frequency response function**

The response function for the RC low pass filter can be written

$$T_{RC(\omega)} = \frac{1}{1 + i\omega RC} \qquad (1)$$

Similarly, the amplitude frequency response function for a mechanical seismometer is

$$T_{d(\omega)} = \frac{\omega^2}{\omega_0^2 - \omega^2 + i2\omega\omega_0 h} \qquad (2)$$

In general, the response function could be any complex function. It turns out that $T(\omega)$ for all systems made from discrete mechanical or electrical components can be represent exactly by rational functions of $i\omega$ like

$$T(\omega) = \frac{a_0 + a_1(i\omega) + a_2(i\omega)^2 + ...}{b_0 + b_1(i\omega) + b_2(i\omega)^2 + ...} \tag{3}$$

Where $a_i$ and $bi$ are constants. The number of terms in the polynomials will depend on the complexity of the system.

It is seen from equation (1), that the RC filter exactly looks like (3), while the mechanical seismometer response must be slightly rewritten to

$$T_{d(\omega)} = \frac{-(i\omega)^2}{\omega_0^2 + 2i\omega\omega_0 h + (i\omega)^2} \tag{4}$$

So for a seismometer $a_0 = 0$, $a_1 = 0, a_2 = -1, b_0 = \omega_0^2, b_1 = \omega_0 h$, $b_2 = 1$. This general representation is sometimes used and is one of the accepted ways of giving response in SEED (Standard for Exchange of Earthquake Data) format. However, (4) can be written in an alternative and simpler way. Considering that a polynomial can be factorized, equation (4) can be written

$$T(\omega) = c\frac{(i\omega - z_1)(i\omega - z_2)(i\omega - z_3)...}{(i\omega - p_1)(i\omega - p_2)(i\omega - p_3)...} \tag{5}$$

Where c is the combined normalization constant for nominator and denominator polynomials, z are the zeros (or roots) of the nominator polynomial while the zeros of the denominator polynomial are the poles p. Using equation (5) to represent $T(\omega)$ is the so called poles and zeros representation, which has become the most standard way. Representing response curves in terms of poles and zeros is often described in a very complicated way, where it is necessary to understand terms like Laplace transforms and complex s-plane

**2. 3 Understanding Poles and Zeros**

The transfer function provides a basis for determining important system response characteristics without solving the complete differential equation. As defined, the transfer function is a rational function in the complex variable $s = \sigma + j\omega$, that is

$$H(s) = \frac{b_m s^m + b_{m-1}s^{m-1} + ... + b_1 s + b_0}{a_n s^n + a_{n-1}s^{n-1} + ... + a_1 s + a_0} \tag{6}$$

It is often convenient to factor the polynomials in the numerator and denominator, and to write the transfer function in terms of those factors:

$$H(s) = \frac{N(s)}{D(s)} = K\frac{(s-z_1)(s-z_2)...(s-z_{m-1})(s-z_m)}{(s-p_1)(s-p_2)...(s-p_{n-1})(s-p_n)} \tag{7}$$

Where the numerator and denominator polynomials, $N(s)$ and $D(s)$, have real coefficients defined by the system's differential equation and $K = b_m / a_n$. As written in Eq. (7) the $z_i's$ are the roots of the equation

$$N(s) = 0, \tag{8}$$

And are defined to be the zeros, and the $p_i's$ are the roots of the equation

$$D(s) = 0, \tag{9}$$

And are defined to be the system poles. In Eq. (7) the factor in the numerator and denominator are written so that when $s = z_i$ the numerator $N(s) = 0$ and the transfer function vanishes, that is

$$\lim_{s \to z_i} H(s) = 0.$$

And similarly when $s = p_i$ the denominator polynomial $D(s) = 0$ and the value of the transfer function becomes unbounded,

$$\lim_{s \to p_i} H(s) = \infty.$$

All of the coefficients of polynomial $N(s)$ and $D(s)$ are real, therefore the poles and zeros must be either purely real, or appear in complex conjugate pairs. In general for the poles, either $p_i = \sigma_{i,}$ or else $p_i, p_{i+1} = \sigma_i \pm j\omega_i$. The existence of a simple complex pole without a corresponding conjugate pole would generate complex coefficients in the polynomial $D(s)$. Similarly, the system zeros are either real or appear in complex conjugate pairs.

The poles and zeros are properties of the transfer function, and therefore of the differential equation describing the input-output system dynamics. Together with the gain K they completely characterize the differential equation, and provide a complete description of the system.

The pole-Zero Plot

A system is characterized by its poles and zeros in the sense that they allow reconstruction of the input/output differential equation. In general, the poles and zeros of a transfer function may be complex, and the system dynamics may represent graphically by plotting their locations on the complex s-plane, whose axes represent the real and imaginary parts of the complex variable s. Such plots are known as pole-zero plots. It is usual to mark a zero location by a circle (○) and a pole location a cross (x). The location of the poles and zeros provide qualitative insights into the response characteristic of a system. Many computer programs are available to determine the poles and zeros of a system from either the transfer function state equations. Figure 2.3 is an example of a pole-zero plot for a third-order system with a single real zero, a real pole and a complex conjugate pole pair, that is;

$$H(s) = \frac{(3s+6)}{(s^3+3s^2+7s+5)} = 3\frac{(s-(-2))}{(s-(-1))(s-(-1-2j))(s-(-1+2j))}$$

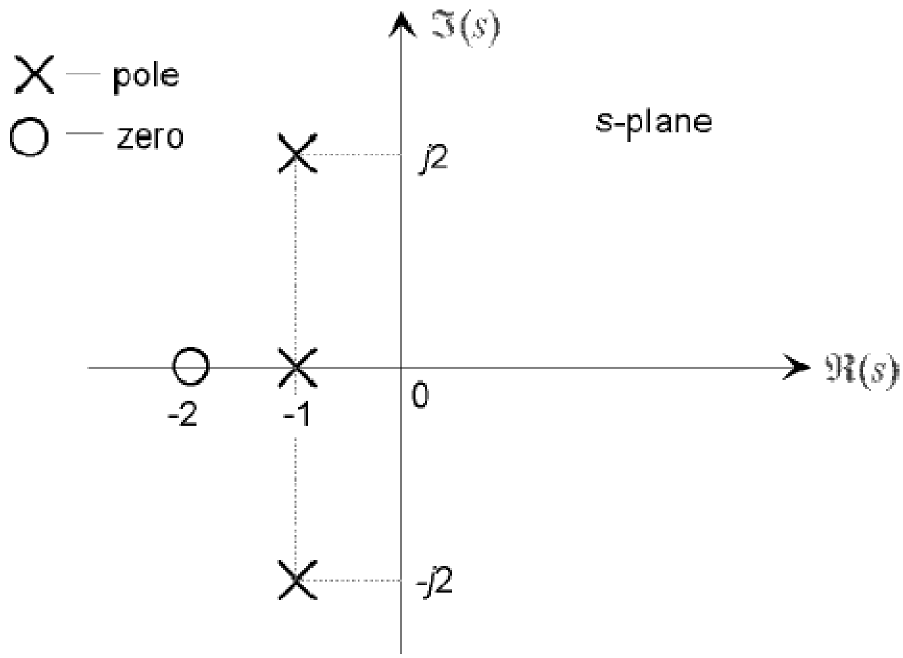


Figure 2.3 The pole-zero plot of a typical third-order system with one real pole and a complex conjugate pole pair, and a single real zero.

System Poles and the Homogeneous Response

Because the transfer function completely represents a system differential equation, its poles and zeros effectively define the system response. The unforced response of a linear system to a set of initial conditions is

$$y_h(t) = \sum_{i=1}^{n} C_i e^{\lambda_i t} \tag{10}$$

Where the constants $C_i$ are determined for the given set of initial conditions and the exponents $\lambda_i$ are the roots of the characteristic equation or the system eigenvalues. The characteristic equation is

$$D(s) = s^n + a_{n-1}s^{n-1} + ... + a_0 = 0, \tag{11}$$

And its roots are the system pole, that is $\lambda_i = p_i$, leading to the following important relationship:

The transfer function poles are the root of the characteristic equation, and also the eigenvalues of the system A matrix.

The homogeneous response may therefore be written

$$y_h(t) = \sum_{i=1}^{n} C_i e^{p_i t} \tag{12}$$

The location of the poles in the s-plane therefore define n components in the homogeneous response described below:

1. A real pole $p_i = -\sigma$ in the left-half of the s-plane defines an exponentially decaying component, $Ce^{-\sigma t}$, in the homogenous response. The rate of the decay is determined by the pole location; poles far from the origin in the left-half plane correspond to components that decay rapidly, while poles near the origin correspond to slowly decaying components.
2. A pole at the origin $p_i = 0$ defines a component that is constant in amplitude and defined by the initial conditions.
3. A real pole in the right-half plane corresponds to an exponentially increasing component $Ce^{\sigma t}$ in the homogeneous response, thus defining the system to be unstable.
4. A complex conjugate pole pair $\sigma \pm j\omega$ in the left-half of the s-plane combine to generate a response component that is decaying sinusoid of the form $Ae^{-\sigma t}\sin(\omega t + \phi)$ where $A$ and $\phi$ are determined by the initial conditions. The rate of decay specified by $\sigma$; the frequency of oscillation is determined by $\omega$.
5. An imaginary pole pair, that is a pole pair lying on the imaginary axis, $\pm j\omega$ generates an oscillatory component with a constant amplitude determine by the initial conditions.
6. A complex pole pair in the right half plane generates an exponentially increasing component.

These results are summarized in Figure 2.4

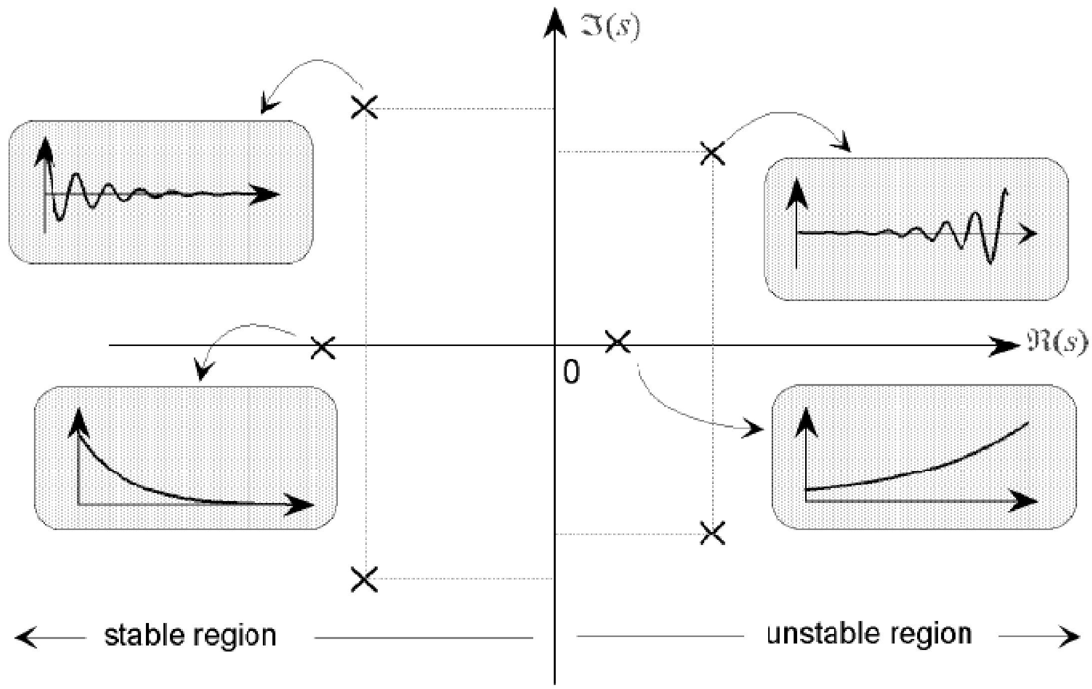


Figure 2.4 The specification of the form of components of the homogeneous response from the system pole locations on the pole-zero plot

## 2.4 Noise Models

Earth noise model have been part of the science at least since Brune and Oliver (1959) published curves of high and low seismic background displacement bases on a worldwide survey of station noise. They have been useful as baselines for evaluating and comparing station site characteristics, for defining instrument specifications, and for predicting the response of sensor systems to quiet and noisy background conditions.

The USGS low-noise model (LNM) originated form a low noise composite of SRO and ASRO data constructed by Peterson (1980) over the period range from 0.1 to 100 sec. The composite was derived from individual station PSD by overlaying the spectral plot and selecting low noise points while ignoring narrow spectral peaks and valleys. Soon after, The SRO/ASRO composite was extended to longer periods by patching it at 100-sec period with IDA gravimeter data published by Agnew and Berger (1978), and extended to shorter period by patching it at 0.5-sec period with low noise spectra form Lajitas, Texas, published by Li and others (1981). The combined composite was approximated by a sequence of linear segments to make it easier to process in a computer, and the result was called a low noise model (LNM). A high-noise model (HNM) was constructed in essentially the same fashion using SRO data from coastal and island sites.

## 2.5 New Noise Model

As STS-1 data became available from the China and IRIS broadband networks, it became clear that the LNM needed modification, especially at long periods. The construction of the new noise models has followed the same procedure to develop the original noise models. In this case, straight line segments were graphically fitted to the lower and upper envelopes of the spectral overlay shown in Figure 2.5. The purpose was to preserve the general structure of the Earth noise without excessive attention to the narrow peaks and minor excursions of individual spectra.

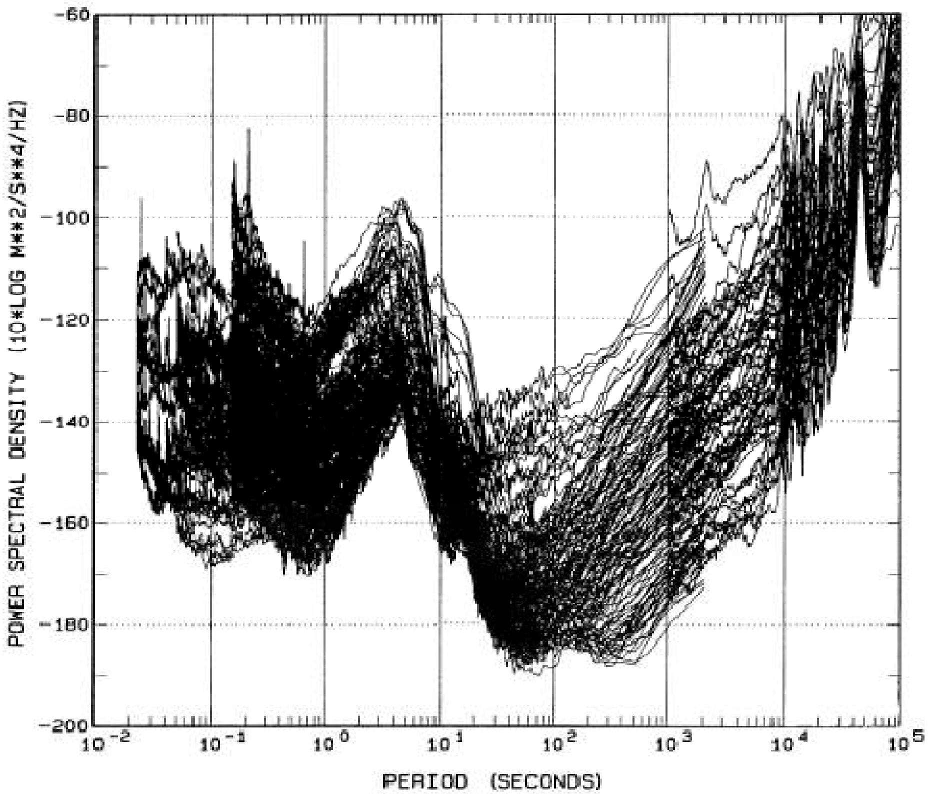


Figure 2.5 An overlay of most station spectra presented by Peterson 1993.

Like the original low-noise model (OLNM), the NLNM is a composite of station spectra obtained from many different instruments, vaults, geologic environments, and geographic regions. It is a hypothetical background spectrum that is unlikely to be duplicated at any single location on Earth.

The variables defining the PSD-axis intercepts and slopes of the NLNM and NHNM line segments are list in Tables 2.1 and 2.2, respectively. For graphical presentation, the noise model curves were generated by a C program that computes 100 points per decade. Both, the original and new noise models are plotted together in Figure 2.4. The OHNM was based on SRO borehole data, which accounts for the large difference between the OHNM and NHNM curves a long periods.

Table 2.1 Line parameters for constructing the NLNM curve given the period (P). (Peterson 1993)

| $NLNM_{acc} = A + B \log_{10}(P)$ dB referred to 1 $(m/sec^2)^2/Hz$ | | |
|---|---|---|
| P | A | B |
| 0.10 - | -162.36 | 5.64 |
| 0.17 - | -166.7 | 0.00 |
| 0.40 - | -170.00 | -8.30 |
| 0.80 - | -166.40 | 28.90 |
| 1.24 - | -168.60 | 52.48 |
| 2.40 - | -159.98 | 29.81 |
| 4.30 - | -141.10 | 0.00 |
| 5.00 - | -71.36 | -99.77 |
| 6.00 - | -97.26 | -66.49 |
| 10.00 - | -132.18 | -31.57 |
| 12.00 - | -205.27 | 36.16 |
| 15.60 - | -37.65 | -104.33 |
| 21.90 - | -114.37 | -47.10 |
| 31.60 - | -160.58 | -15.28 |
| 45.00 - | -187.50 | 0.00 |
| 70.00 - | -216.47 | 15.70 |
| 101.00 - | -185.00 | 0.00 |
| 154.00 - | -168.34 | -7.61 |
| 328.00 - | -217.43 | 11.90 |
| 600.00 - | -258.28 | 26.60 |
| 10000.00 - 100000.00 | -346.88 | 48.75 |
| $NLNM_{vel} = NLNM_{acc} + 20.0\log_{10}(P/2\pi)$ dB ref 1 $(m/sec)^2/Hz$ | | |
| $NLNM_{displ} = NLNM_{acc} + 20.0\log_{10}(P^2/4\pi^2)$ dB ref 1 $m^2/Hz$ | | |

Table 2.2 Line parameters for constructing the NHNM curve given the period (P). (Peterson 1993)

| $NHNM_{acc} = A + B \times \log_{10}(P)$ dB referred to 1 $(m/sec^2)^2/Hz$ | | |
|---|---|---|
| P | A | B |
| 0.10 - | -108.73 | -17.23 |
| 0.22 - | -150.34 | -80.50 |
| 0.32 - | -122.31 | -23.87 |
| 0.80 - | -116.85 | 32.51 |
| 3.80 - | -108.48 | 18.08 |
| 4.60 - | -74.66 | -32.95 |
| 6.30 - | 0.66 | -127.18 |
| 7.90 - | -93.37 | -22.42 |
| 15.40 - | 73.54 | -162.98 |
| 20.00 - | -151.52 | 10.01 |
| 354.80 - 100000.00 | -206.66 | 31.63 |
| $NHNM_{vel} = NHNM_{acc} + 20.0 \times \log_{10}(P/2\pi)$ dB ref 1 $(m/sec)^2/Hz$ | | |
| $NHNM_{displ} = NHNM_{acc} + 20.0 \times \log_{10}(P^2/4\pi^2)$ dB ref 1 $m^2/Hz$ | | |

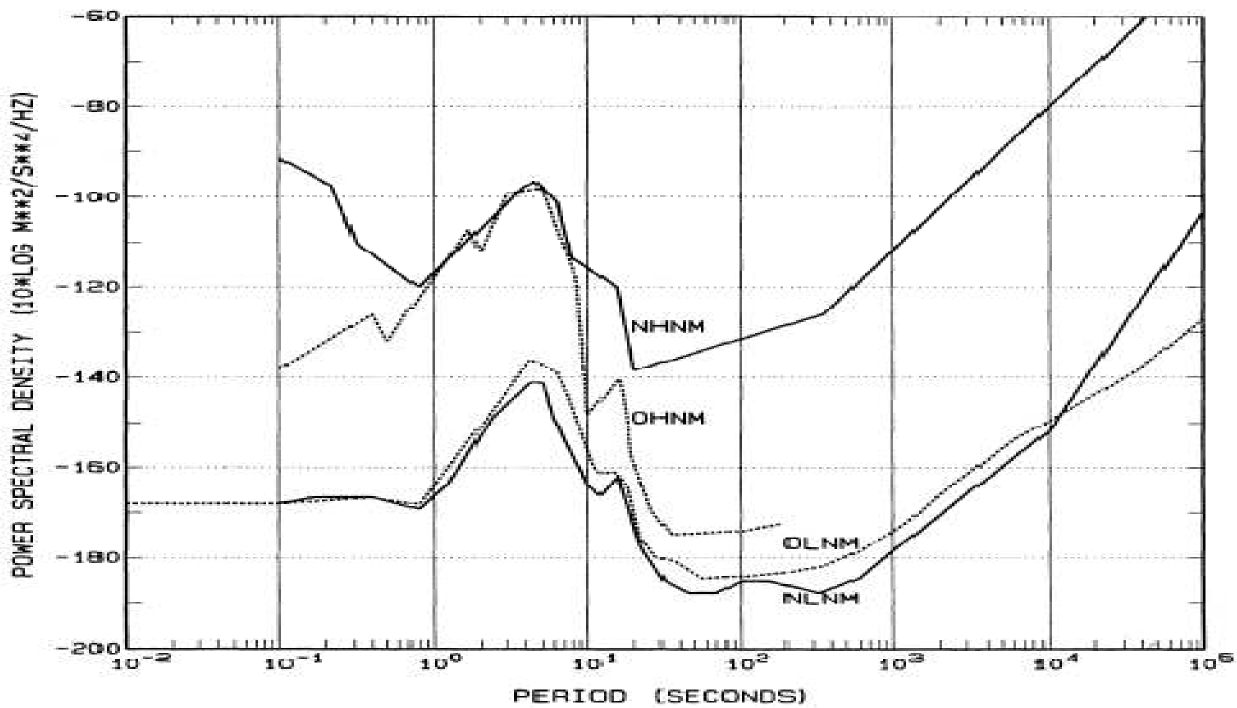

Figure 2.6 Comparison of new and original noise models. (Peterson)

## 2.6 Power Spectral Density

The standard method for quantifying seismic background noise is to calculate the noise power spectral density (PSD). The most common method for estimating the PSD for stationary random seismic data is called the direct Fourier transform or Cooley-Tukey method (Cooley et al 1965). The method computes the PSD via a finite range fast Fourier transform (FFT) of the original data and is advantageous for its computational efficiency.

The FFT of a periodic time series y (t) [m/s] is given by:

$$Y(f,T_r) = \int_o^{T_r} y(t)e^{-j2\pi ft}\,dt \qquad [m/Hz] \tag{13}$$

Where $T_r$ = length of time series segment [s].

$f$ = Frequency [Hz]

nfft= (N/2) +1=16385, number of frequency amplitudes estimated.

For discrete frequency values, $f_k$ The Fourier components are defined as:

$$Y_k = \frac{Y(f_{k,}T_r)}{\Delta t} \quad [\frac{m}{s \cdot Hz}] \tag{14}$$

For, $f_k = \frac{k}{N\Delta t}$ where $k = 1,2,..., N$

Where $\Delta t =$ sample interval (0.025s),

$N =$ Number of samples in each time series segment, $N = \frac{T_r}{\Delta t}$

Hence, using the Fourier component above then, the total power spectral density estimated is defined as:

$$P_k = \frac{2\Delta t}{N}|Y_k|^2 \quad [\frac{m^2}{s^2 \cdot Hz}] \tag{15}$$

From equation (15) it is noted that, the total power $P_k$, is simply the square of the amplitude spectrum with a normalization factor $\frac{2\Delta t}{N}$.

Finally, the seismometer instrument response is removed by dividing the PSD estimate by the instrument transfer function to acceleration (Havskov et al 2002), in the frequency domain.

$$P_a = P_k \cdot \omega^2 = P_v \cdot \omega^2, P_k = P_v, [(m/s^2)^2/Hz.] \tag{16}$$

For direct comparison of the low noise model and high noise model [10], the PSD estimate is converted into decibels (dB) with respect to acceleration $(m/s^2)^2/Hz$.

$$P_{a(dB)} = 10 \cdot \log_{10} P_a \text{, [dB]} \tag{17}$$

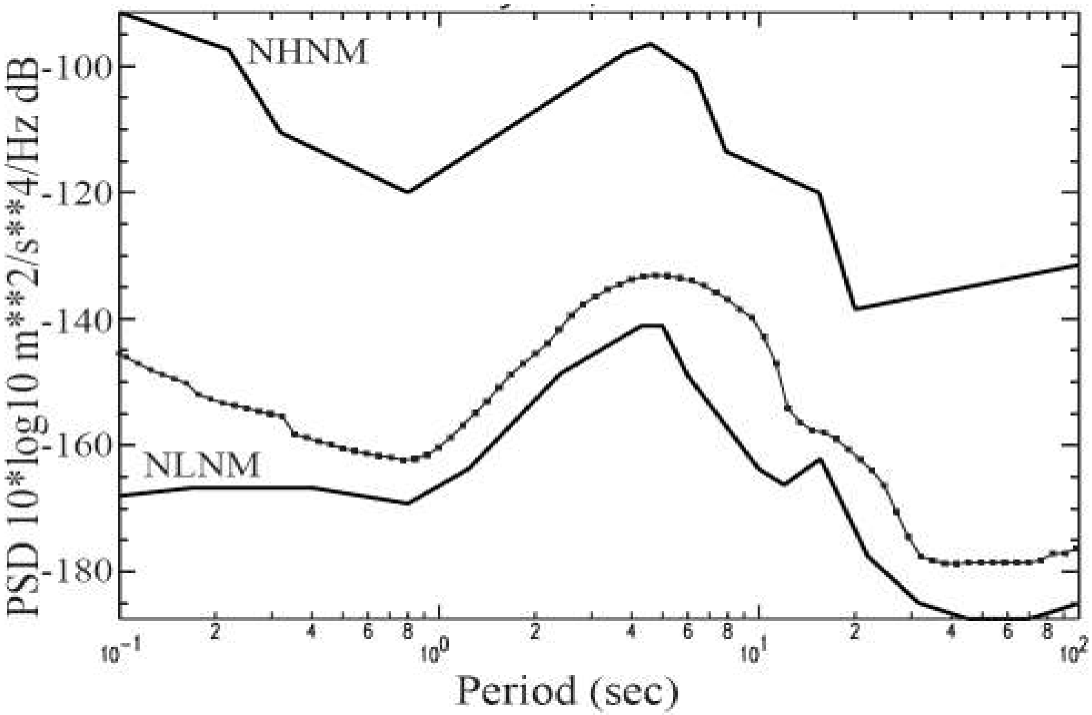


Figure 2.7 Example of a PSD (McNamara et al 2004)

In the Figure 2.7, the dot lines represent the values obtained with the PSD method described above. The new global high (NHNM) and low noise model (NLNM) (Peterson 1993), are curves that represent the upper and lower bounds of cumulative compilation of representative ground acceleration power spectral densities determined for noisy and quiet periods at 75 distributed worldwide digital station.

## 2.7 Probability Density Function

To estimate the true variation of noise at a given station seismic background noise is generated using probability density functions (PDF) from thousands of PSDs processed according to the previous section.

In order to adequately sample the PSDs, full octave averages are taken in 1/8 intervals. This procedure reduces the number of frequency by a factor of 169 from the number of fast fourier transform, nfft=16385 to 97. Thus, power is averaged between a short period (high frequency) corner, $T_s$ and a long period (low frequency) corner of $T_l$=2*$T_s$, with a center period, $T_c$=sqrt ( $T_s * T_l$) is the geometric mean period within the octave. The geometric means are evenly spaced in log space. The average power for that octave, period range from $T_s$ to $T_l$, is stored with the center period of the octave, $T_c$ for future analysis. $T_s$ is incremented by one octave such that $T_s = T_s * 2^{0.125}$, to compute the average power for the next period bin. $T_l$ and $T_c$ are recomputed, powers are averaged within the next period range $T_s$ to $T_l$ and the process continue until reaches the longest resolvable period given the time series window length of the original data, $T_r/10$. This process is repeated for every one hour PSD estimate, resulting of thousand of smooth PSD estimates for each station component. Powers are accumulated in 1 dB intervals to produce frequency distribution plots (histograms), for each period (Fig. 2.8), (McNamara et al 2006).

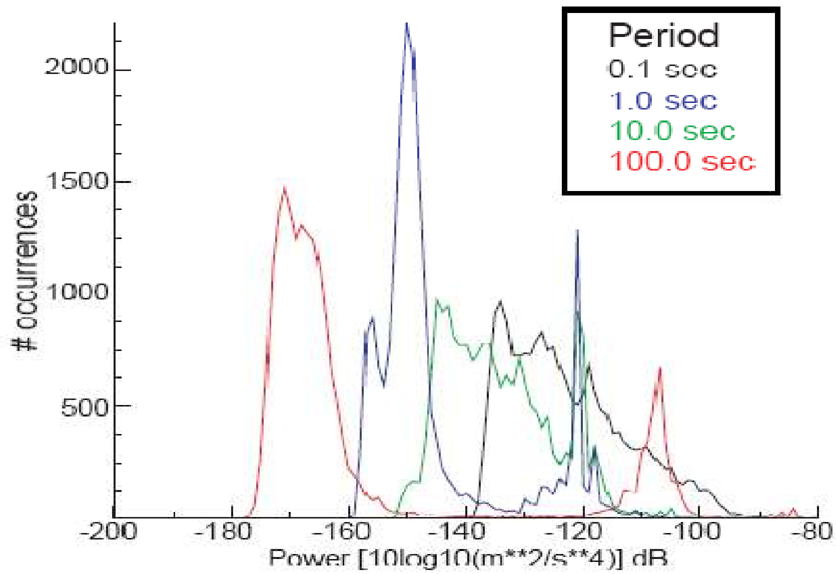


Figure 2.8 Histograms of powers, in 1dB bins, at four separate period bands (McNamara et al 2004)

The next step is to plot the distribution of powers for period, as observed in Figure 2.8, using a probability density function (PDF). The PDF, for a given center period, $T_c$ can be estimated as:

$$P(T_c) = N_{PT_c} / N_{T_c}$$

Where $N_{PT_c}$ is the number of spectral estimates that fall into a 1 dB power bin, P, with a range from -200 to -80 dB, and a center period, $T_c$; then plots the probability of occurrence of a given power at a particular period for direct comparison to the high and low noise model Figure 2.9.

In the Figure 2.9 below, it shows an example of a PDF for the station AOPR locate at Arecibo Astronomic Observatory. It has different values for a period range from 0.1-100 sec. In this figure, see the mode, maximum values and minimum values of PSD. Also the probability of occurrence in a color bar code is shown. This PDF is in dB with respect to acceleration $(m/s^2)^2/Hz$. The data length corresponds to one week.

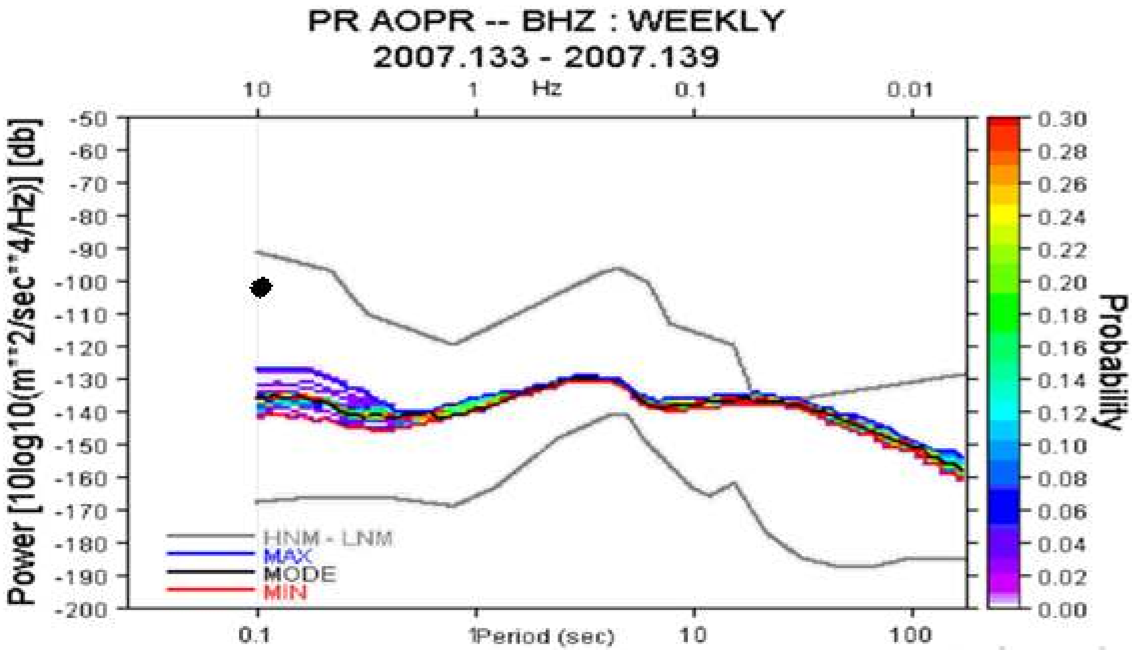


Figure 2.9 PDF of Arecibo Astronomic Observatory Seismic Station.

In the previous figure also shows two curves in gray color: HNM (High noise model) and LNM (low noise model). These curves represent the standard way of measuring the noise in a seismic station. These curves were obtained from an average of thousand of PSD of the world seismic station by Peterson in 1993. Also, there is a black point representing a magnitude 3.0, 100 km of distance to the station, earthquake, this earthquake has enough power to be over the noise level of the station

## 2.8 Seismic Background Noise Characterization

The seismic noises that will be characterized are described bellow:

1. **Cultural noise**: The most common source of seismic noise is from the actions of human activity at or near the surface of the Earth. This noise has a frequency band from 1-10 Hz. (1-0.1s). Cultural noise originates from the coupling of traffic and machinery energy cause by human activity into the earth.

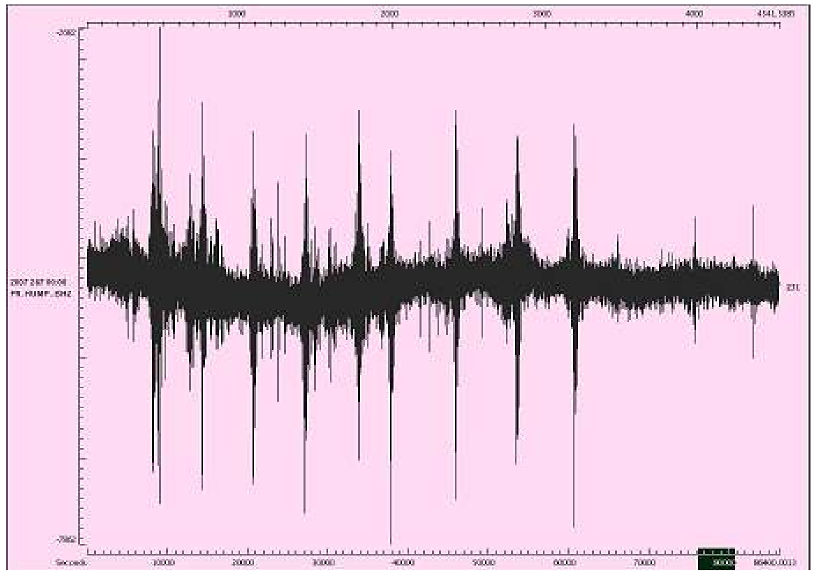

Figure 2.10 Example of car noise in the time domain

2. **Wind, water, and geological noise**: Objects move when responding to wind and this movement, when coupled can be major source of noise. Additional noise includes running water, surf, volcanic activity or long period tilt due to thermal instabilities from poor station design. In the Figure 2.9, there is a PDF of the seismic station Barro Colorado in Panamá. Since the period of 60 seconds, there is water noise generated by the Canal de Panama.

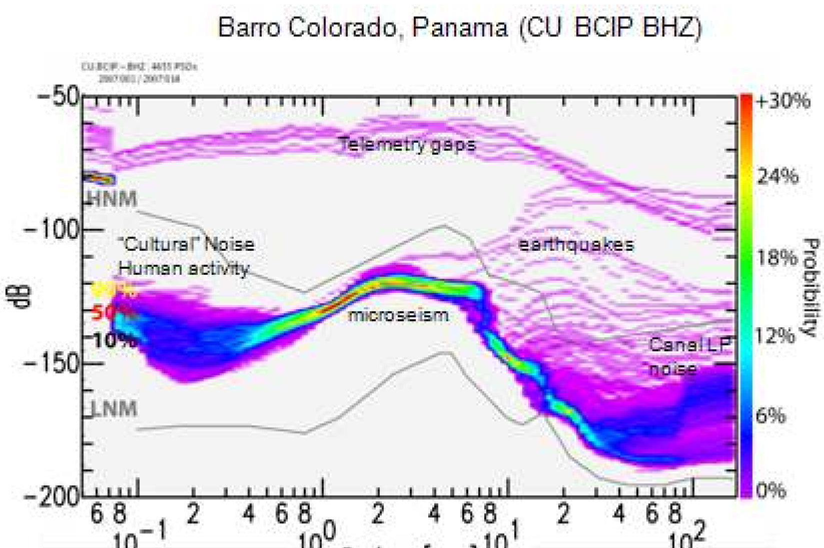


Figure 2.11 PDF of the seismic station Barro Colorado, Panama

3. **Microseisms**. These are two dominant peaks in the seismic noise spectrum that are both widespread and easily recognizable at all broadband seismic station worldwide. One peak is the single frequency peak (T=10-16s) that is generated in shallow coastal waters where ocean wave energy is converted into seismic energy either trough vertical pressure

variations, and the other peak is the double frequency peak (T= 4-8s) that is generated by the superposition of ocean waves of same period traveling in opposite directions. The figure 2.12 shows an example.

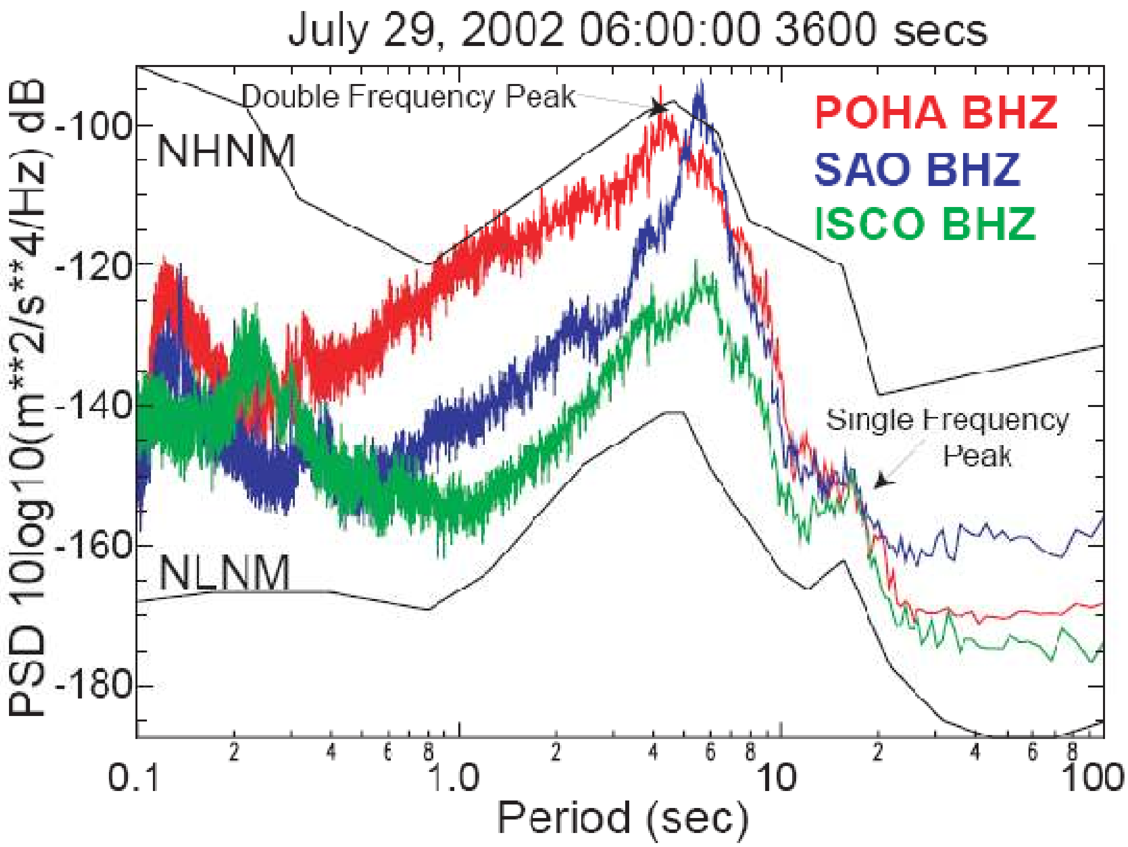


Figure 2.12 microseisms (McNamara)

4. **System artifact in the PDF noise field**. These are system transients as data gaps and sensor glitches. Data gaps are data loss by hardware or communication problems and are filled by zero. Sensor glitches are divided in two parts: calibration pulse and auto mass re-center. Calibration Pulses are pulses used to test the calibration of the seismic sensor according to the manufacture calibration sheet. Auto mass re-center are pulse send to the seismic sensor to center the mass when it loss the middle position. The Figure 2.13 and 2.14 show these three signals in the time domain and in the PDF.

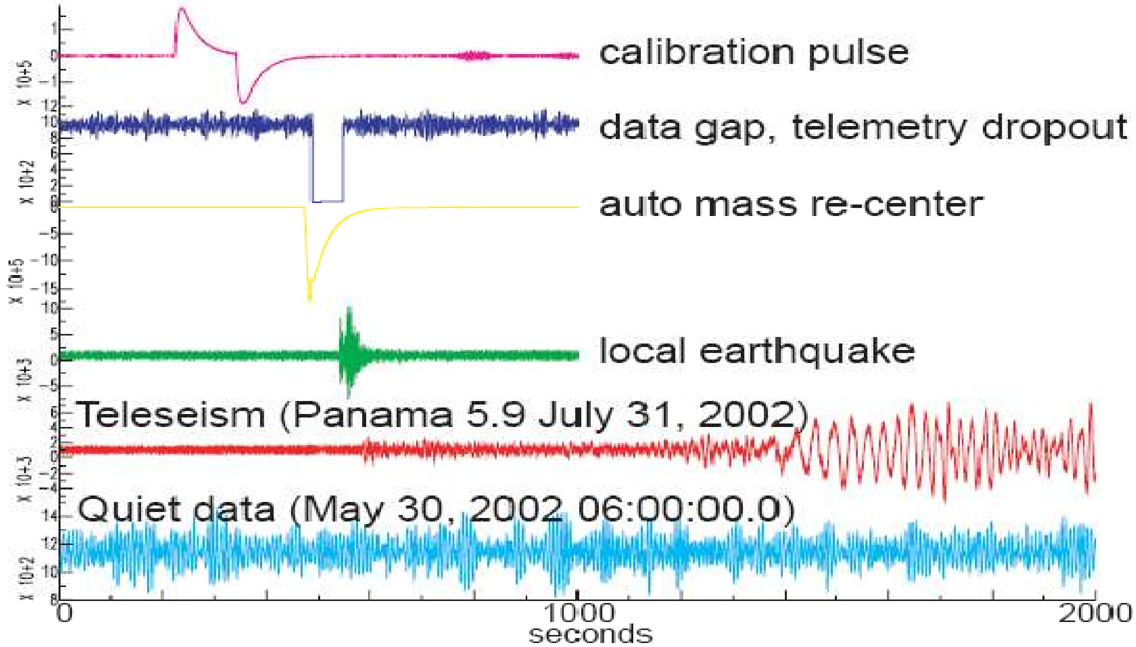


Figure 2.13 System artifact (McNamara et al 2004)

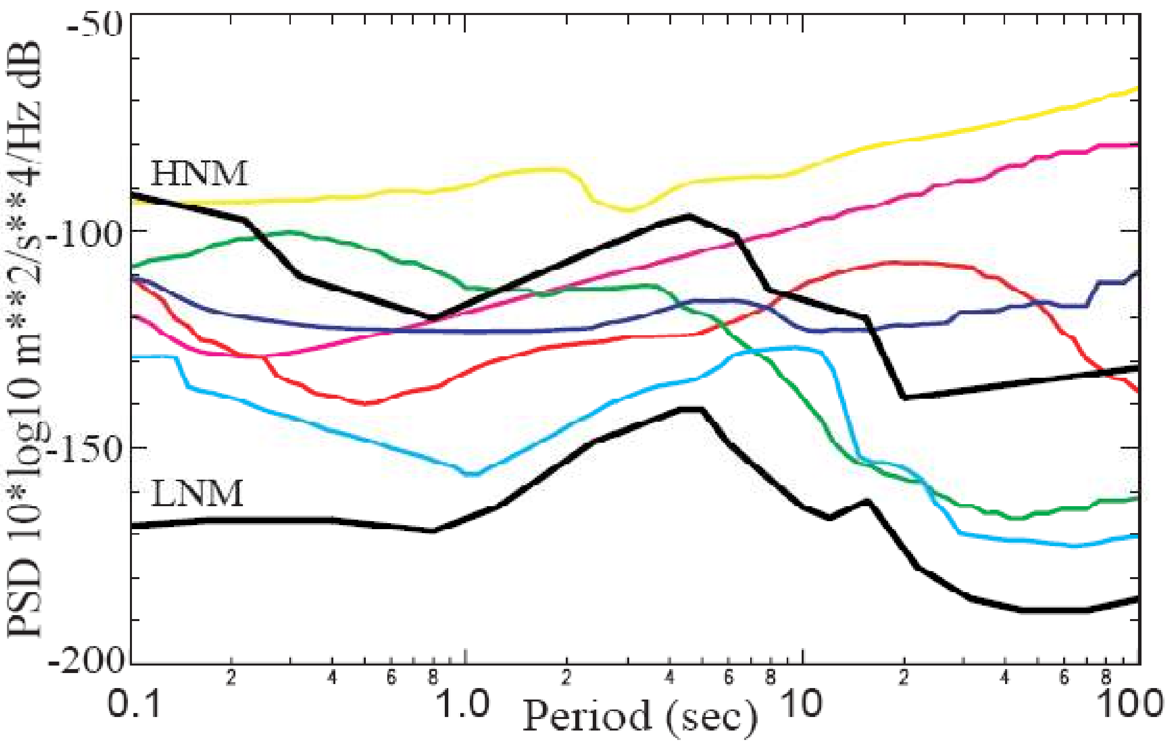


Figure 2.14 PDF representing system artifacts (McNamara et al 2004)

5. **Earthquakes**: An earthquake is the result of a sudden release of energy in the earth's crust that generates seismic waves. There are three types of earthquakes that we have to define clearly in order to study the noise signals caused by them. The first are the local earthquakes, which are earthquakes with a distance of approximately 0-200km to the

seismic station. The second one is the regional earthquakes which are earthquake with a distance of 200-1000 km and the last one is the teleseismic which are earthquake with a distance more than 1000km.

There are two types of seismic waves, body waves and surface waves. Body waves travel through the interior of the earth. They follow raypath bent by the varying density and modulus of the earth's interior, they behave like the light with the refraction. They are dominated by a period of <1s. Surface waves are analogous to water waves and travel just under the earth's surface. They are dominated by a period of >10s. (Shearer 1999)

Typical speeds of body waves are 330 m/s in air, 1450 m/s in water and about 5000 m/s in granite. Surface waves are slower than body waves, roughly 70% of the velocity of body waves

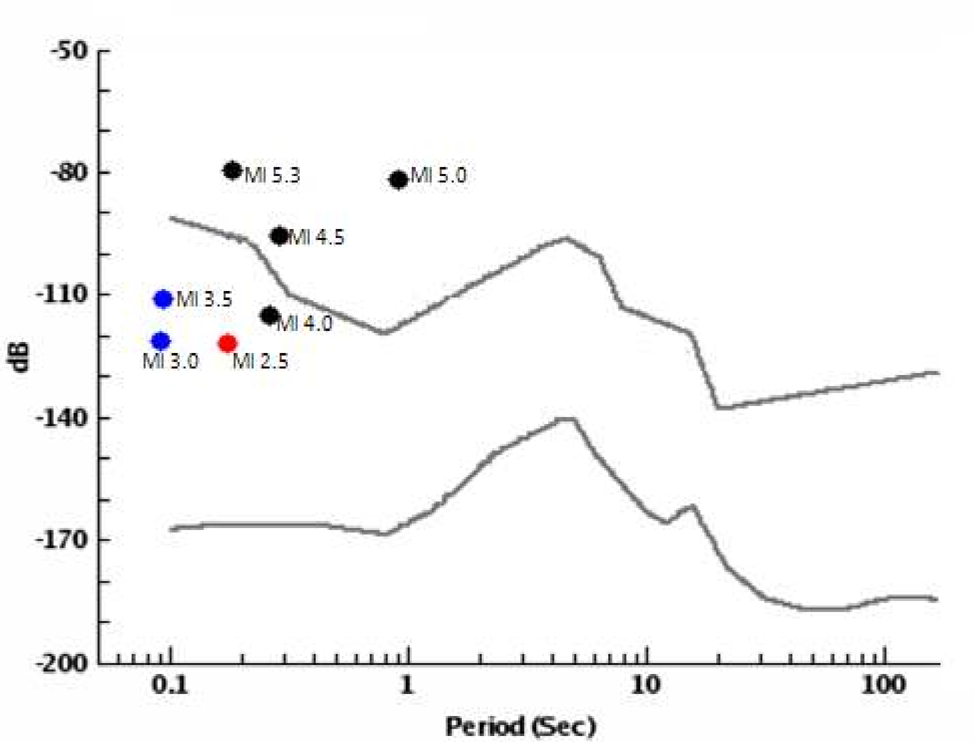


Figure 2.15 Earthquakes on a PSD

The Figure 2.15 shows different points which represent local earthquakes of different magnitudes in the Richter scale and different distances to the seismic station that detected them. The black points are earthquakes within a distance of 200 kilometers to the seismic station and their magnitudes are within 4.0 and 5.3. The blue points are earthquakes within a distance of 100 kilometers to the seismic station and their magnitudes are within 3 and 3.5. Finally the red point is an earthquake within a distance of 10 kilometer to the seismic station and its magnitude is 2.5.

**2.9 Diurnal Variations**

Diurnal variations is the variation of the amplitude of the acceleration in dB respect to 1(m**2/s**4)/Hz during the hours of the day respect to period ranging from 0.1-100sec.

The diurnal variation of seismic noise is analyzed by accumulating the PSDs in hourly bins and computing a PDF for each hour of the day over a three-year period, and then compute the statistical mode at all periods.

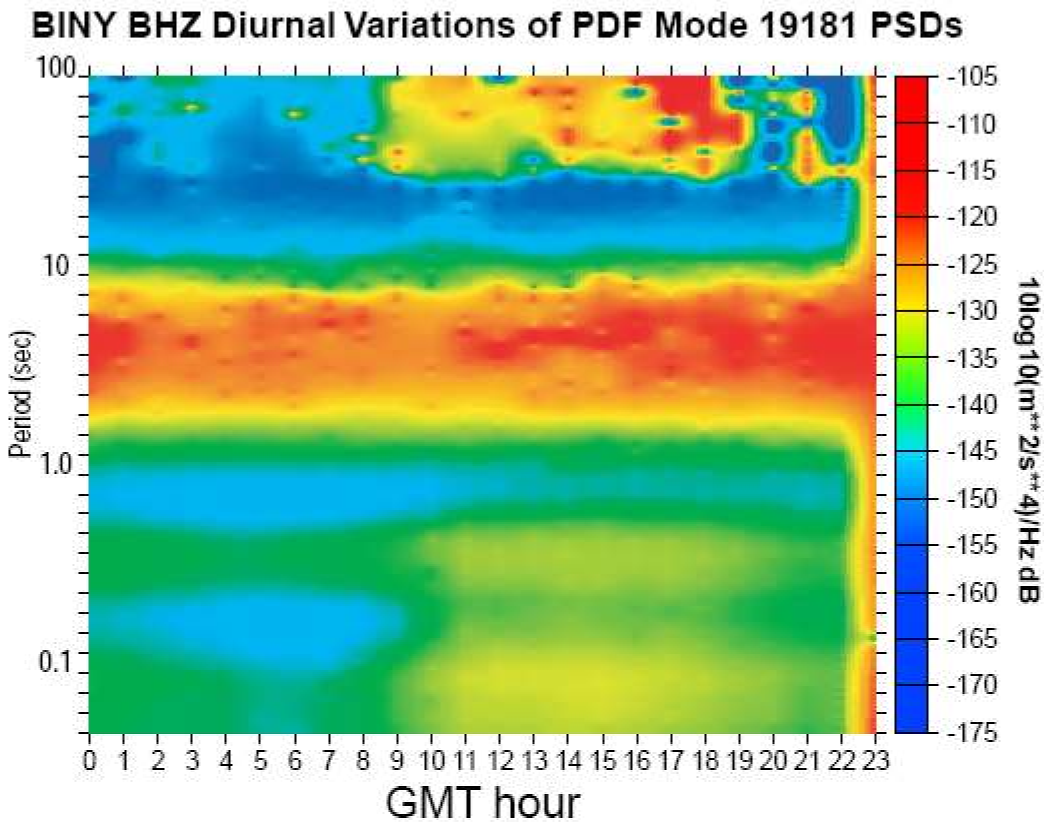


Figure 2.16 BINY Diurnal Variations (McNamara et al 2004)

Figure 2.16 is a plot of the variation in the PDF mode as a function of hour of the day at station BINY, Binghamton, New York using 19181 hourly PSDs computed from September 2000 to September 2003.

**2.10 Seasonal Variations**

Seasonal variations is the variation of the amplitude of the acceleration in dB respect to 1(m**2/s**4)/Hz during the months of the years respect to period ranging from 0.1-100sec.

Seasonal variations are computed in the same way as diurnal variations. A separate PDF for each month of the year over a three-year period is computed. Then compute the statistical mode for all periods for each monthly PDF.

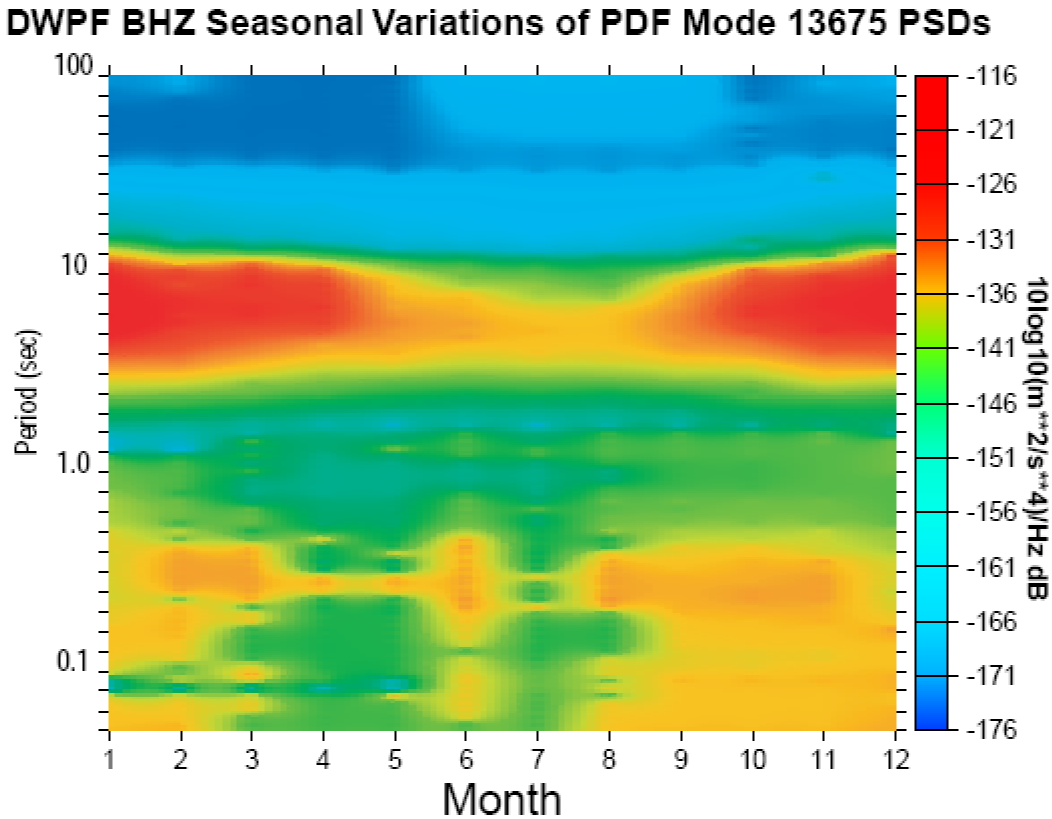

Figure 2.17 DWPF Seasonal Variations (McNamara et al 2004)

Figure 2.17 is a plot of the seasonal noise variation at station DWPF in Florida.

# CHAPTER 3 METHODOLOGY

The data of the seismic broadband station located in Puerto Rico has been analyzed; below there is a Table 3.1 of the stations that were used, followed by a map showing their geographical position, Figure 3.1.

Table 3.1 Seismic broadband stations located in Puerto Rico.

| Station Code | Site | Sensor / Digitalizador | LOCATION | | |
|---|---|---|---|---|---|
| | | | LAT (°N) | LON (°W) | ELEVATION (m) |
| AGPR | Aguadilla, PR | 0.0027-50 Hz Q330 | 18.4675 | 67.1111 | 119.9 |
| AOPR | Arecibo, PR | 0.05-50 Hz Reftek 130 | 18.3466 | 66.7539 | 355.2 |
| CBYP | Cubuy, Canóvanas, PR | 0.033-50Hz Reftek 7208 | 18.2716 | 65.8566 | 606.9 |
| CPD | Yabucoa, PR | 0.05-50Hz Reftek 7208 | 18.0368 | 65.9151 | 385.7 |
| CRPR | Cabo Rojo, PR | 0.05-50 Hz Reftek 7208 | 18.0064 | 67.1096 | 65.0 |
| HUMP | Humacao, PR | 0.0027-50 Hz Reftek 130 | 18.1421 | 65.8489 | 79.1 |
| ICM | Isla Caja de Muerto, PR | 0.033-50Hz Reftek 7208 | 17.8933 | 66.5210 | 77.2 |
| MPR | Mayagüez, PR | 0.0027-50 Hz Netdas | 18.2117 | 67.1398 | 22.4 |
| MTP | Vieques, PR | 0.01-50 Hz Reftek 7208 | 18.0972 | 65.5525 | 120.0 |
| OBIP | Ponce, PR | 0.033-50Hz Netdas | 18.0428 | 66.6062 | 102.6 |
| SJG | Cayey, PR | 0.01-50 Hz Q680 | 18.1001 | 66.1502 | 456.9 |

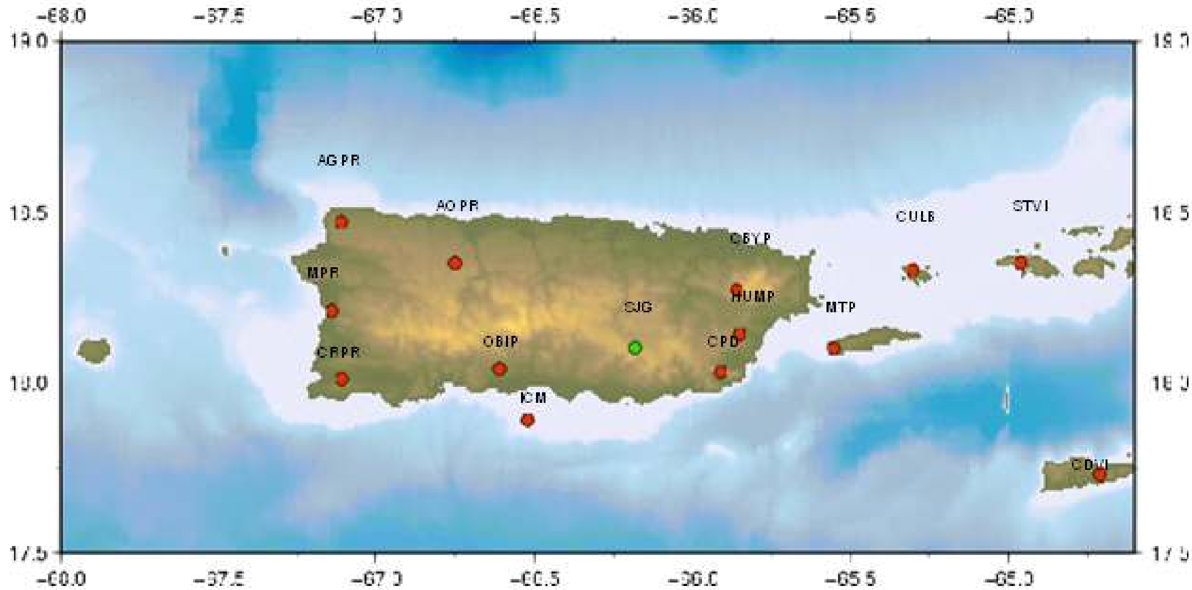


Figure 3.1 Geographical Position of all PRSN seismic stations (Pujols et al 2008).

To take a station into account, it should have a maximum of three year of data for each station, in some cases this was not be possible, so an approximation was used.

The database of the whole transfer function of each seismic station was compiled specifying the complete values for the seismometer Laplace transform and digitizer Z transform of the whole PRSN seismic station, this database is usually called the dataless. This dataless is done in The Standard for the Exchange of Earthquake Data (SEED), is an international standard format for the exchange of digital seismological data.

In order to get the ambient earth vibration at a seismic station, it is mandatory to have these information, because these information tells the calibration at each seismic station, so when the ground motion is measured with the seismometer, it gets true ground values.

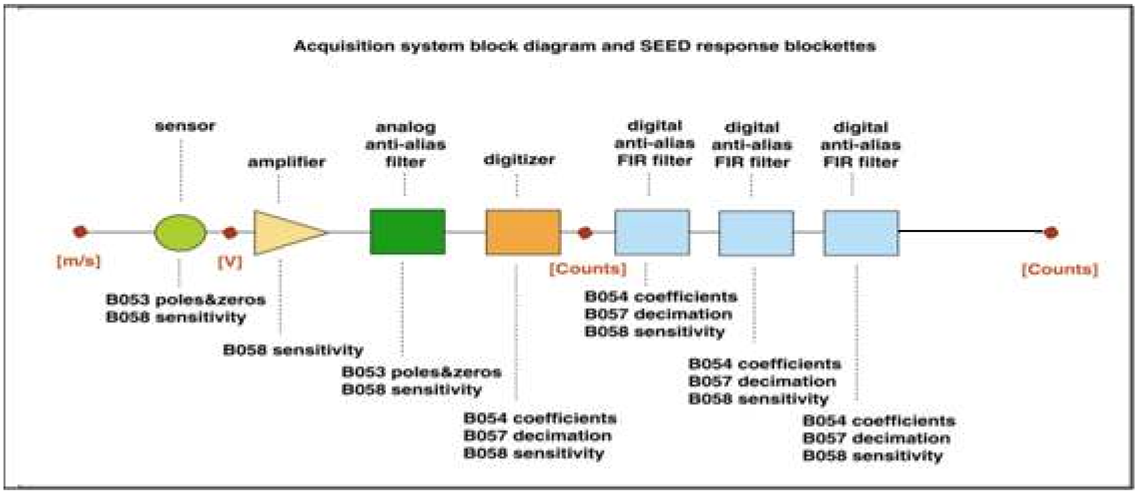

Figure 3.2 Block diagram of seismometer and digitizer in SEED

In the Figure 3.2 there is a block diagram describing how to make the dataless for the PRSN. First the sensor response it input by the poles and zeros and sensitivity. Its input is m/s and its output is Volts, then there is an amplifier which in the case of PRSN has a gain of one. In addition the green rectangle is the anti-aliasing filter which is described by poles and zeros and sensitivity. The principal function of this box is to eliminate all the frequency above 18Hz. Besides, an orange rectangle represent the number of bit that the digitizer can resolve, its output is in Counts. Finally you have three stage of Finite Impulse Response (FIR) filter which mission is to decimate and filter the data.

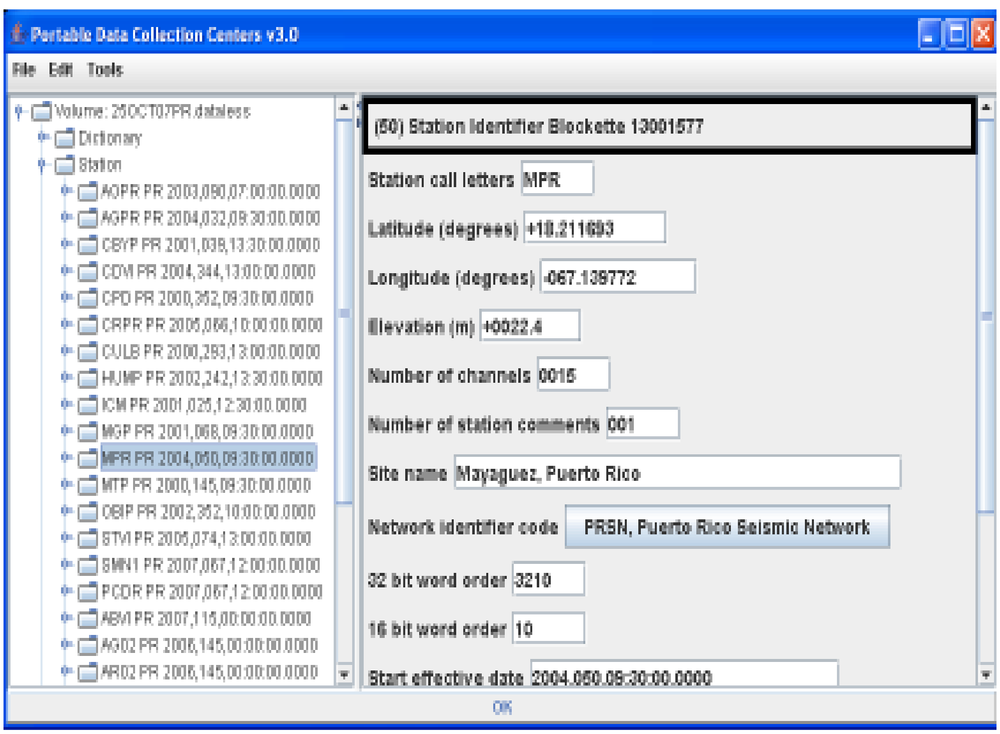

Figure 3.3 Portable Data Collection Center (PDCC)

The seismic data and their calibration file were put in a database in SEED format (see Figure 3.2 and 3.3), then the calibration values was tested via magnitude computation using the Scherbaum computer program (see figure 3.4) (Scherbaum 2002).

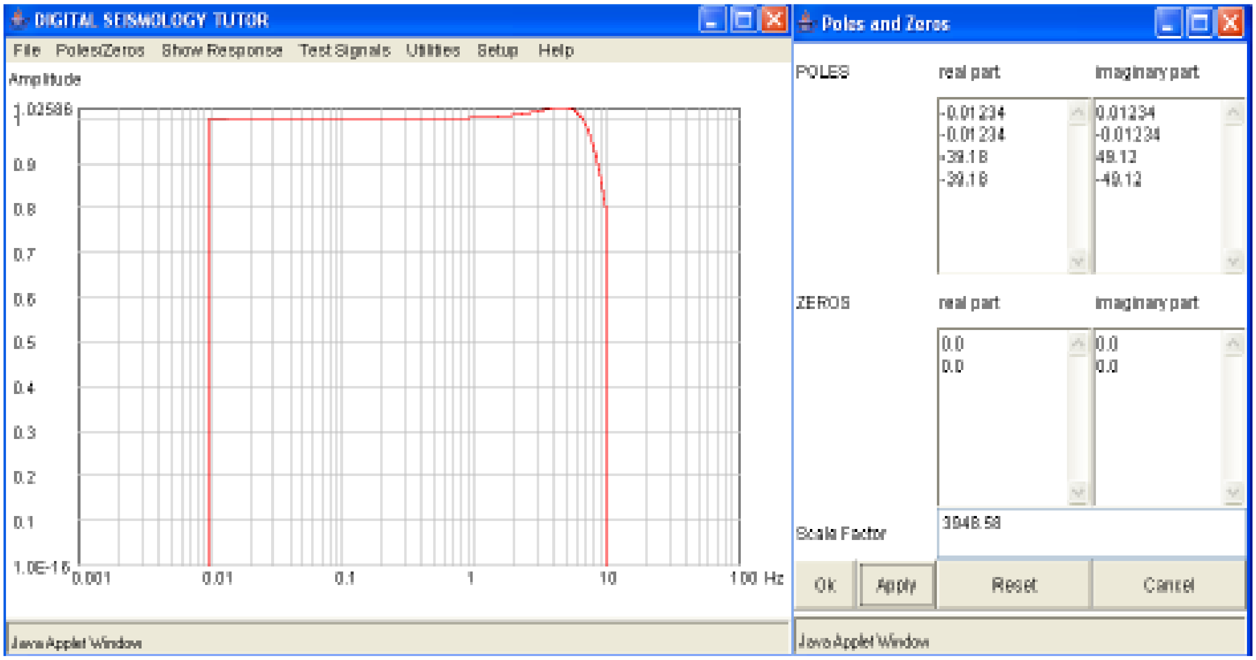


Figure 3.4 Scherbaum Program

Now the description of what was done with the three year of data.

First, the data was converted from the format of the West Coast and Alaska Tsunami Warning Center (WCATWC) to the Standard for the Exchange of Earthquake data (SEED). The program used to make this task was the atwc2mseed.exe. This program run on Windows and must be installed with the program mseedWriter.exe in the same directory.

The syntax to use the program atwc2mseed.exe was a follows:

Atwc2mseed paramsfile.d month/day/year 00:00:00 1440 intel

Where the paramsfile.d is the file that contain the seismic station that was converted to mseed. Also it includes the input and output directory.

Month/day/year is the month, day and year, respectively that is converted to mseed.

00:00:00 is the initial time for the data to be converted.

1440 is the total minutes corresponding to one day.

Intel is the platform use, the other is Sun.

To automate the process of converting data, a Disk Operating System (DOS) script was created. The name of the script is mseed.bat. The principal mission of this script is to change the day automatically in the atwc2mseed program so it is not necessary the input of the users to change any params.

Then a program called rafael.tcl is used to rename the data from Gregorian calendar to the day of the year. In this program the user specifies the input and output directory.

After that the installation of the program PQLX must be done. This program runs on a LINUX, MAC OS and SOLARIS. The README.txt file of the PQLX program must be read in order to install this program. Once the PQLX has been installed the program PQLX must be run to view the PDF. The Figure 3.5 shows some PDF calculate with the PQLX program. It is recommend to process one channel per year in order the program to run, this depend on the speed of the computer used.

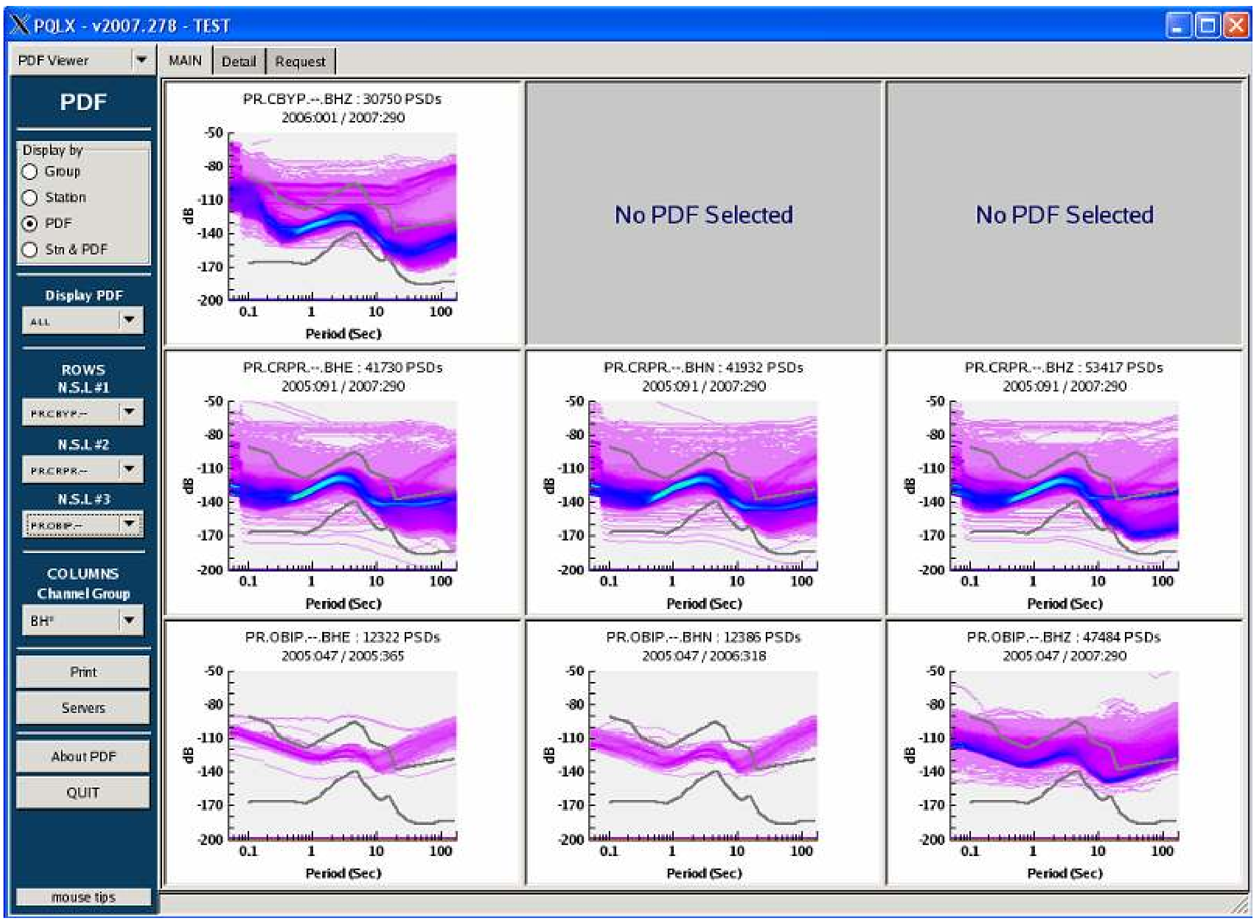


Figure 3.5 PQLX Program

In the directory where the bin file are created called $PQLXBIN there is program call exPSDhour that is used to extract the data to construct the PDF mode. The user introduces the range of the data that want to extract to get the PSD in the manner below:

./exPSDhour PRSN PR AOPR -- BHZ 2006-04-03 2006-05-03 02:00 14:00

Where PRSN is the name of the database for requesting the data, PR is the network code of the seismic station, AOPR is the station to be retrieve, -- is the location code, BHZ is the vertical channel. Also there are the date and time range in the request.

### 3.1 The PDF mode noise plot

First the script exPSDhour must be used to extract the data from the PQLX database, then the program psd_binstats is used to make basic statistic with the data. It computed the minimum, maximum, average, median, 90$^{th}$ and mode. The mode has to be chosen to make the PDF mode noise plot. The scripts pdf.m was done in Matlab to plot the PDF mode noise plot. To choose only the mode the user must use the program pdf.exe

### 3.2 The diurnal variation plot

First the script exPSDhour must be use to extract the data from the PQLX database, in this case, the user introduce the range of the data that is interested. For example:

./exPSDhour PRSN PR AOPR -- BHZ 2005-03-01 2007-09-30 00:00 00:00

This outputs all the PSD for the hour 00:00, if the user wants another hour, just have to change it.

Then the program psd_binstats is used to make basic statistic with the data. The mode has to be chosen to make the diurnal variation plot with the program pdf.exe. Moreover the user has to introduce manually in the file a column with the number of the hour. The same procedure is repeated for the hour 01 until 23.

Finally the user puts this file in a Linux machine with a Global Mapping Tool (GMT) installed to run the script diurnal.sh to make the diurnal variation plot.

### 3.3 The seasonal variation plot

First the script exPSDhour must be used to extract the data from the PQLX database, in this case, the user introduce the range of the data that is interest. For example:

./exPSDhour PRSN PR AOPR -- BHZ 2005-03-01 2007-03-30 00:00 24:00

This outputs all the PSD for the hour 00:00 to the hour 24:00 for the complete month of March, in this case, if the user wants another month, just have to change it.

Then the program psd_binstats is used to make basic statistic with the data. The mode has to be chosen to make the seasonal variation plot with the program pdf.exe. Moreover the user has to introduce manually in the file a column with the number of the month of the year. The same procedure is repeated for every month.

Finally the user put this file in a Linux machine with a Global Mapping Tool (GMT) installed to run the script seasonal.sh to make the seasonal variation plot.

### 3.4 Geographical Variation Plot

To make the geographical variation the user must create the file geo.xyz which has three columns of data, the first one is the latitude, the second is the longitude and the third is an average of the power of the PDF Mode between the frequencies of interest.

Then the user run the scripts grid.sh, after that run the program grd2xyz with the following input

grd2xyz geo.grd > geo1.xyz

Then will use the program compareLG to compare the file land.xyz with geo1.xyz and the output will be redirect to newgrid.xyz. The user need to compare land.xyz with geo.xyz to extract the area of interest with in this case is the land.

compareLG > newgrid.xyz

Then the user needs to run the scripts newgrid.sh and then the mapa.sh.

### 3.5 Frequency Response Plot.

To create the frequency response plot, the user must have to use the program JPlotResp. The user has to input the Network Code PR, the station AOPR and the channel BHZ. Also the user has to browse the filename that correspond to the station calibration. After that the user has to click on the Plot bottom to plot the AOPR frequency response. To plot another station the user has to change the name of the station and also to browse the calibration file that correspond to that seismic station. The Figure 3.6 shows a view of the input of the program JPlotResp.

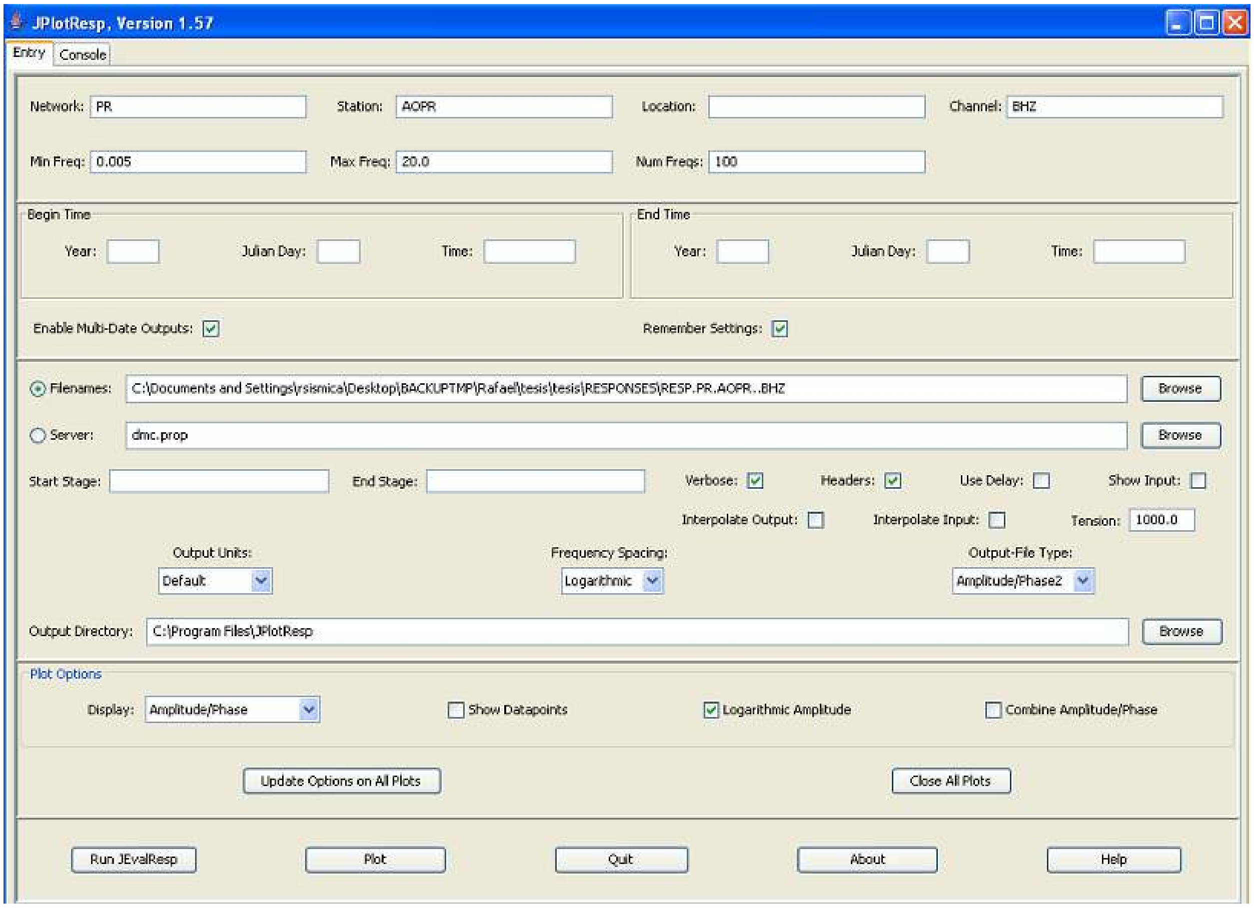

Figure 3.6 The program JPlotResp

Now the process of choosing the record length and preprocessing will be described.

### 3.6 Record Length

For our analysis, continuous time series was parsed, for each station component, into one hour ( $T_h$=3600s) finite length time series segments, overlapping by 50 percent, distributed continuously in time. Overlapping time series segments are used to reduce variance in the power spectral density (PSD) estimate (Bendat et all 1971). For this work, the seismic data, each 3600s times series segment is sampled at 40 sample per second (sps), for a total N=144000 data points.

### 3.7 Preprocessing

Preprocessing of each one hour time segment consists of several operations (Cooley et all 1965). First, to significantly improve the Fast Fourier Transform (FFT) speed ratio, by reducing the number of operations, the number of samples in the time series, N, is truncated to the next lowest power of two, $2^{17}$ leaving N=131072, thereby reducing the series length such that $T_h$=3276.8s. Second, in order to reduce the variance of the final PSD estimates, each roughly one hour time series record is divided into 13 segments, overlapping by 75 percent, where the length of the new time series record is now, $T_r = T_h$/4=819.2s, with N=32768=$2^{15}$. The sample size N is chosen based on the longest period of interest, $T_l$ (lowest frequency, $fl$). In general the record length, $T_r = N\Delta t$, is chosen such that it is 10 times the longest resolvable period, $T_l$. Given this, $T_l$= $T_r$ /10=90s. The shortest period, $T_s$ (highest frequency, $fh$) is equivalent to the Nyquist folding frequency, $fc = 1/2 \cdot t = 20Hz$= 0.05s. Third, in order to minimize long period contamination, the data is transformed to a zero mean value. Fourth, to suppress side lobe leakage in the resulting FFT, a 10 percent sine taper is applied at the ends of the time series. Tapering the time series has the effect of smoothing the FFT and minimizing the effect of the discontinuity between the beginning and the end of the time series. The time series variance reduction can be quantified by the ratio of the total power in the raw FFT to the total power in the smoothed filter (1.142857) and will be use to correct absolute power in the final spectrum (Bendat et al 1971).

The figure 3.7 show a figure simplifying the PSD/ PDF methods.

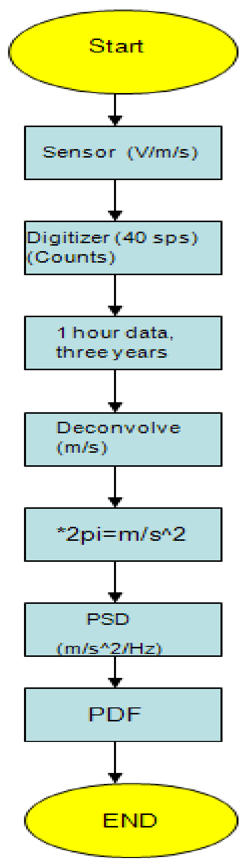


Figure 3.7 Block diagram representing the methodology

To run all this program the user needs a computer with UNIX operating system, because the program PQLX and GMT run under UNIX system, with 160 GB space in hard disk to store the seismic data and with a 2GHz processor to make the programs PQLX and GMT to work faster.

# CHAPTER 4 RESULT AND DISCUSSION

## 4.1 SJG, Cayey

This station belongs to the Global Seismic Network (GSN). This network is used to monitor earthquakes around the world. The instruments used in this station are a Q680 digitizer and a STS1 seismometer. In the Figure 4.1, there is a photo of the site were the station is installed.

Figure 4.1 SJG seismic station

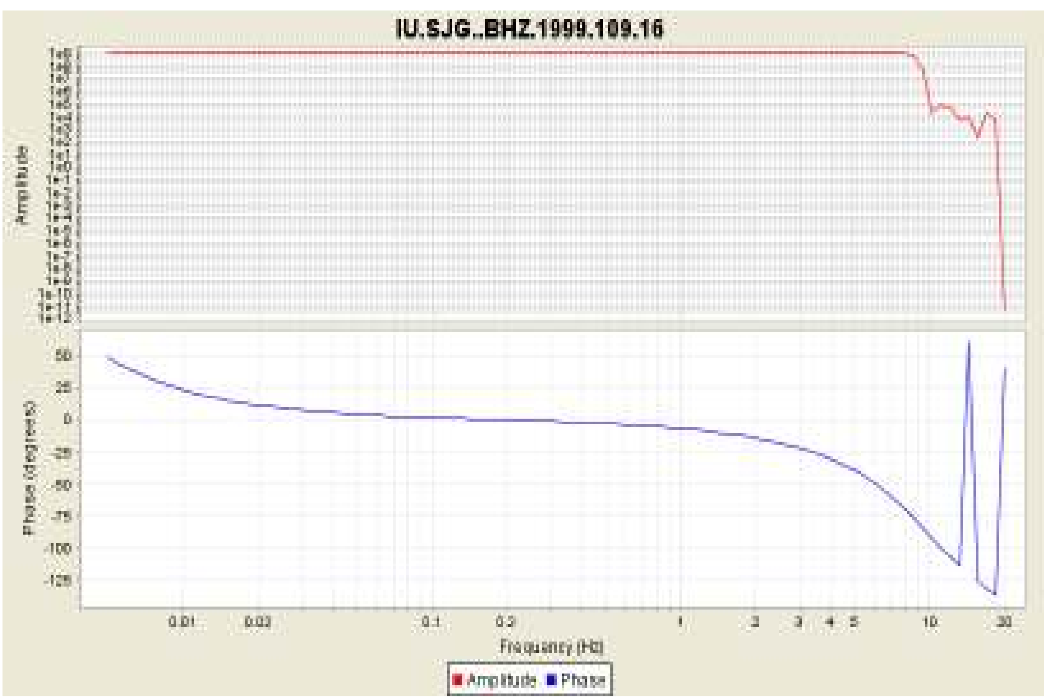


Figure 4.2 SJG Frequency response

The Figure 4.2 shows the frequency response of the SJG seismic station. This is the frequency response of the digitizer and seismometer. It has a flat response in the frequency range of (0.01Hz-10Hz). The phase change from 50 to 125 degrees in the flat response of the magnitude. This station has a flat response until 10Hz and not until 16Hz because it is sampled to 20sps and for the Nyquist frequency it only reaches to digitize 10Hz as the maximum frequency. This frequency response includes the seismometer and the digitizer used.

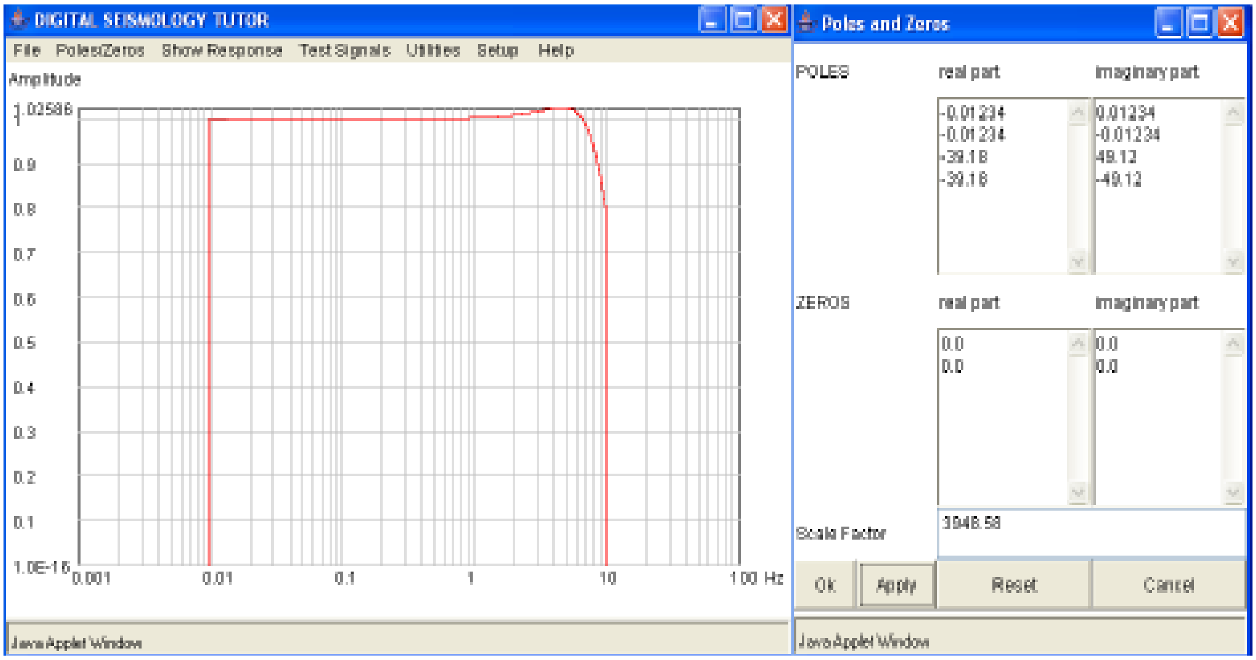

Figure 4.3 SJG Poles and Zeros

The Figure 4.3 shows the poles, zeros and scale factor for the frequency response for seismometer used in this station which is a STS1. The right of the plot shows the poles and zeros used to make the figure to the left. The figure to the left shows that it has a frequency response from 0.01Hz to 10Hz and also has an amplitude of 1.

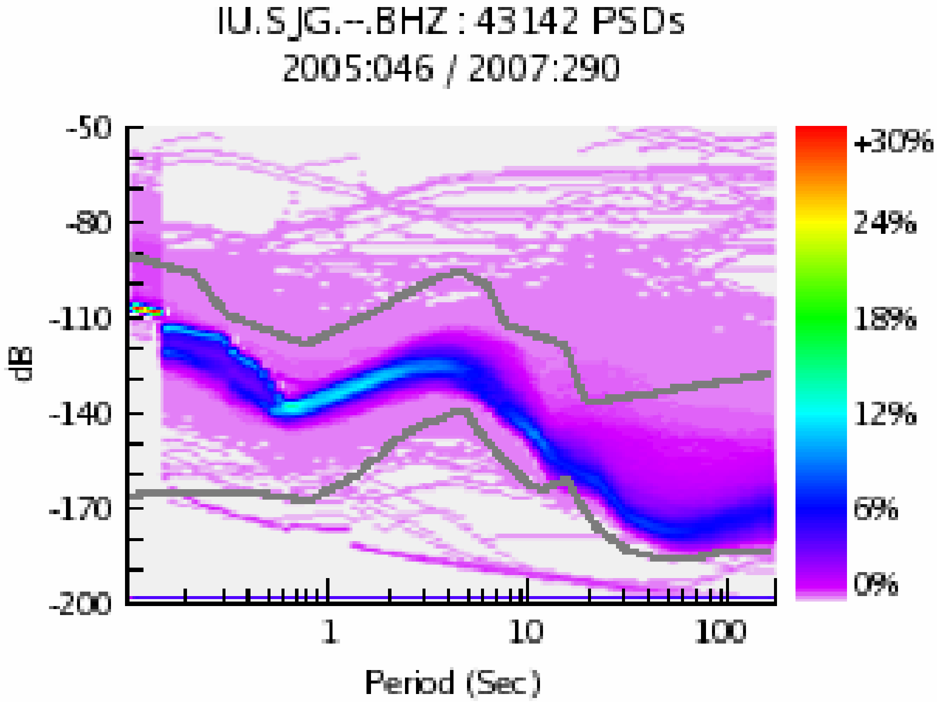


Figure 4.4 SJG PDF

The Figure 4.4 shows the SJG PDF plot. This station has a good performance because the blue color maintains between the grey curves which represents the NHNN and NLNM curves. The right of the plot shows the probability of occurrence of each PSD in a colorbar. This probability of occurrence is normalized from 0% to 30%. In the period between 0.1-0.6 sec. shows two curves due to diurnal variation in the cultural noise band. The figure 4.5 is taken from this PDF using the mode values. Finally this PDF is constructed with 43142 PSDs in the range shown.

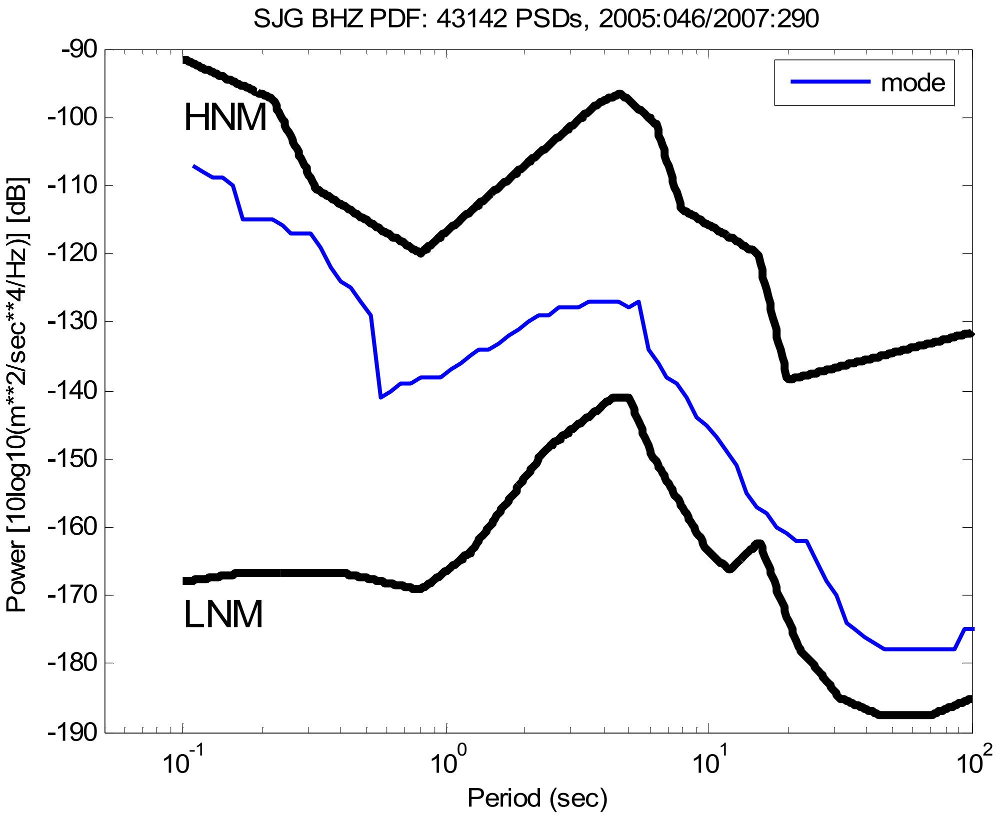


Figure 4.5 SJG PDF MODE

In the Figure 4.5 shows how the pdf mode is approximately 70dB over the LNM curve in the cultural noise band (0.1-1sec), this affects the body waves in local earthquakes. At microseisms frequency and surface wave the PDF mode is 10dB over the LNM curves.

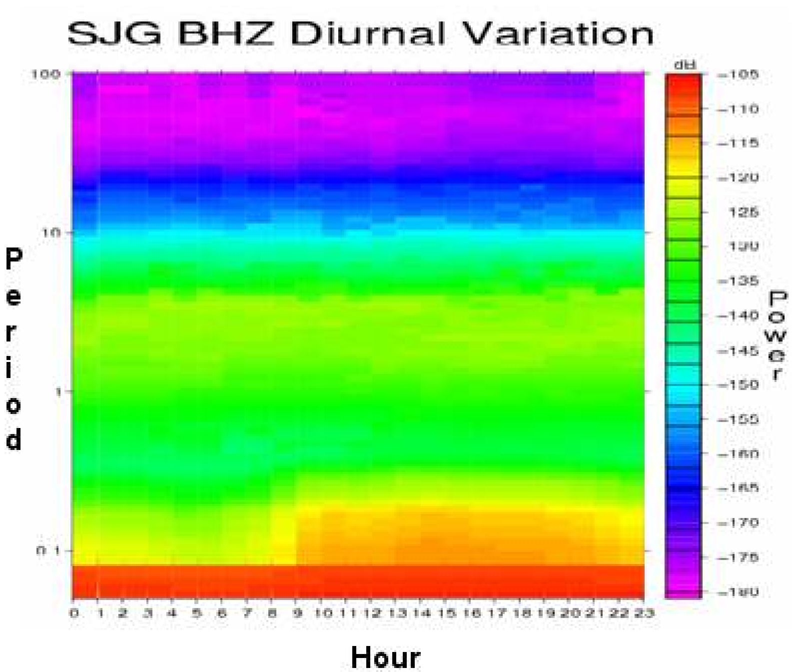


Figure 4.6 SJG Diurnal Variations

The Figure 4.6 shows the diurnal variation for the SJG seismic station. In the cultural noise period band (0.1-1sec) the power vary by 30-40dB. In the microseism band (4-16 sec.) the power vary by 25-30dB. In the long period band (20-100sec) the power vary by 10-15dB. In the period of 0.1sec., part of the cultural noise period band, it shows an increase of power during the hours of the day of 10dB due to increase of daylight working hours.

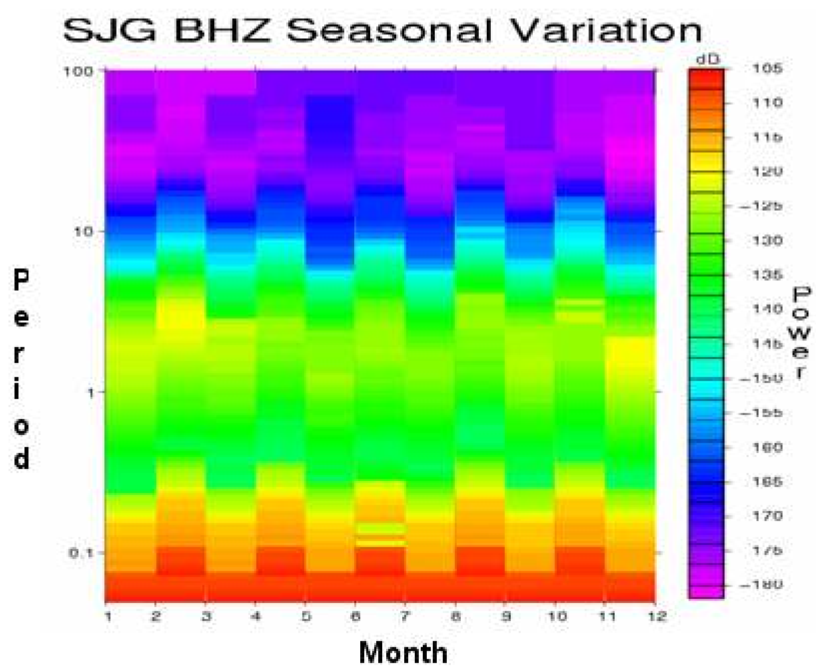


Figure 4.7 SJG Seasonal Variation

The Figure 4.7 shows the seasonal variation for the SJG seismic station. In the cultural noise period band (0.1-1sec) the power vary by 20-25dB. In the microseism band (4-16 sec.) the power vary by 25-30dB. In the long period band (20-100sec) the power vary by 5-10dB. There is not seasonal change due to the different month of the years.

In the figures of seasonal variations, the seasonal variation do not present any important pattern for this station and the others because there are not temperature and atmospheric fluctuation (Beauduin et al 1996) in the island of Puerto Rico as its shown in the Figure 4.8 and 4.9.

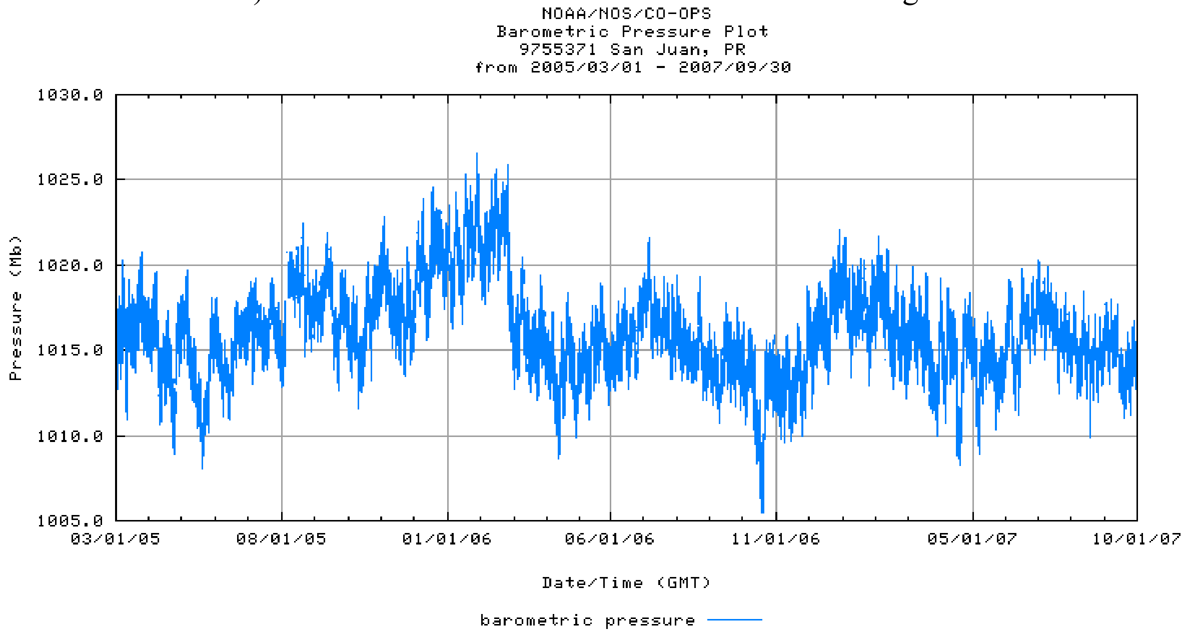

Figure 4.8 Barometric Pressure

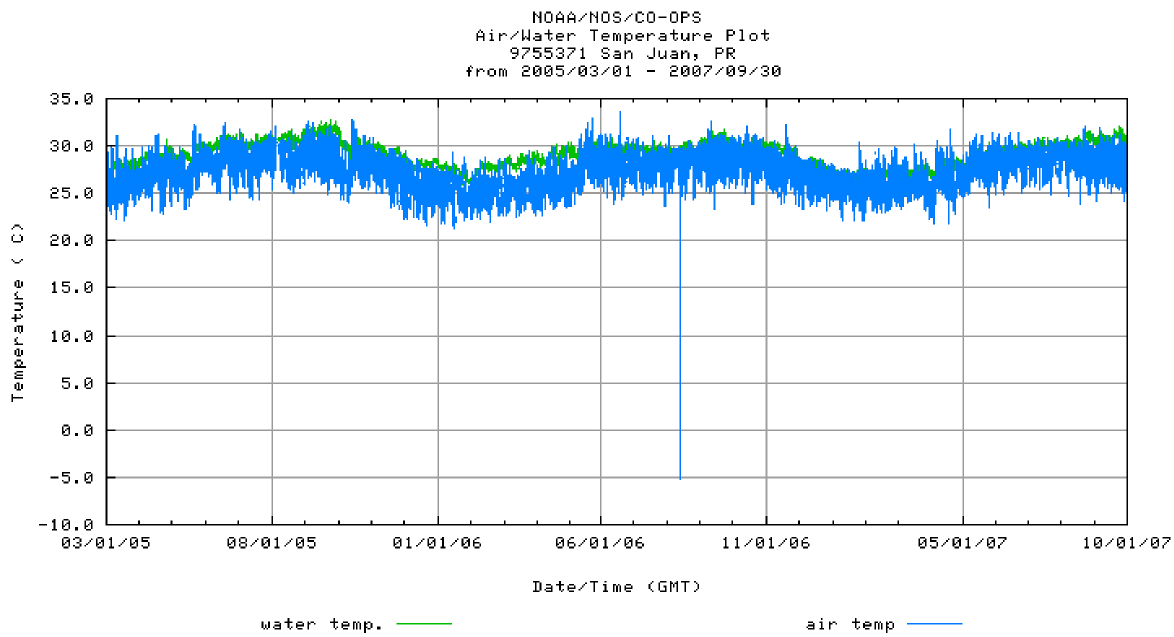

Figure 4.9 Air Temperature

## 4.2 AGPR, Aguadilla

Figure 4.10 AGPR Seismic Station

This seismic station is instrument with a Q330 digitizer and Guralp 3T Seismometer. The Figure 4.10 shows the AGRP Seismic Station.

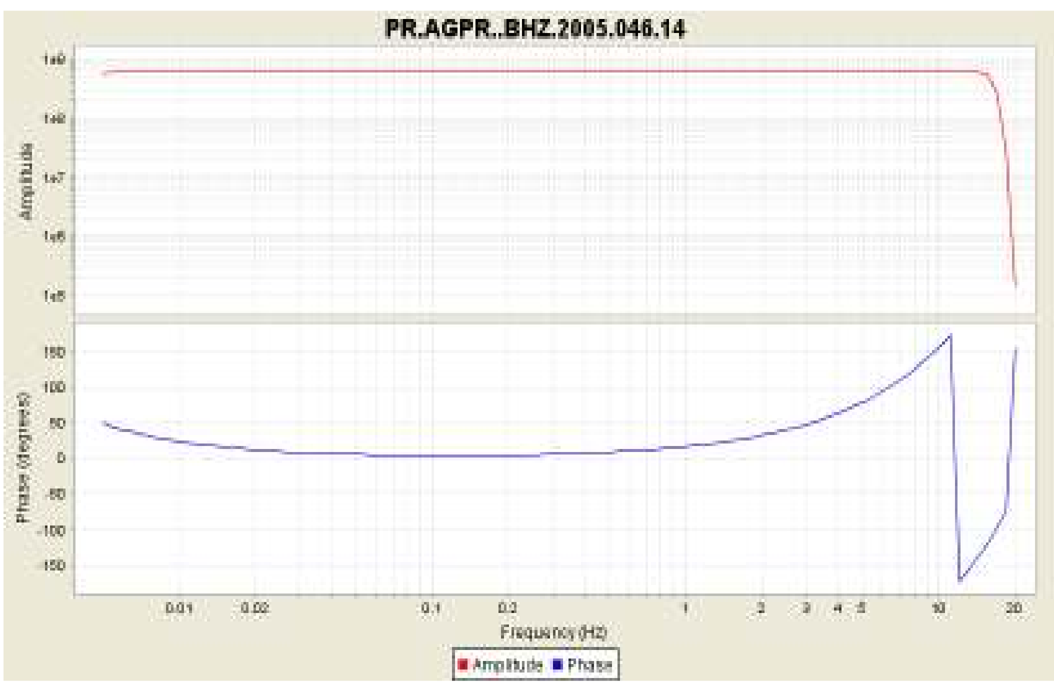


Figure 4.11 AGPR Frequency Response 1

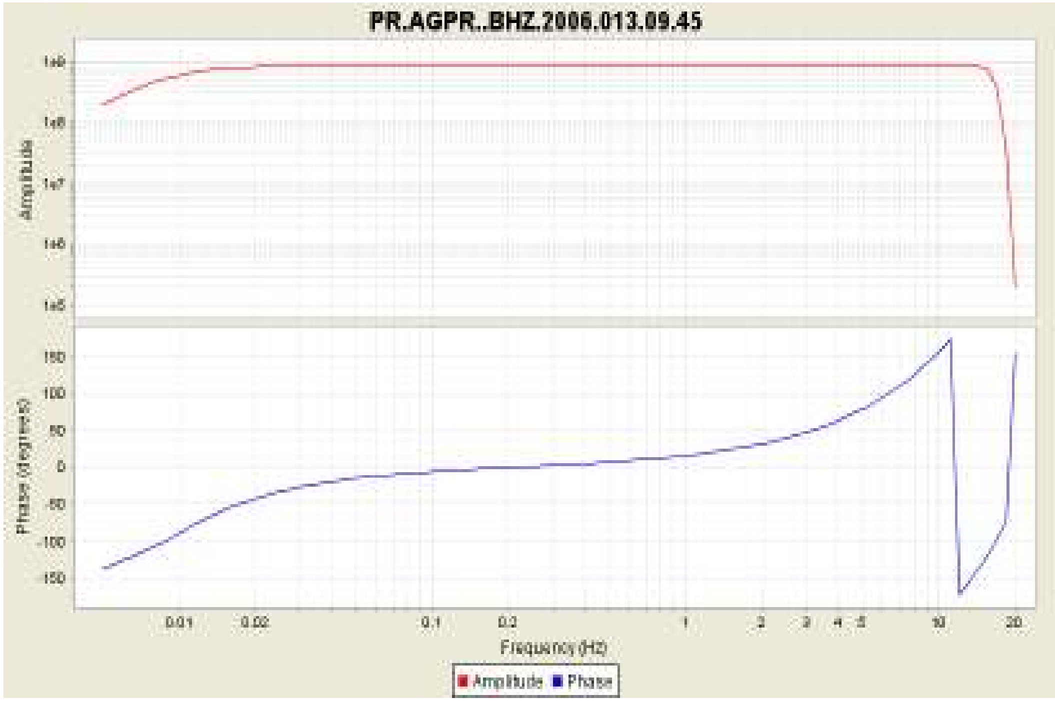

Figure 4.12 AGPR Frequency Response 2

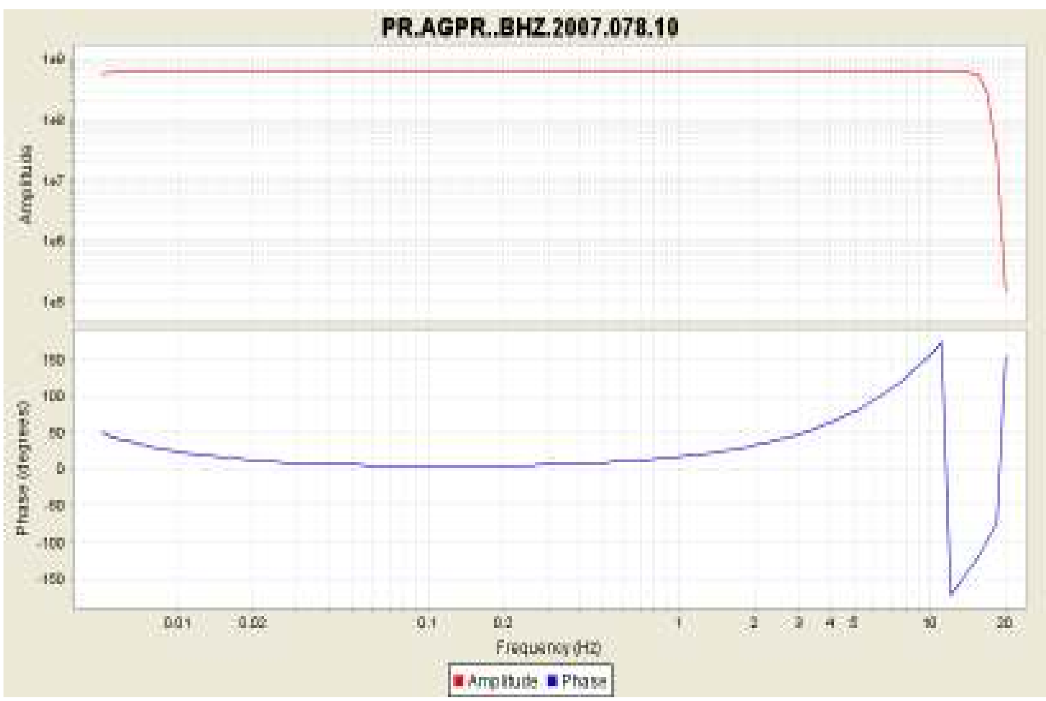

Figure 4.13 AGPR Frequency Response 3

In the Figures 4.11, 4.12 and 4.13 show the different frequency response of the station AGPR, they show a flat response for the frequency band of .01Hz until 16Hz. In Figure 4.11 and 4.13 the phase changes from 50 degree to 100 degree in the flat response of the magnitude, in the Figure 4.12 the phase change from -150 to 100 degree. There are three different frequency responses because this station used three different seismometer during the period of time that the data has been analyzed.

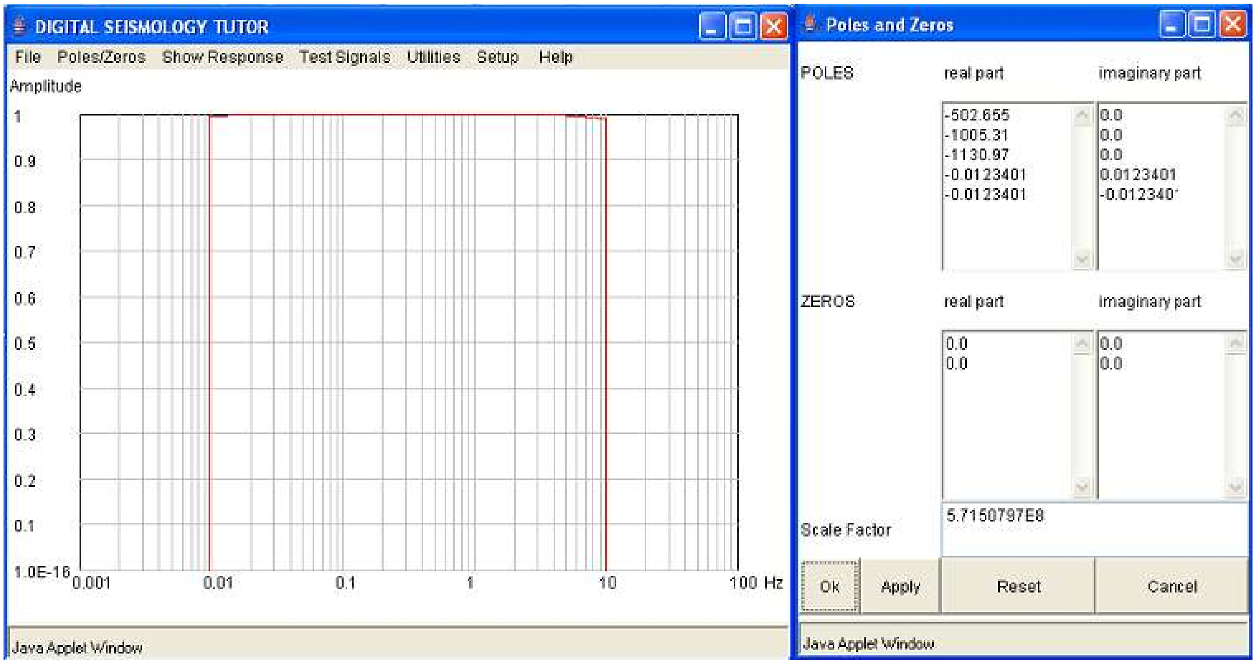


Figure 4.14 AGPR Poles and Zeros

The Figure 4.14 shows the poles, zeros and scale factor for the frequency response for seismometer used in this station which is a 100 sec. seismometer. The right of the plot presents the poles and zeros used to make the figure to the left. The figure to the left shows that it has a frequency response from 0.01Hz to 10Hz and also has an amplitude of 1

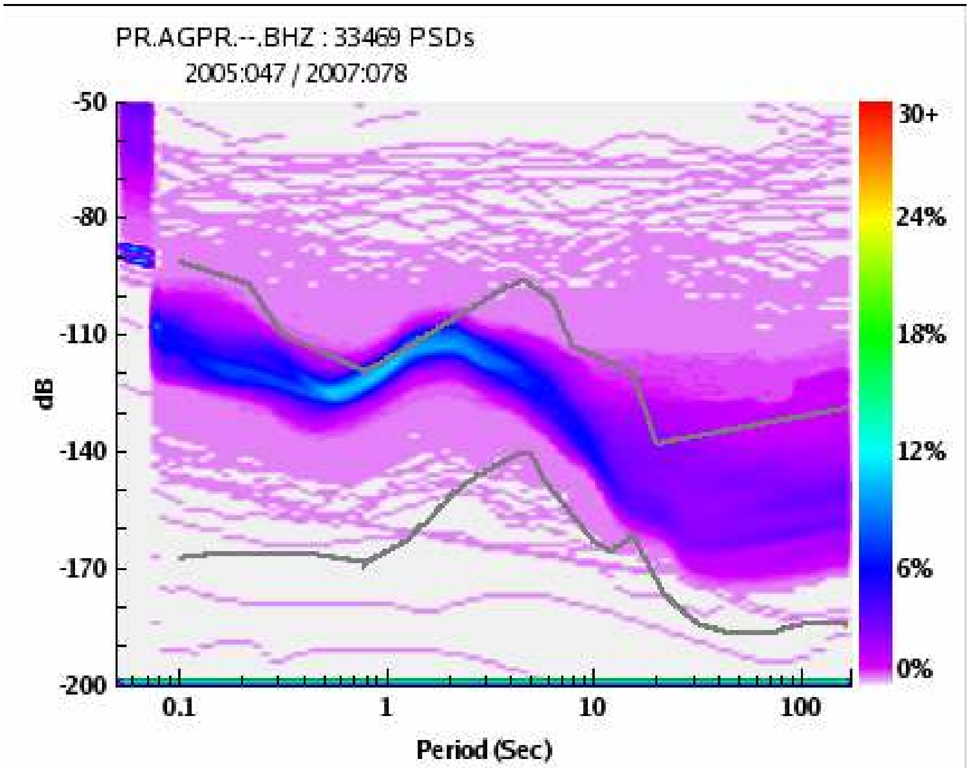

Figure 4.15 AGPR PDF

The Figure 4.15 shows the AGPR PDF plot. This station has a good performance because the blue color maintains between the grey curves which represents the NHNN and NLNM curves. The right of the plot shows the probability of occurrence of each PSD in a colorbar. This probability of occurrence is normalized from 0% to 30%. In the period between 0.1- 0.6 sec. shows two curves due to diurnal variation in the cultural noise band. The figure 4.16 is taken from this PDF using the mode values. Finally this PDF is constructed with 33469 PSDs in the range shown. The most important to note in the figure 4.15 for the 1sec period the blue line almost cross the HNM, this means that cultural noise is very strong in this station. The blue line is less intense from the period of 20 sec. until 100 sec., this is due to the change of seismometer of different frequency response as it is mentioned before in this seismic station.

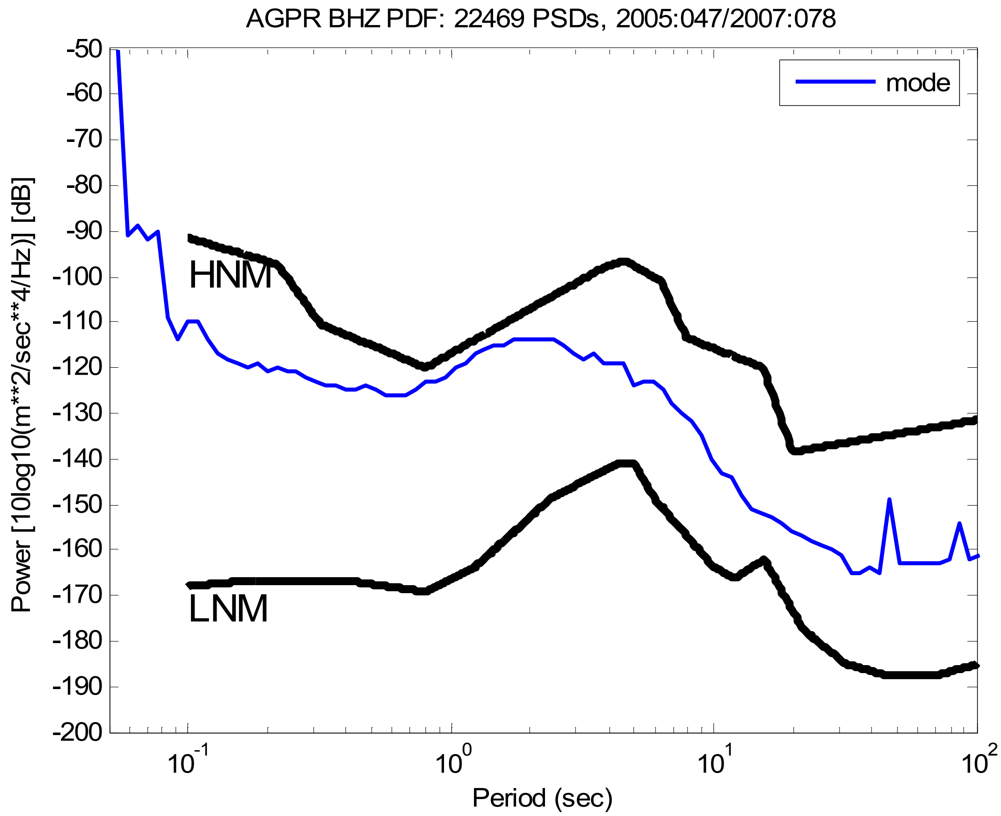


Figure 4.16 AGPR PDF MODE

The Figure 4.16 shows the AGPR PDF mode, in this picture is shown in the cultural noise band (0.1-1sec) how the noise is approximately 70dB over the LNM curve, this affect the body waves in local earthquakes. At microseisms frequency and long period there is 10dB over the LNM curves.

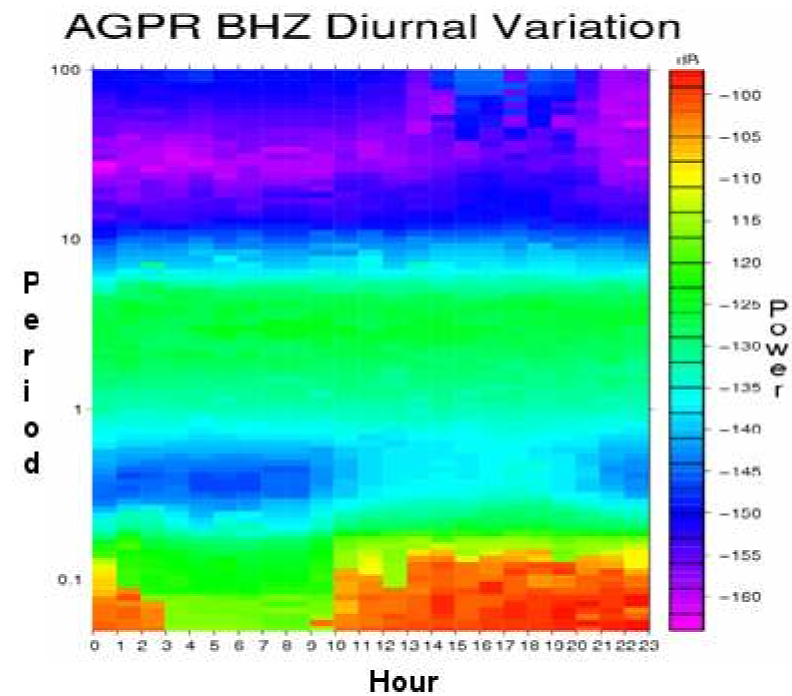

Figure 4.17 AGPR Diurnal Variation

The Figure 4.17 shows the diurnal variation for the AGPR seismic station. In the cultural noise period band (0.1-1sec) the power vary by 20-25dB. In the microseism band (4-16 sec.) the power vary by 20-25dB. In the long period band (20-100sec) the power vary by 10-15dB. In the period of 0.1sec., part of the cultural noise period band, it shows an increase of power during the hours of the day of 20dB due to increase of daylight working hours.

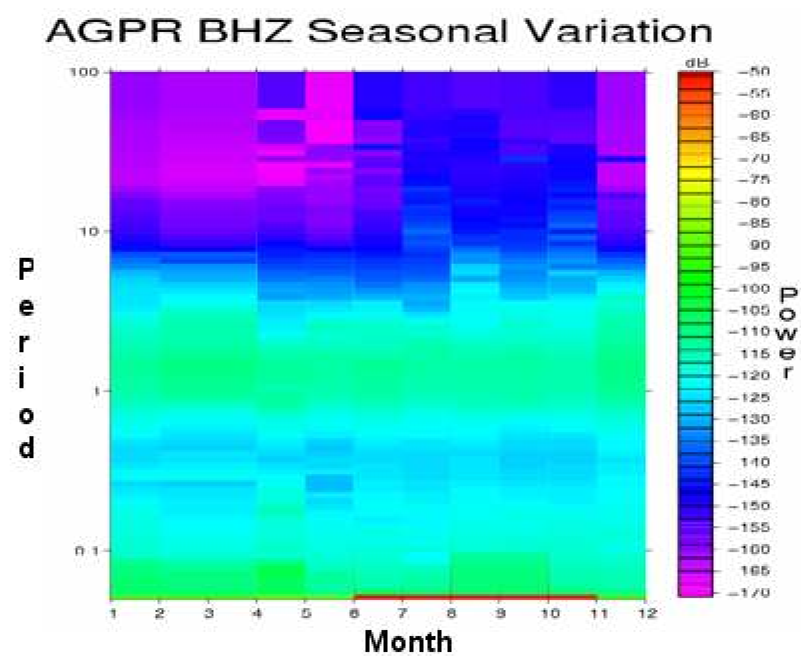

Figure 4.18 AGPR Seasonal Variation

The Figure 4.18 shows the diurnal variation for the AGPR seismic station. In the cultural noise period band (0.1-1sec) the power vary by 20-25dB. In the microseism band (4-16 sec.) the power vary by 15-20dB. In the long period band (20-100sec) the power vary by 10-15dB. There is no seasonal change due to the different month of the years.

### 4.3 AOPR, Arecibo

Figure 4.19 AOPR Seismic Station

This seismic station is instrumented with a Reftek 130 digitizer and a Guralp CMG-40T seismometer**.** The Figure 4.19 shows the places where the seismometer is installed.

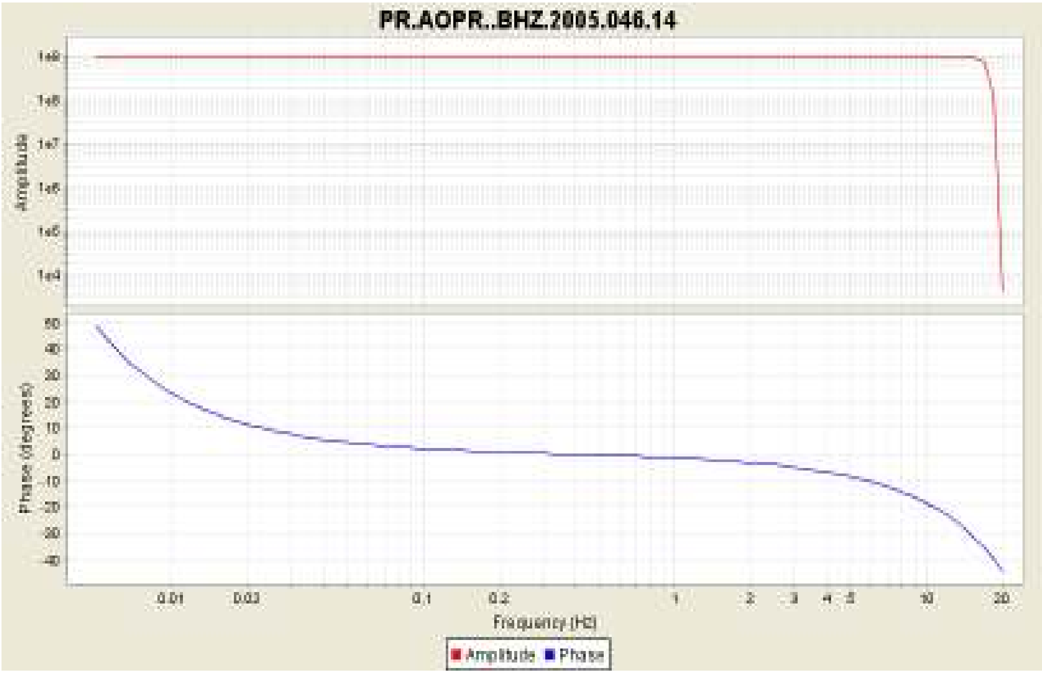

Figure 4.20 AOPR Frequency Response 1

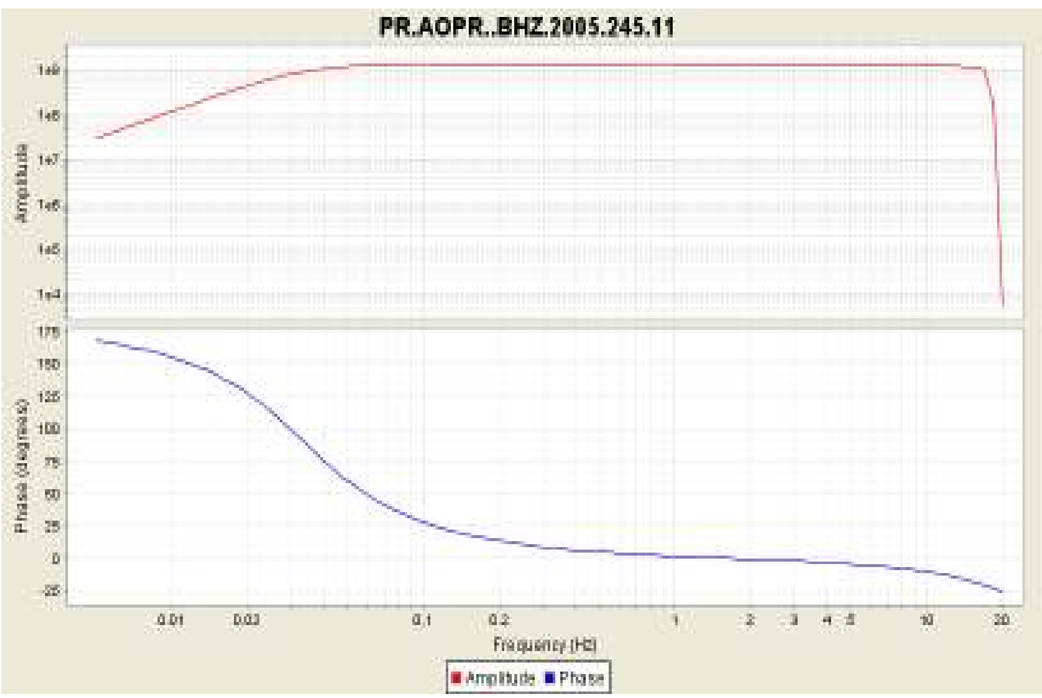

Figure 4.21 AOPR Frequency Response 2

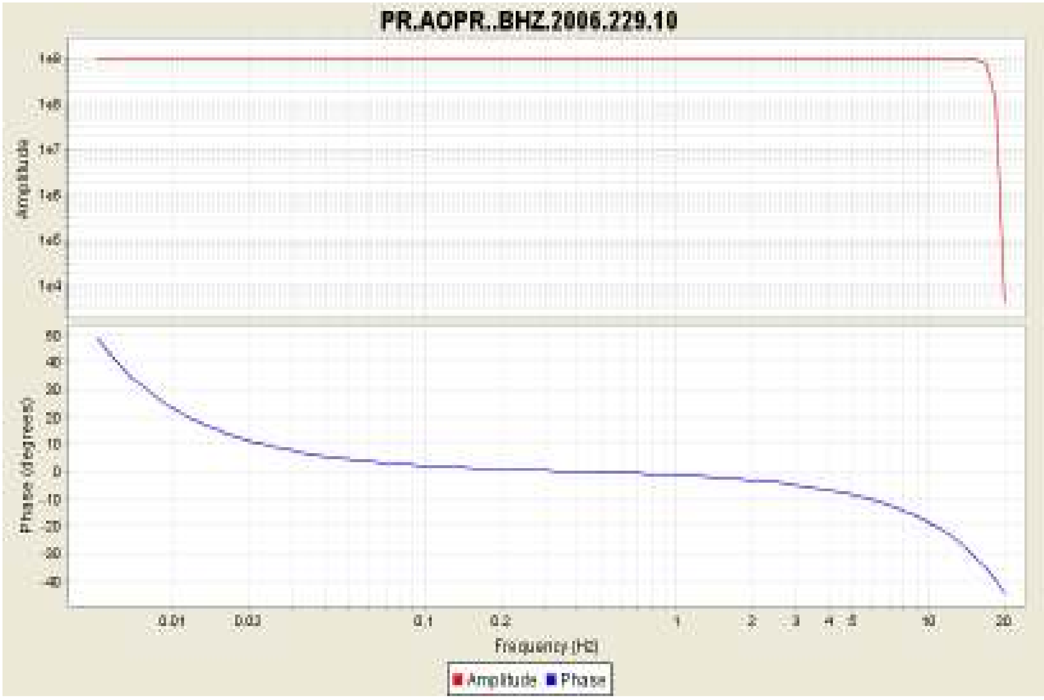

Figure 4.22 AOPR Frequency Response 3

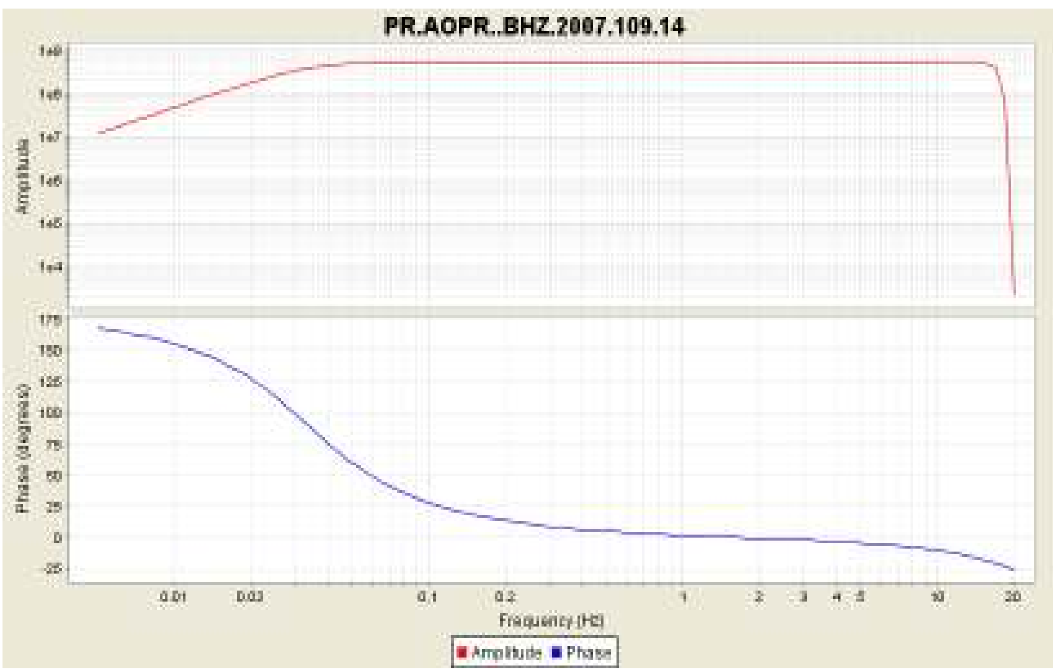

Figure 4.23 AOPR Frequency Response 4

In the Figure 4.20, 4.21 , 4.22 and 4.23 show the frequency responses for the station AOPR, these figures show different plots of frequency response because of change of the seismic sensor. In the last Figure you observe that the frequency response is not flat until frequency 0.01Hz. causing the station not to resolve PSD until that frequency, also present the change in phase from 175 to -25 degrees.

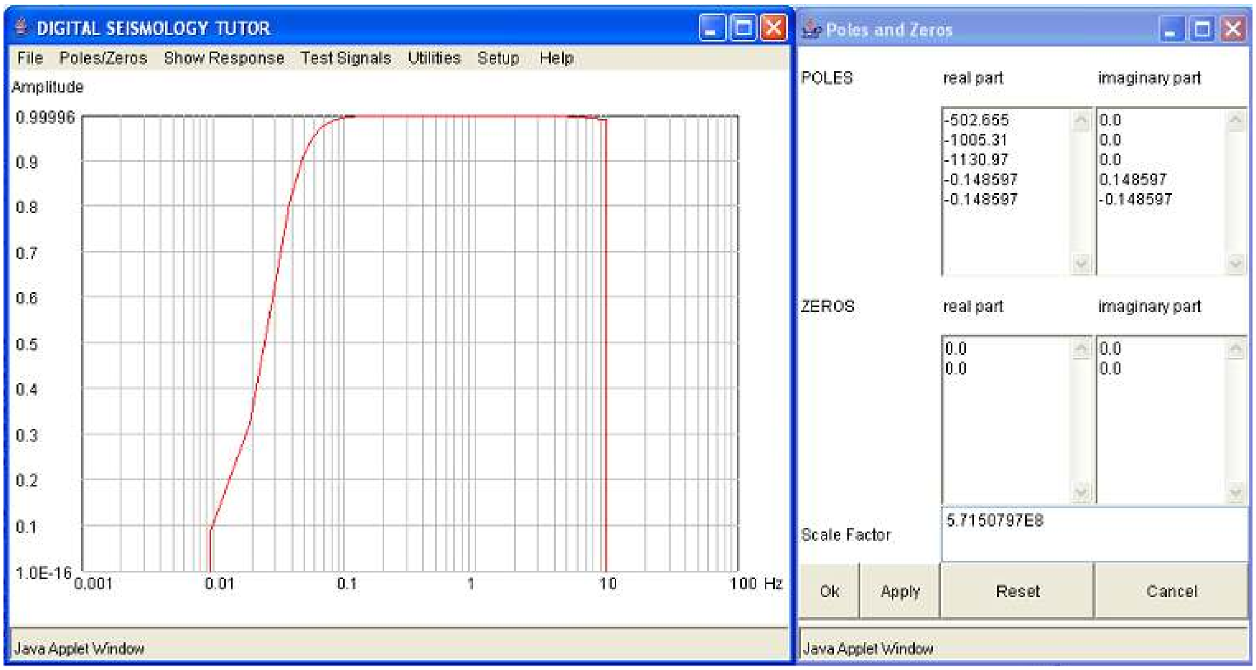

Figure 4.24 AOPR Poles and Zeros

The Figure 4.24 shows the poles, zeros and scale factor for the frequency response for seismometer used in this station which is a 20sec. The right of the plot presents the poles and zeros used to make the figure to the left. The figure to the left shows that it has a frequency response from 0.05Hz to 10Hz and also has an amplitude of 1.

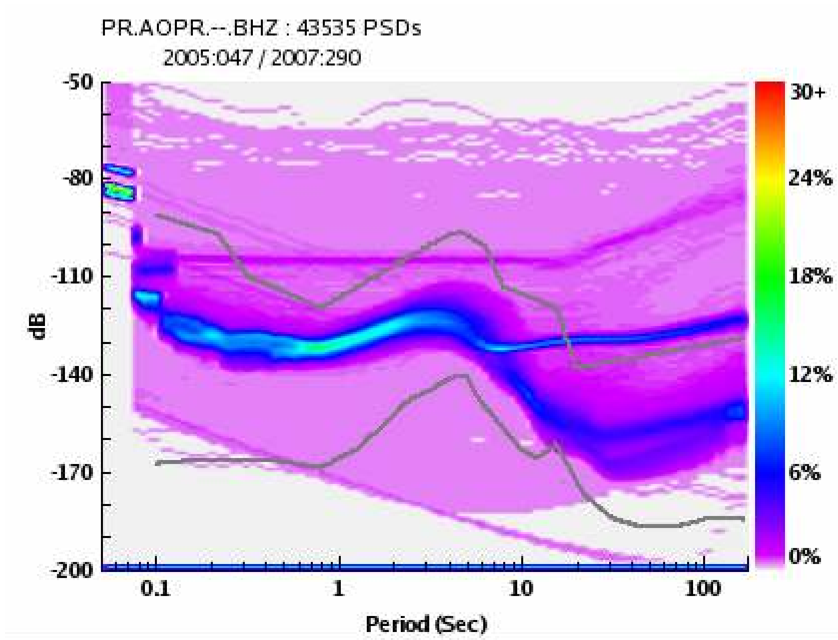

Figure 4.25 AOPR PDF

The Figure 4.25 shows the AOPR PDF plot. This station does not have a good performance because the blue color goes over the upper grey curves which represent the NHNM. The right of the plot shows the probability of occurrence of each PSD in a colorbar. This probability of occurrence is normalized from 0% to 30%. In the period of 10 sec. until 100 sec. shows two curves due to change of seismometer of different frequency response. The figure 4.26 is taken from this PDF using the mode values. Finally this PDF is constructed with 45535 PSDs in the range shown.

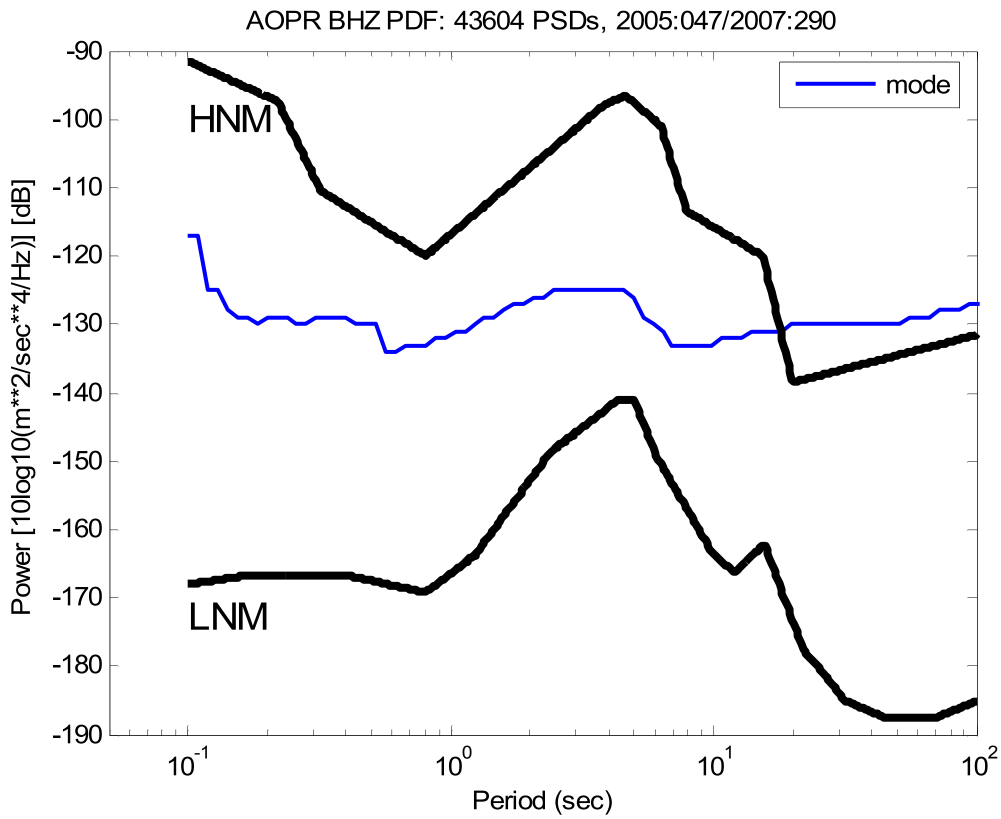

Figure 4.26 AOPR PDF Mode

In the Figure 4.26 the most important to note is that the statical mode go over the HNM for the long period due to the principal reason that the seismic sensor most of the time do not have good perfomance in the long period band (20-100sec). Also, there is an interference in this band with the cable use in the Arecibo Observatory to tense the antenna.

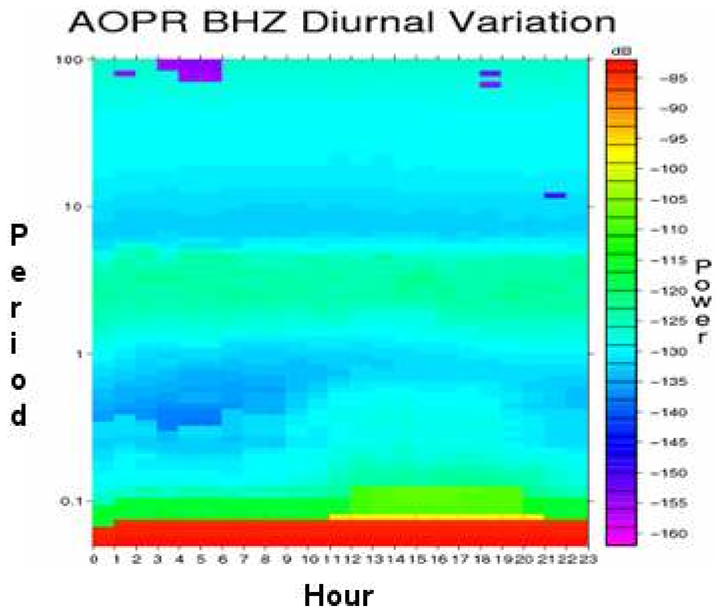

Figure 4.27 AOPR Diurnal Variation

The Figure 4.27 shows the diurnal variation for the AOPR seismic station. In the cultural noise period band (0.1-1sec) the power vary by 10-15dB. In the microseism band (4-16 sec.) the power vary by 5dB. In the long period band (20-100sec) the power do not change. In the period of 0.1sec., part of the cultural noise period band, it shows an increase of power during the hours of the day of 10dB due to increase of daylight working hours.

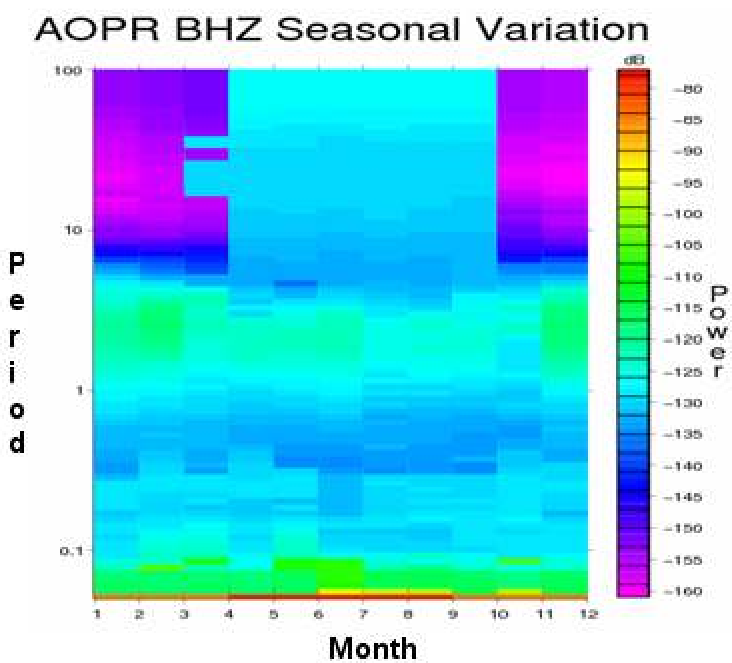

Figure 4.28 AOPR Seasonal Variation

The Figure 4.28 shows the seasonal variation for the AOPR seismic station. In the cultural noise period band (0.1-1sec) the power vary by 5-10dB. In the microseism band (4-16 sec.) the power vary by 40-45dB. In the long period band (20-100sec) the power vary by 20-30dB. There is no seasonal change due to the different month of the years.

### 4. 4 CBYP, Cubuy

Figure 4.29 CBYP Seismic Station

This seismic station is instrumented with a Reftek 7208 digitizer and a Guralp CMG-3ESP seismometer**.** The Figure 4.19 shows the places where the seismic station is installed.

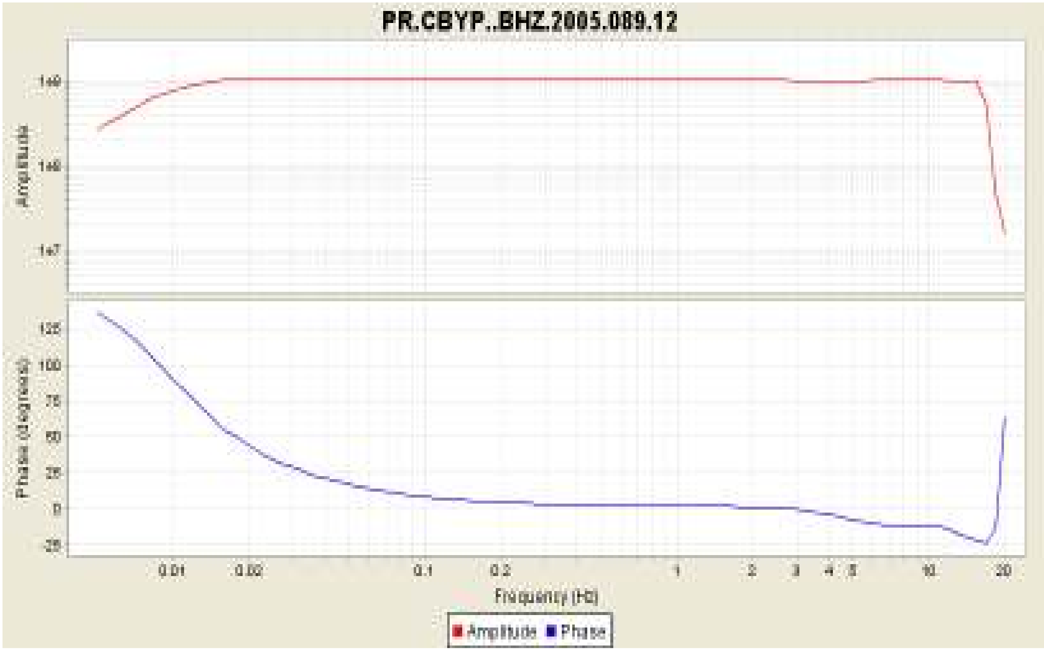

Figure 4.30 CBYP Frequency Response 1

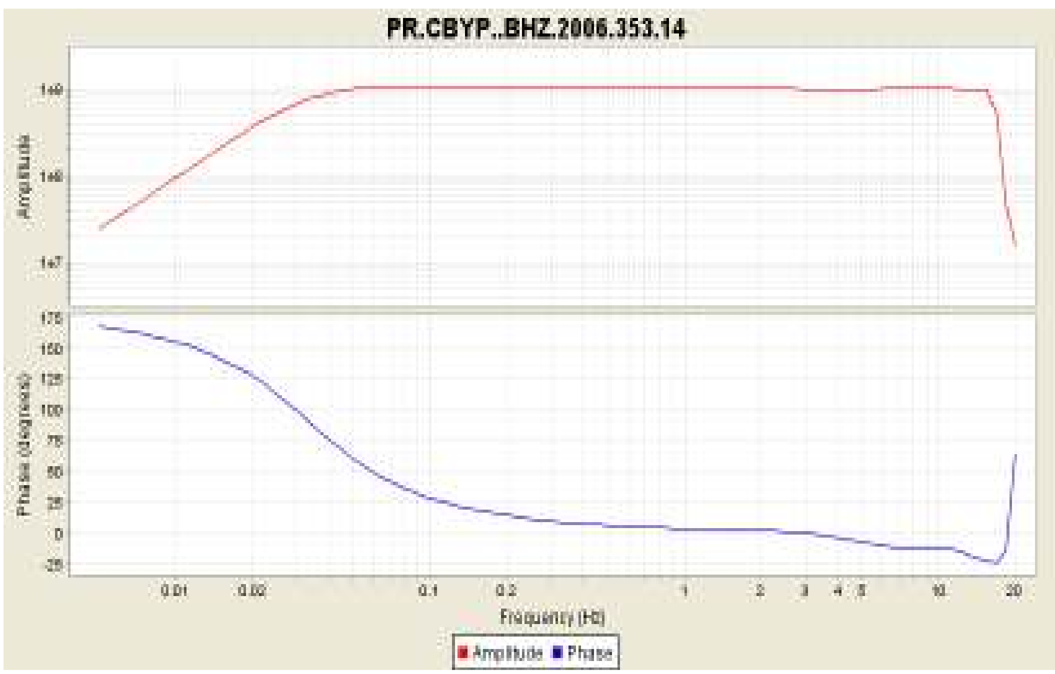

Figure 4.31 CBYP Frequency Response 2

The Figure 4.30 and 4.31 shows the different frequency responses used in the station of CBYP. The Figure 4.30 show a flat response until 0.01Hz while the figure 4.31 does not have a flat response until the frequency of 0.01Hz. In the Figure 4.30 the phase changes from 125 to -25 degrees in the flat response of the magnitude. In the Figure 4.31 the phase changes 175 to -25 degrees. There are two frequency response plot for this station because is used to have a 100 sec seismometer then it was change to a 30 sec. sensor.

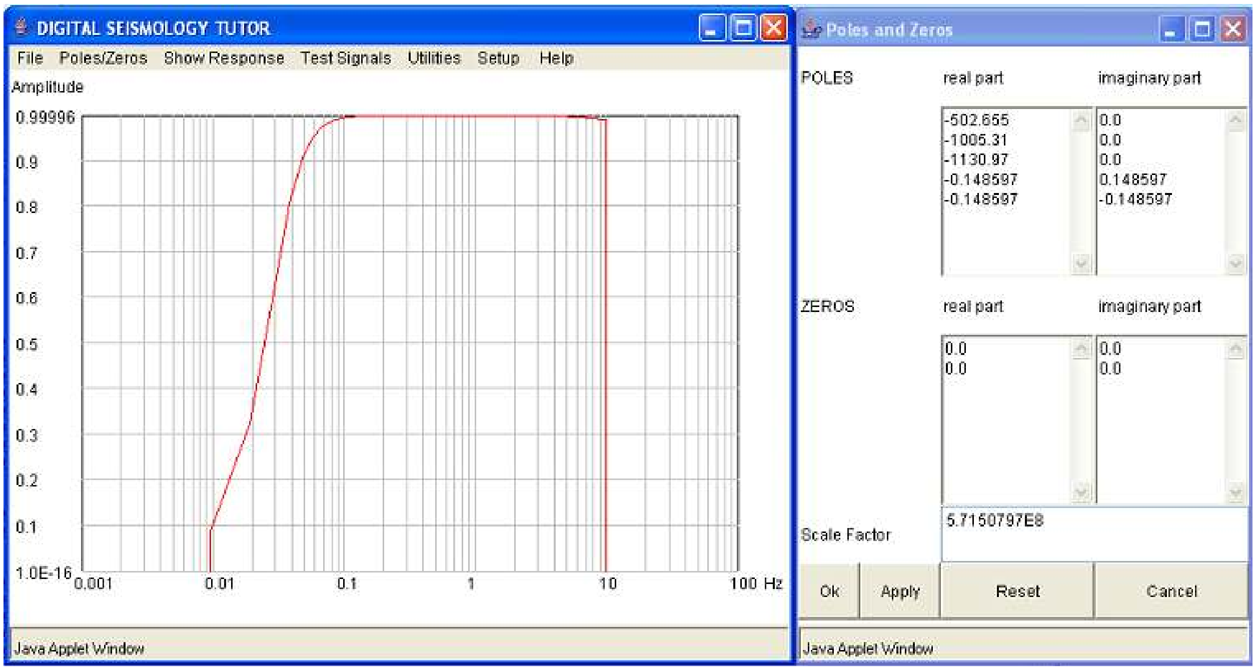

Figure 4.32 CBYP Poles and Zeros

The Figure 4.32 shows the poles, zeros and scale factor for the frequency response for seismometer used in this station which a 20 sec. The right of the plot presents the poles and zeros used to make the figure to the left. The figure to the left shows that it has a frequency response from 0.05Hz to 10Hz and also has an amplitude of 1

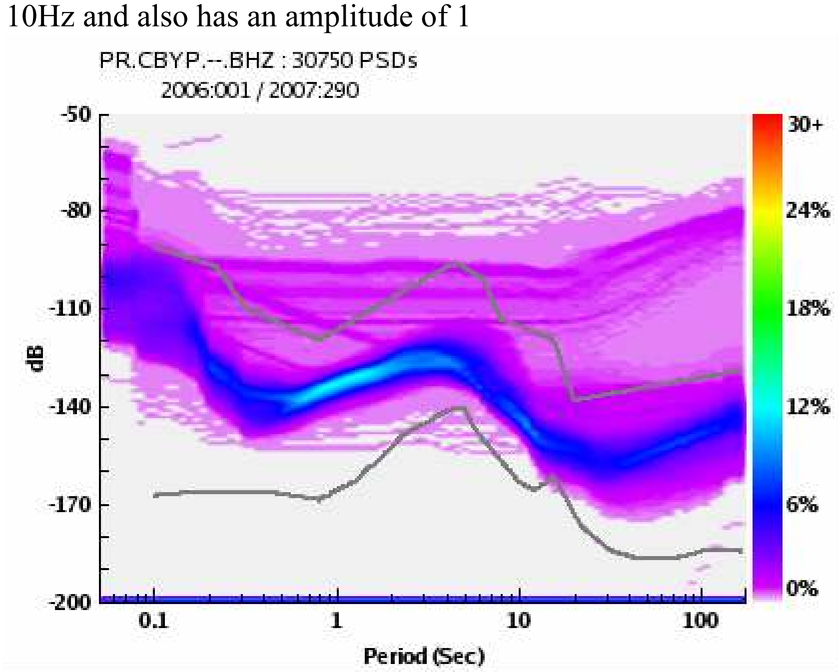

Figure 4.33 CBYP PDF

The Figure 4.33 shows the CBP PDF plot. This station has a good performance because the blue color maintains between the grey curves which represents the NHNN and NLNM curves. The right of the plot shows the probability of occurrence of each PSD in a colorbar. This probability of occurrence is normalized from 0% to 30%. The figure 4.34 is taken from this PDF using the mode values. Finally this PDF is constructed with 30750 PSDs in the range shown.

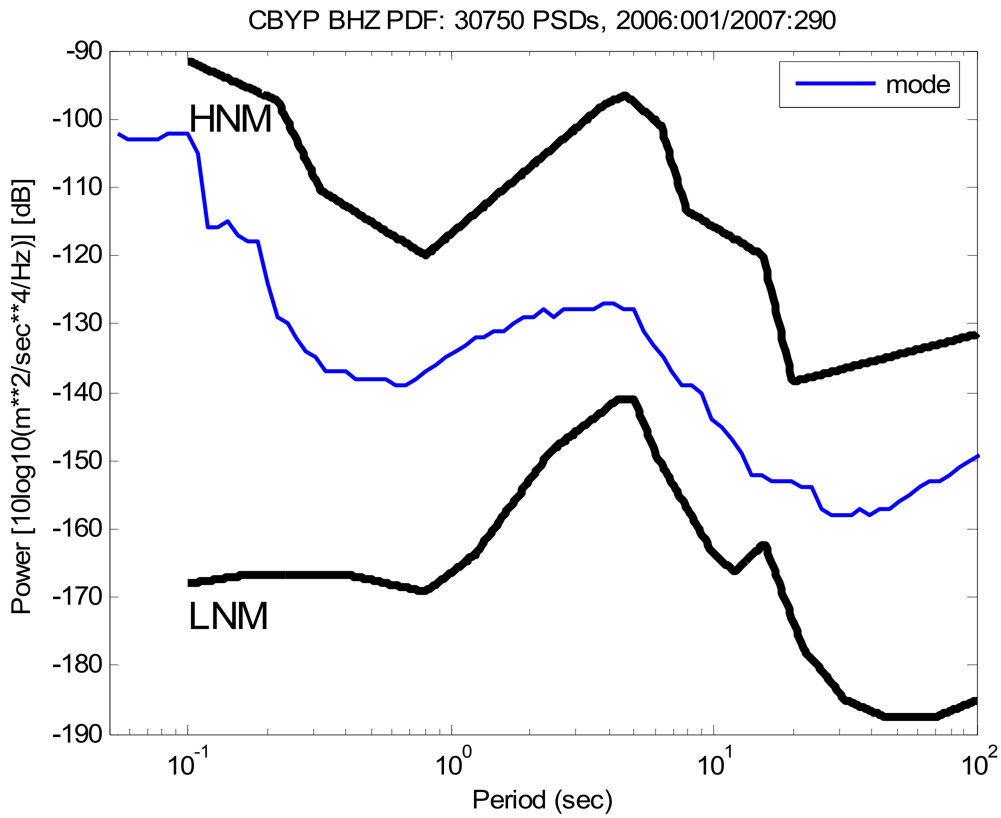

Figure 4.34 CBYP PDF Mode

In the Figure 4.29 the station has 50dB over the LNM curve in the 0.1-0.2sec. In the microseisms band (4-16 sec.) the blue line is 10dB over the LNM curve, finally at the long period band (20-100 sec.) begin with 20dB over the LNM curve and finish with 30dB over this curve.

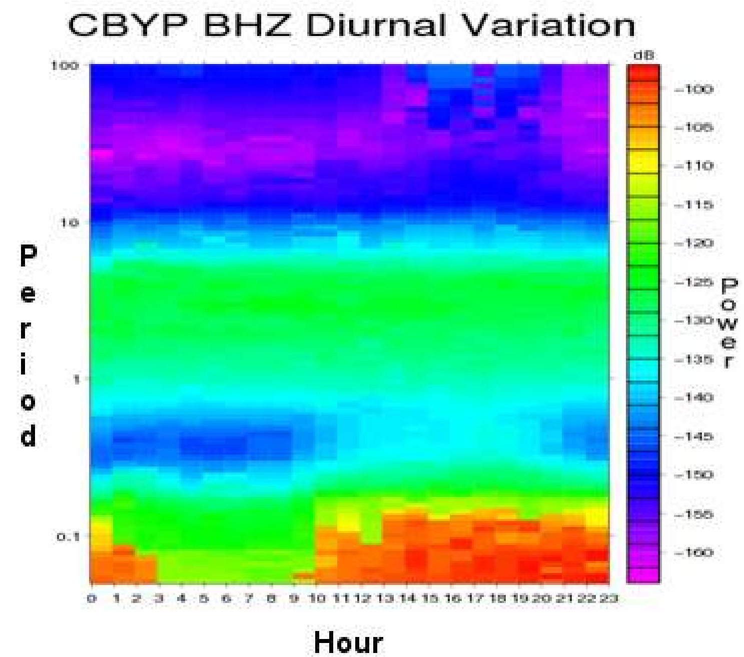

Figure 4.35 CBYP Diurnal Variation

The Figure 4.35 shows the diurnal variation for the CBYP seismic station. In the cultural noise period band (0.1-1sec) the power vary by 20-25dB. In the microseism band (4-16 sec.) the power vary by 20-25dB. In the long period band (20-100sec) the power vary by 10-15dB. In the period of 0.1sec., part of the cultural noise period band, it shows an increase of power during the hours of the day of 20dB due to increase of daylight working hours.

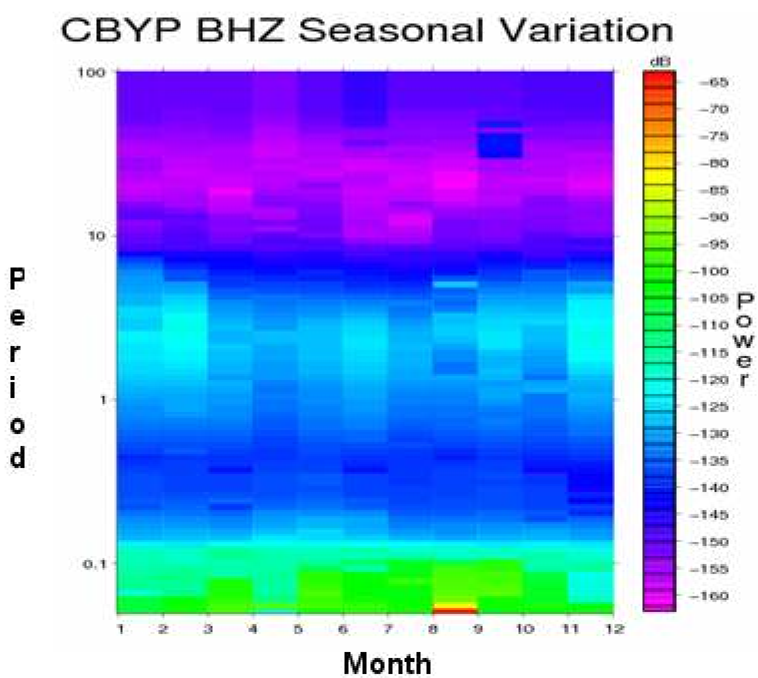

Figure 4.36 CBYP Seasonal Variation

The Figure 4.36 shows the seasonal variation for the CBYP seismic station. In the cultural noise period band (0.1-1sec) the power vary by 20-25dB. In the microseism band (4-16 sec.) the power vary by 25-30dB. In the long period band (20-100sec) the power vary by 5-10dB. There is no seasonal change due to the different month of the years.

### 4.5 CPD, Yabucoa

Figure 4.37 CPD Seismic Station

This seismic station is instrumented with a Reftek 7208 digitizer and a Guralp CMG-40T seismometer**.** The Figure 4.37 shows the places where the seismic station is installed.

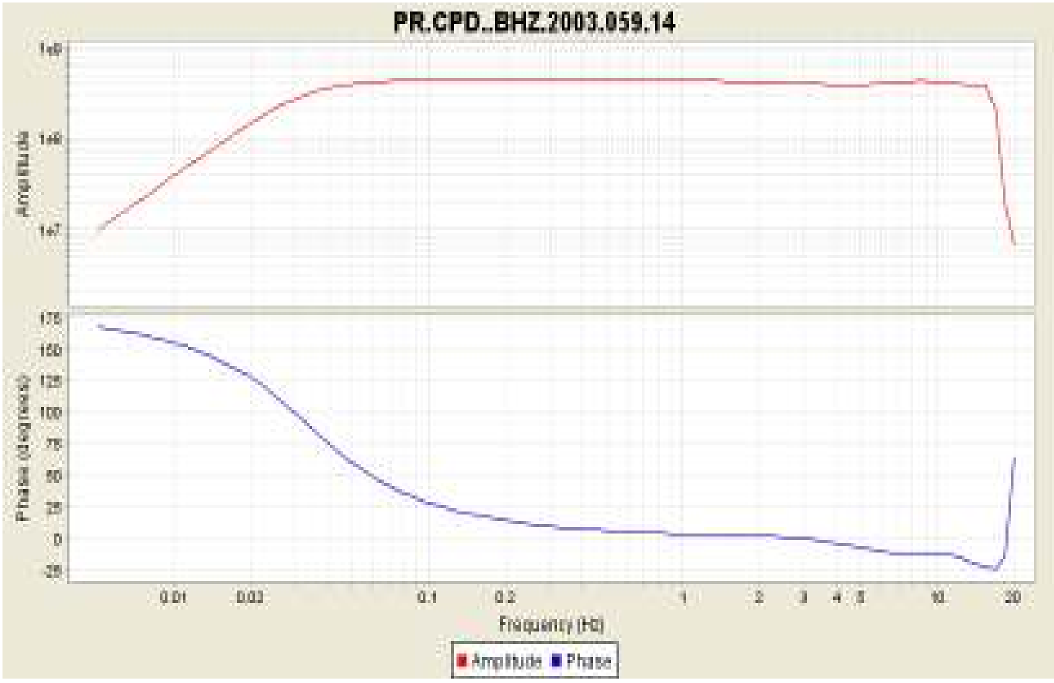


Figure 4.38 CPD Frequency Response 1


Figure 4.39 CPD Frequency Response 2

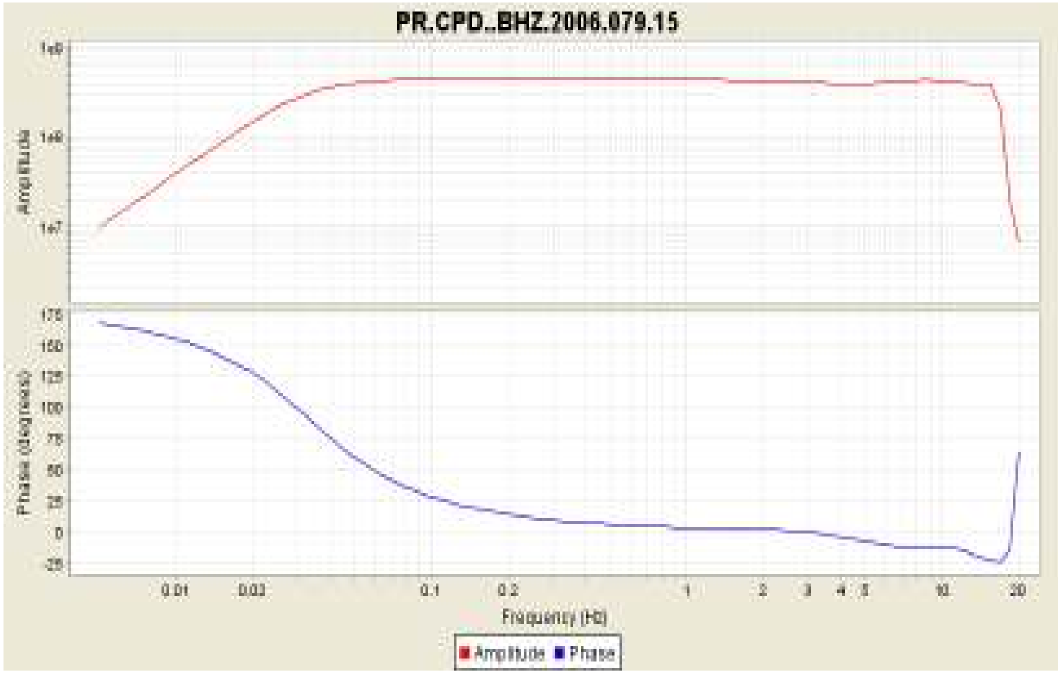


Figure 4.40 CPD Frequency Response 3

In the Figure 4.38, 4.39 and 4.40 is clear that the seismic station do not have a flat response until the frequency of 0.01Hz. The change in phases is from 175 to -25 degrees for the three seismometer used. There are three figures because changing of the seismometer.


Figure 4.41 CPD Poles and Zeros

The Figure 4.41 shows the poles, zeros and scale factor for the frequency response for seismometer used in this station which is a 20 sec. The right of the plot presents the poles and zeros used to make the figure to the left. The figure to the left shows that it has a frequency response from 0.05Hz to 10Hz and also has an amplitude of 1.

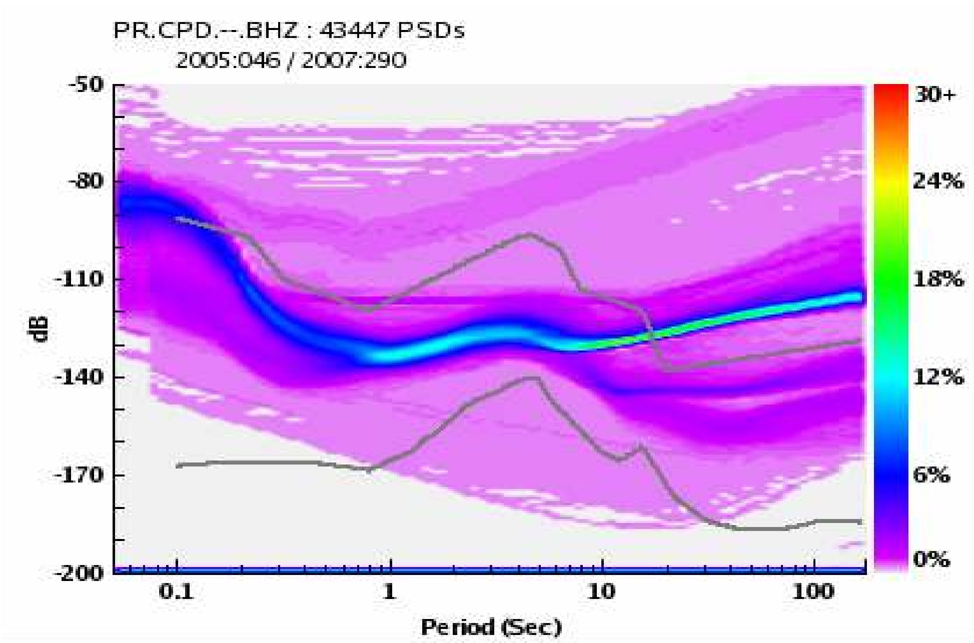


Figure 4.42 CPD PDF

The Figure 4.42 shows the CPD PDF plot. This station does not have a good performance because the blue color goes over the upper grey curve which represents the NHNM. The right of the plot shows the probability of occurrence of each PSD in a colorbar. This probability of occurrence is normalized from 0% to 30%. The figure 4.5 is taken from this PDF using the mode values. Finally this PDF is constructed with 43447 PSDs in the range shown.

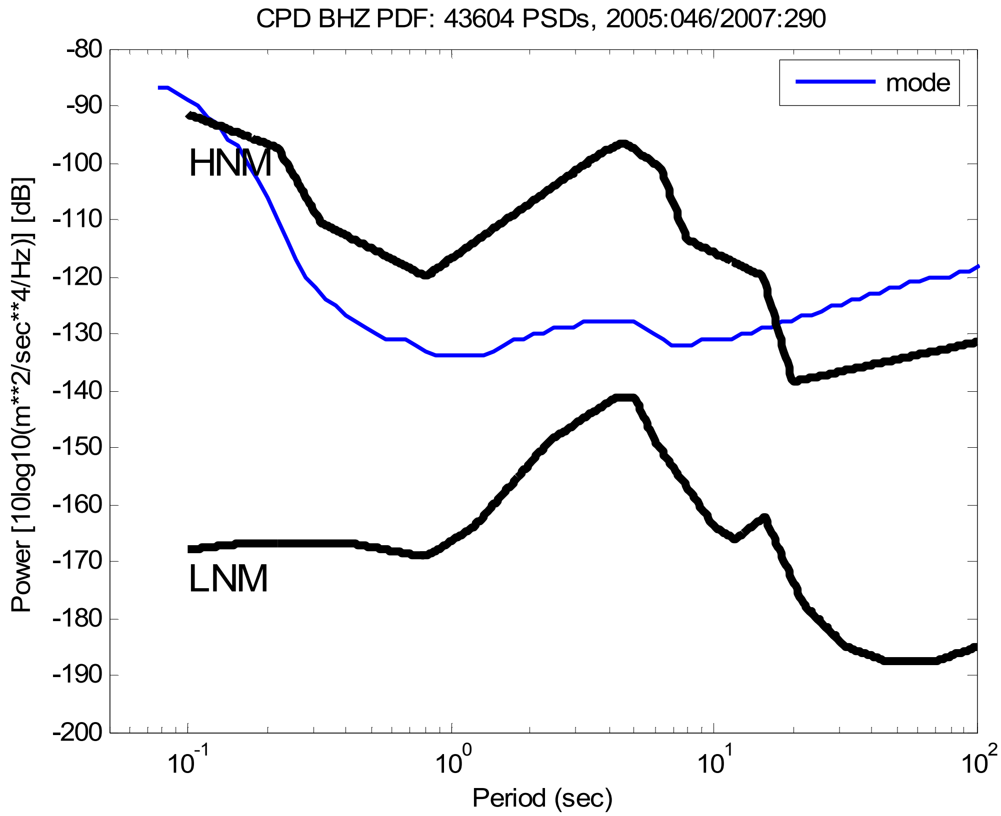

Figure 4.43 CPD PDF Mode

The Figure 4.43 shows the CPD PDF Mode. The seismic station has 70dB over the LNM curve in the 0.1-0.2sec and reach to cross the HNM curve, this affect the signal of local eartqhuakes. In the microseism band (4-16 sec.) the noise level is 15 dB over the LNM curves in the double frequency peak (4-8sec) and 30 dB over the LNM curve in the single frequency peak band (10-16sec). For the long period band it goes 10 dB over  the HNM curve.

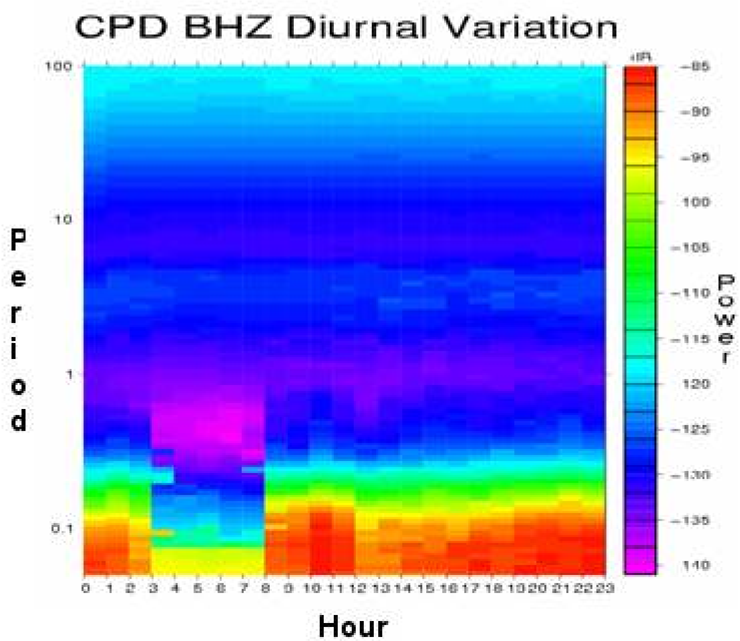

Figure 4.44 CPD Diurnal Variation

The Figure 4.44 shows the diurnal variation for the CPD seismic station. In the cultural noise period band (0.1-1sec) the power vary by 40-50dB. In the microseism band (4-16 sec.) the power vary by 10-15dB. In the long period band (20-100sec) the power vary by 10-15dB. In the period of 0.1sec., part of the cultural noise period band, it shows an increase of power during the hours of the day of 45dB due to increase of daylight working hours.

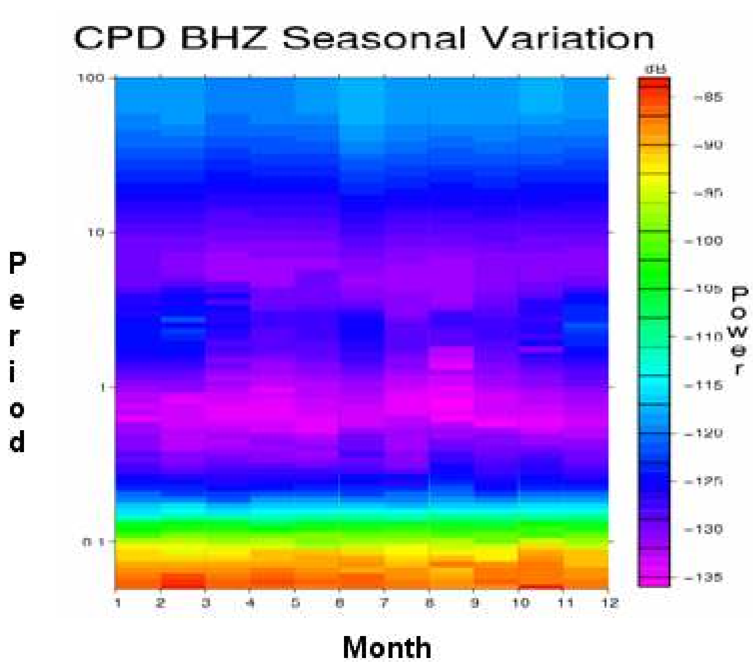

Figure 4.45 CPD Seasonal Variation

The Figure 4.45 shows the seasonal variation for the CPD seismic station. In the cultural noise period band (0.1-1sec) the power vary by 30-35dB. In the microseism band (4-16 sec.) the power vary by 5-10dB. In the long period band (20-100sec) the power vary by 5-10dB. There is not seasonal change due to the different month of the years.

**4. 6 CRPR, Cabo Rojo**

Figure 4.46 CRPR Seismic Station

This seismic station is instrumented with a Reftek 7208 digitizer and a Guralp CMG-40T seismometer**.** The Figure 4.46 shows the place where the seismic station is installed.

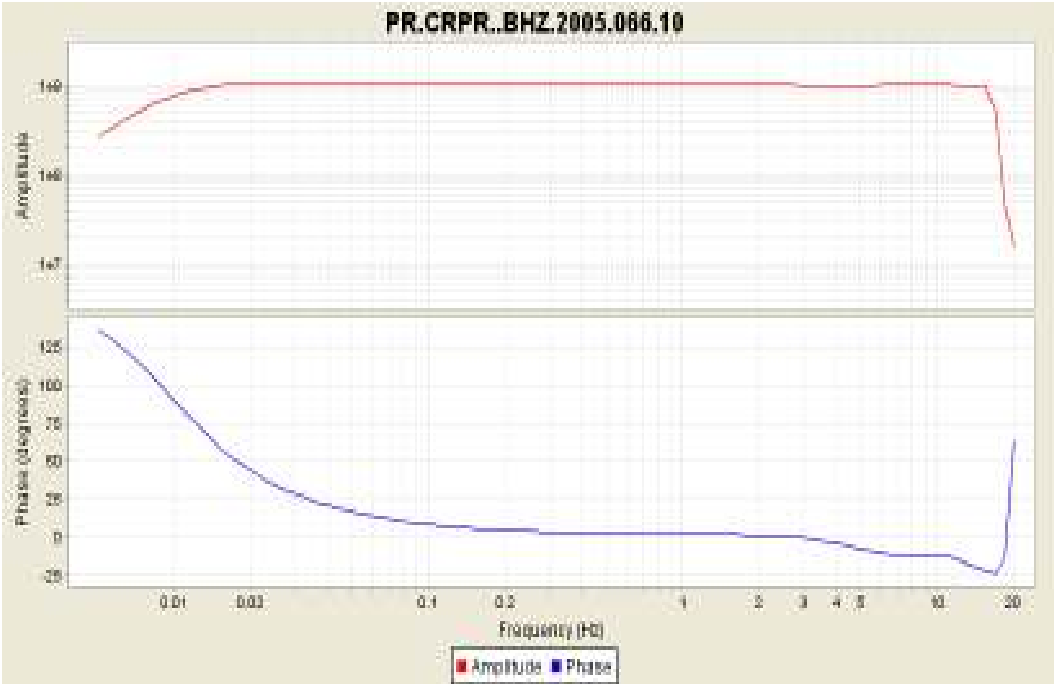

Figure 4.47 CBYP Frequency Response 1

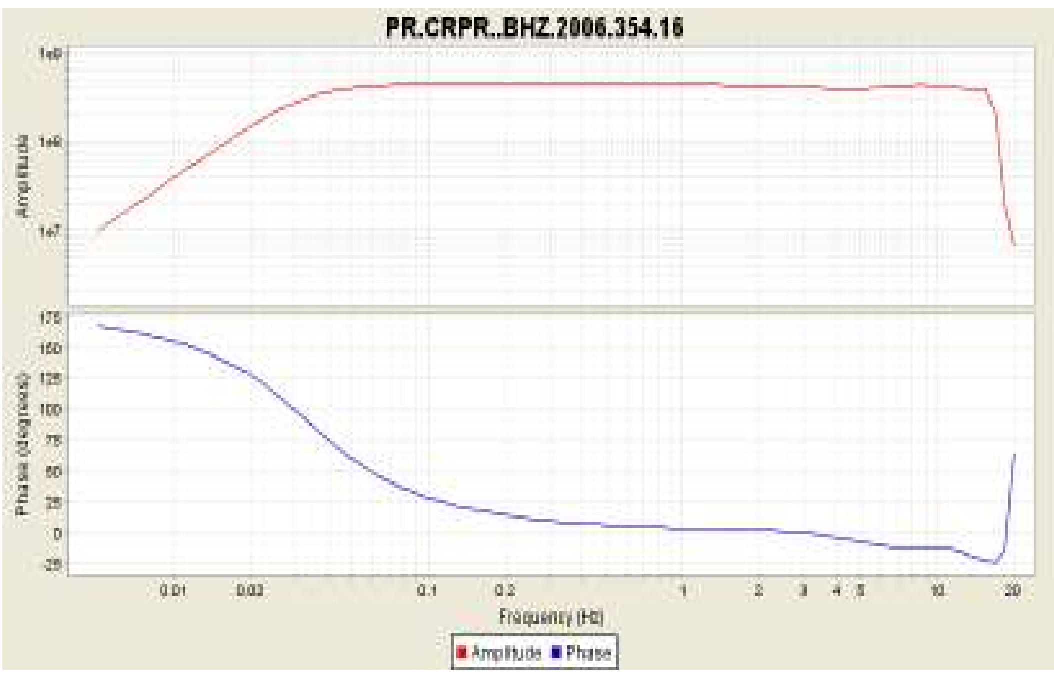

Figure 4.48 CRPR Frequency Response 2

The Figure 4.47 and 4.48 shows the different frequency responses used in the station of CRPR. The Figure 4.47 shows a flat response until 0.01Hz and the phase changes from 125 to -25 degrees while the figure 4.48 does not have a flat response until the frequency of 0.01Hz and the phase changes from 175 to -25 degrees. There are two figures because the change of seismometer.

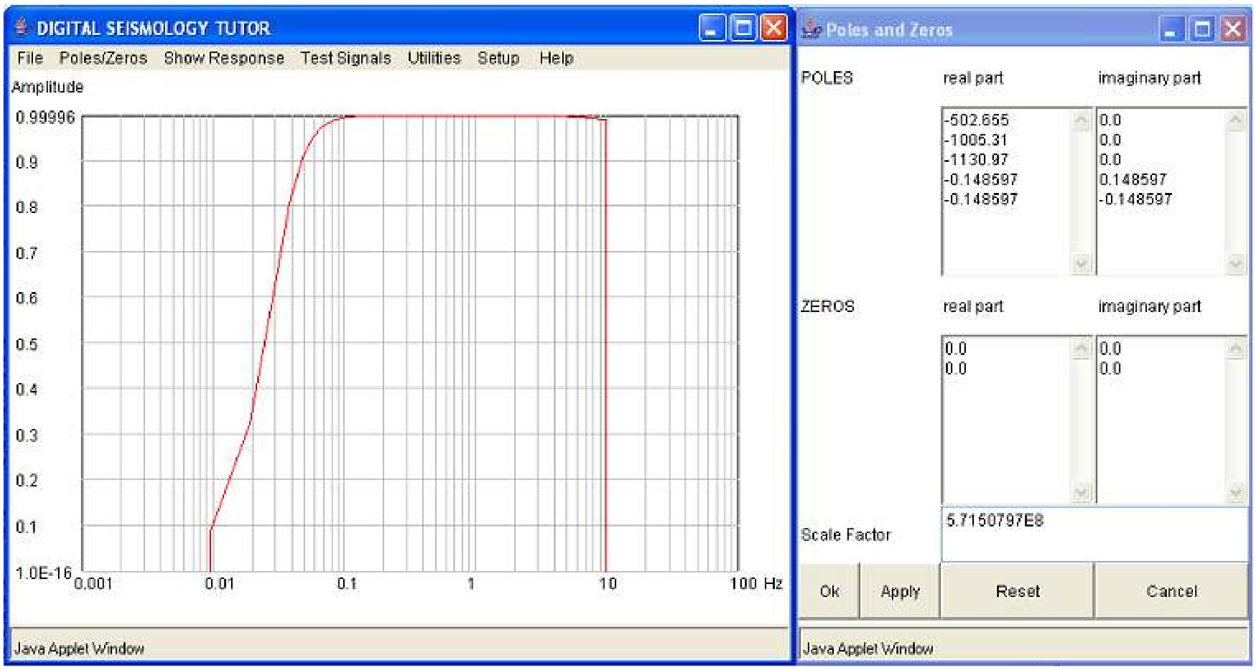


Figure 4.49 CRPR Poles and Zeros

The Figure 4.49 shows the poles, zeros and scale factor for the frequency response for seismometer used in this station which is 20 sec. The right of the plot presents the poles and zeros used to make the figure to the left. The figure to the left shows that it has a frequency response from 0.05Hz to 10Hz and also has an amplitude of 1.

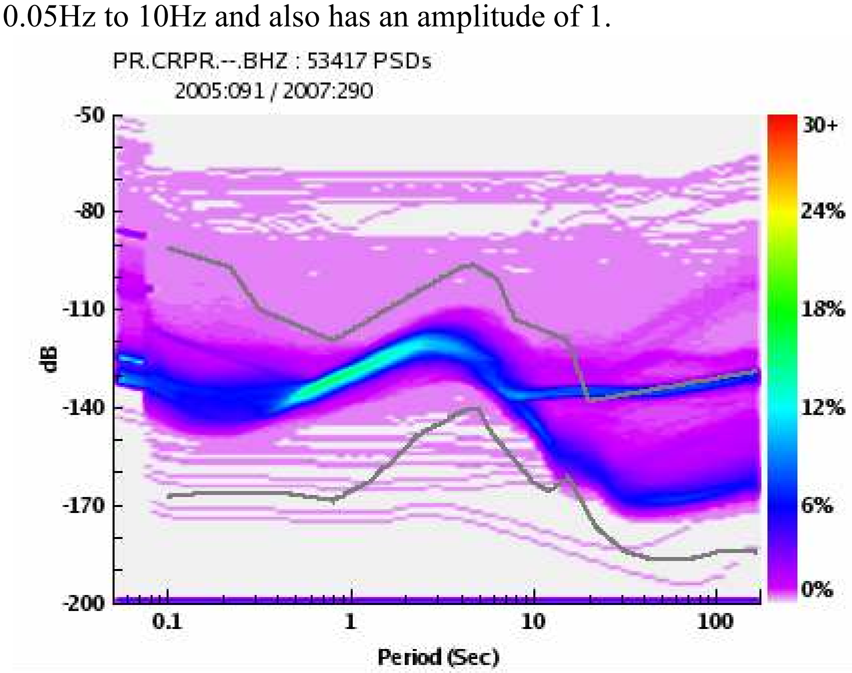


Figure 4.50 CRPR PDF

The Figure 4.50 shows the CRPR PDF plot. This station has a good performance in the cultural noise band because the blue color is over the down grey curve which represents the NLNM in only 25dB. In the long period band has two curves due to getting two seismometer of different frequency response, one of this seismometer reach the period of 100 sec. this is the reason why the down blue curves have only 10 dB over the NLNM, the other go over the NHNM because it is a 20 sec. seismometer. The right of the plot shows the probability of occurrence of each PSD in a colorbar. This probability of occurrence is normalized from 0% to 30%. The figure 4.51 is taken from this PDF using the mode values. Finally this PDF is constructed with 53417 PSDs in the range shown.

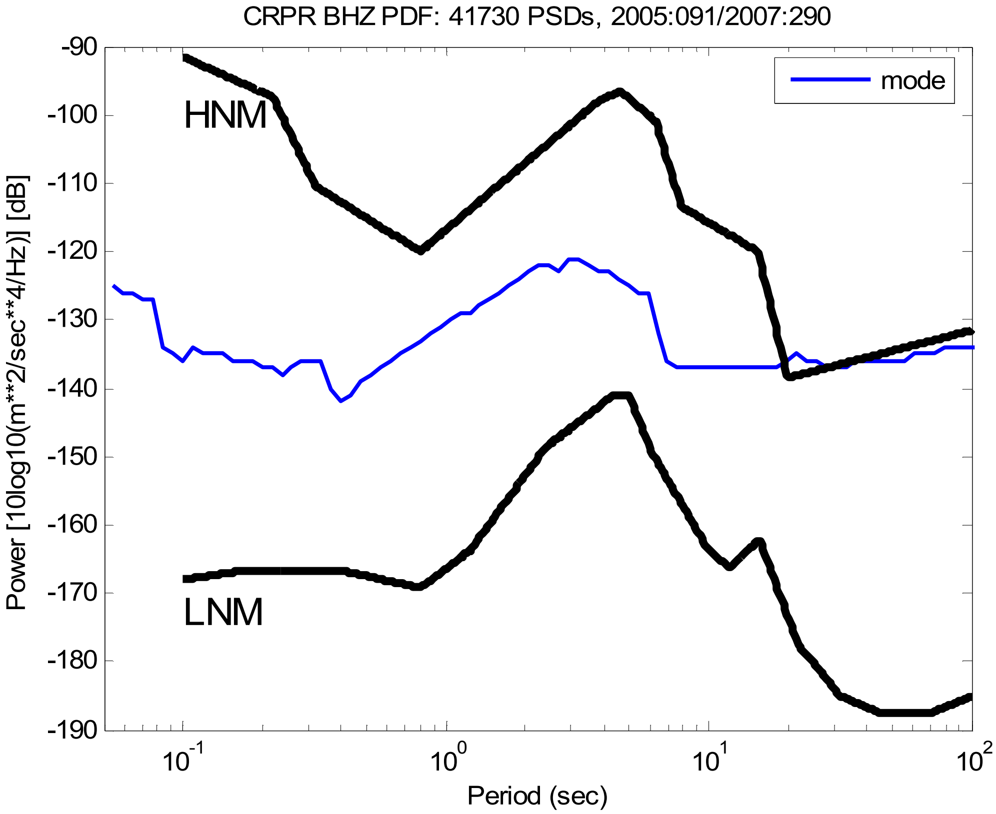


Figure 4.51 CRPR PDF Mode

The Figure 4.51 shows the CRPR PDF Mode. The seismic station has 35dB over the LNM curve in the cultural noise period band (0.1-1sec), this is very good for detecting local earthquakes. In the microseism band (4-16 sec.) the noise level is 15 dB over the LNM curves in the double frequency peak (4-8sec) and 30 dB over the LNM curve in the single frequency peak band (10-16sec).For long period band it goes crossing the HNM curves this is because the frequency response of the seismometer is until the period of 20 sec.

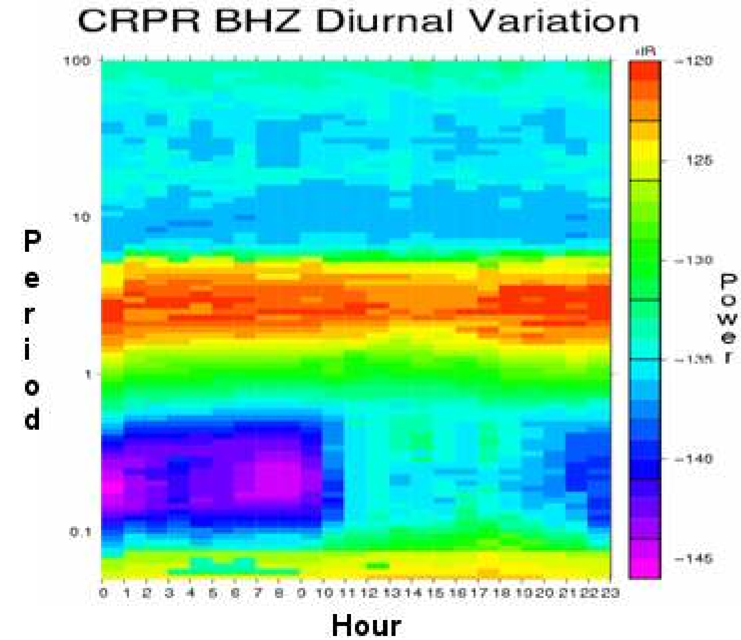


Figure 4.52 CRPR Diurnal Variation

The Figure 4.52 shows the diurnal variation for the CRPR seismic station. In the cultural noise period band (0.1-1sec) the power vary by 10-15dB. In the microseism band (4-16 sec.) the power vary by 30-35dB. In the long period band (20-100sec) the power vary by 5-10dB. In the period of 0.1sec., part of the cultural noise period band, it shows an increase of power during the hours of the day of 5dB due to increase of daylight working hours.

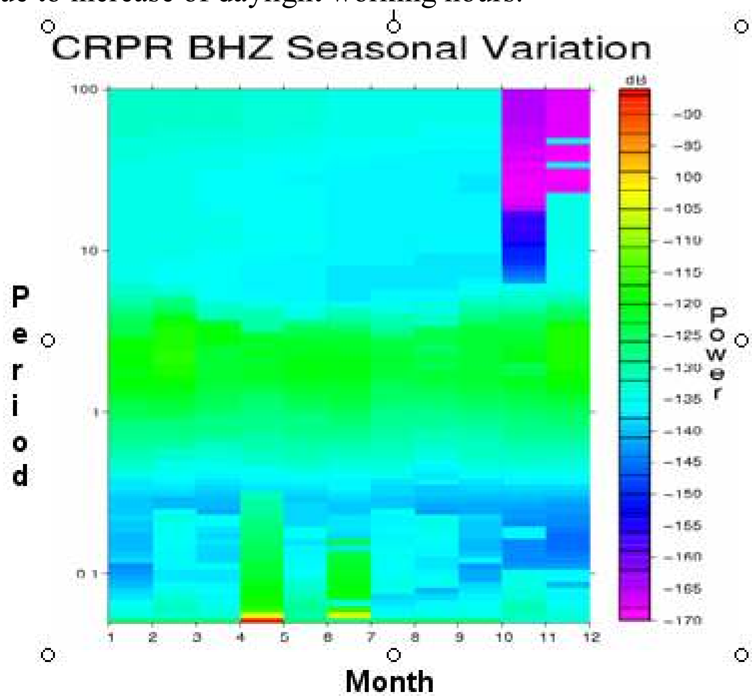


Figure 4.53 CRPR Seasonal Variation

The Figure 4.53 shows the seasonal variation for the CRPR seismic station. In the cultural noise period band (0.1-1sec) the power vary by 15-20dB. In the microseism band (4-16 sec.) the power vary by 30-35dB. In the long period band (20-100sec) the power vary by 25-30dB. There is no seasonal change due to the different month of the years.

**4. 7 HUMP, Humacao**

Figure 4.54 HUMP Seismic Station

This seismic station is instrumented with a Reftek 130 digitizer and a Guralp CMG-3T seismometer**.** The Figure 4.54 shows the places where the seismic station is installed.

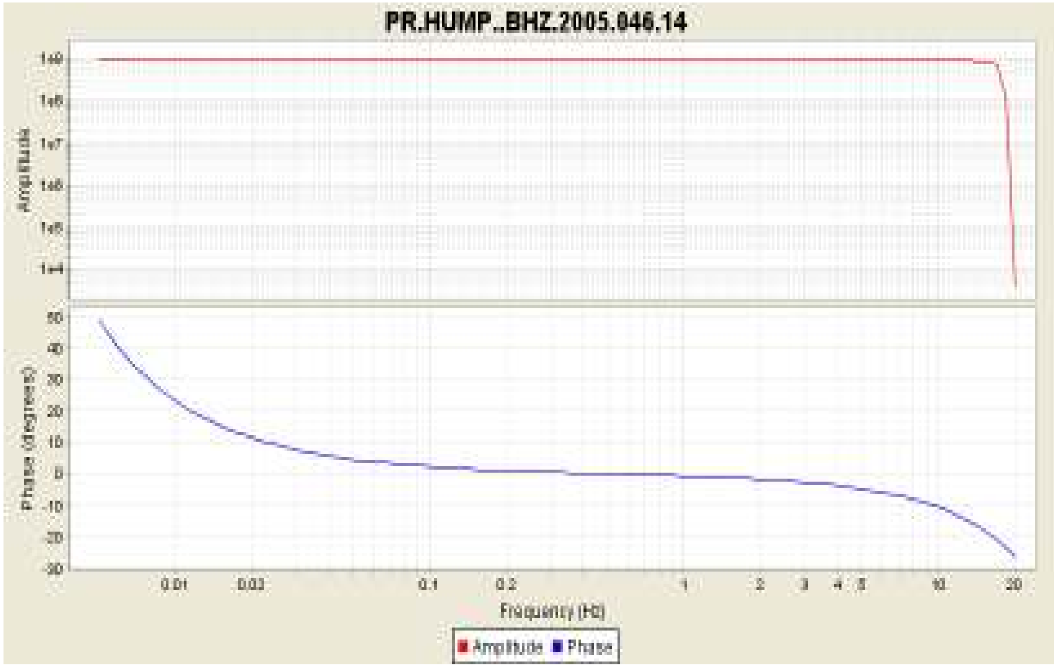

Figure 4.55 HUMP Frequency Response

The Figure 4.55 shows that this station has a flat response for the frequency 0.01Hz. The phase changes from 50 to -25 degrees.

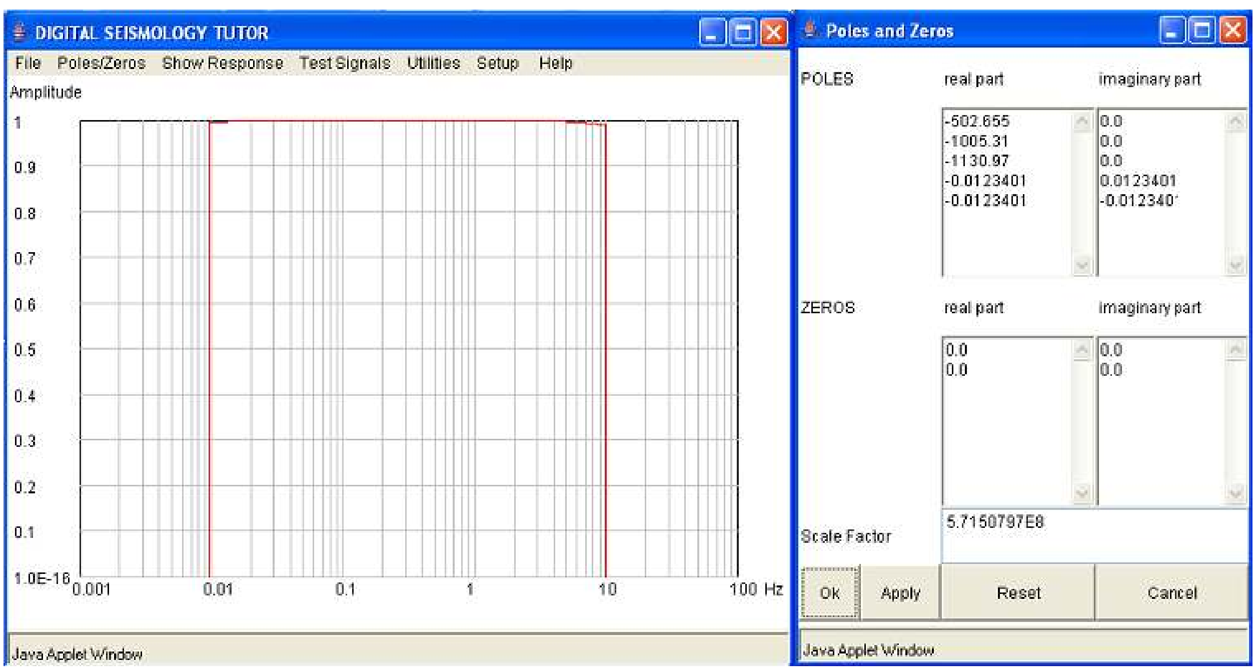

Figure 4.56 HUMP Poles and Zeros

The Figure 4.56 shows the poles, zeros and scale factor for the frequency response for seismometer used in this station which is a 100 sec. The right of the plot presents the poles and zeros used to make the figure to the left. The figure to the left shows that it has a frequency response from 0.01Hz to 10Hz and also has an amplitude of 1.

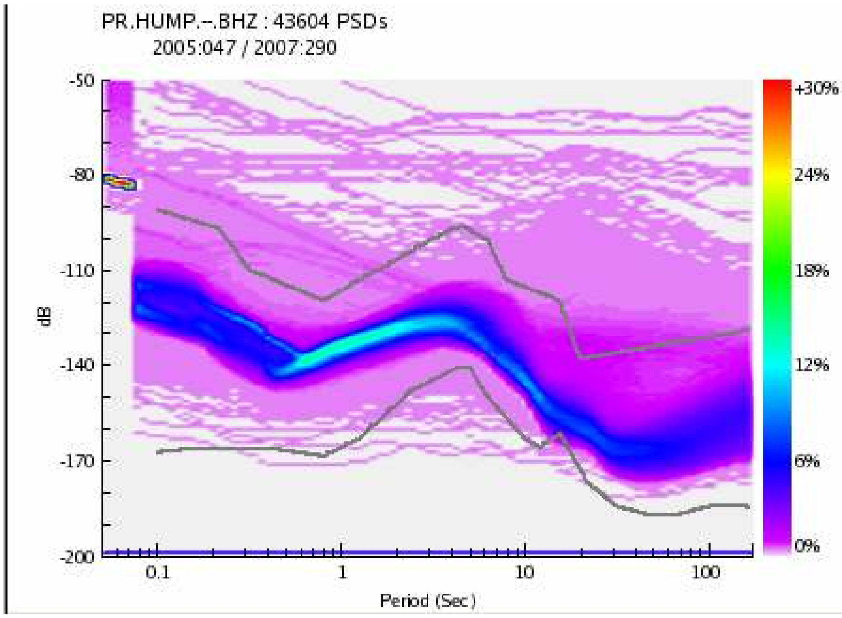


Figure 4.57 HUMP PDF

The Figure 4.57 shows the HUMP PDF plot. This station has a good performance because the blue color maintains between the grey curves which represents the NHNN and NLNM curves. The right of the plot shows the probability of occurrence of each PSD in a colorbar. This probability of occurrence is normalized from 0% to 30%. In the period between 0.1-0.6 sec. shows two curves due to diurnal variation in the cultural noise band. The figure 4.58 is taken from this PDF using the mode values. Finally this PDF is constructed with 43604 PSDs in the range shown.

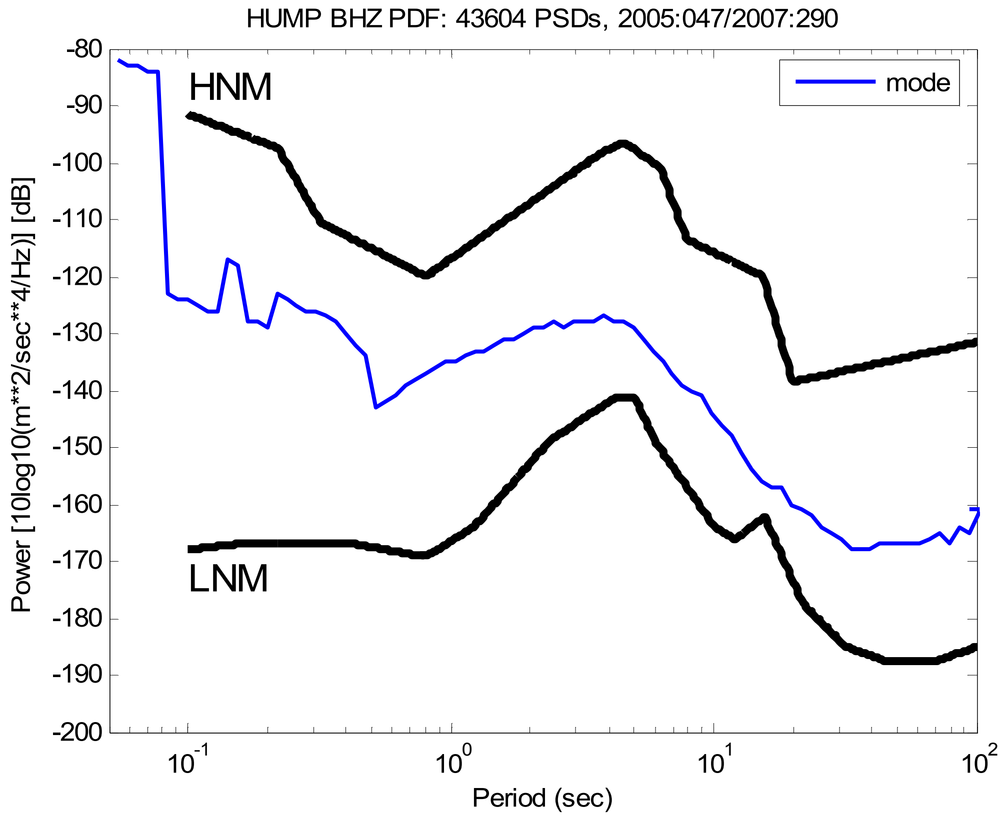


Figure 4.58 HUMP PDF Mode

The Figure 4.58 shows the HUMP PDF Mode. The seismic station has 50dB over the LNM curve in the 0.1-0.5sec period band. This period band belong to the cultural noise band and is very good for detecting local earthquake. In the microseism band (4-16 sec.) the noise level is 10 dB over the LNM curves in the double frequency peak (4-8sec) and 5 dB over the LNM curve in the single frequency peak band (10-16sec).For long period band (20-100sec) it go 20 dB over the LNM curve.

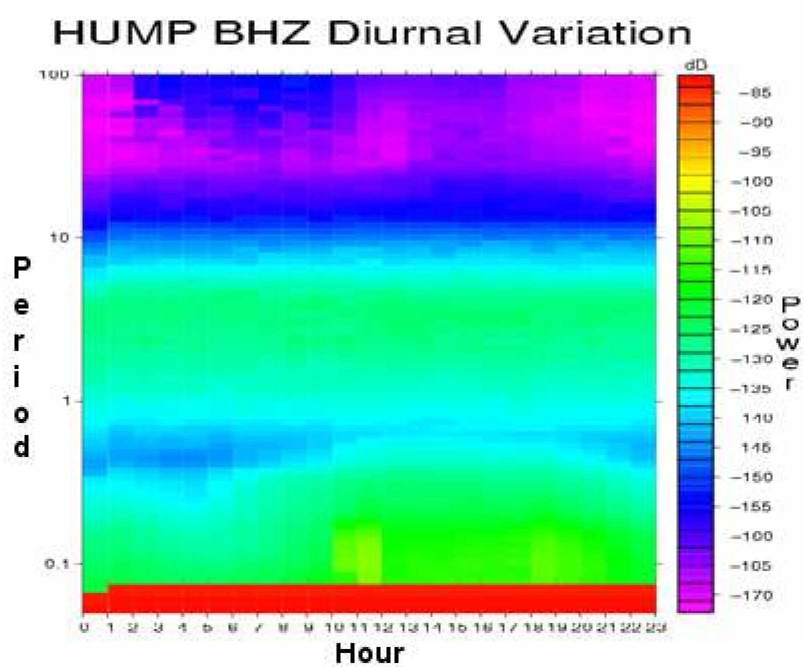


Figure 4.59 HUMP Diurnal Variation

The Figure 4.59 shows the diurnal variation for the HUMP seismic station. In the cultural noise period band (0.1-1sec) the power vary by 25-30dB. In the microseism band (4-16 sec.) the power vary by 30-35dB. In the long period band (20-100sec) the power vary by 10-15dB. In the period of 0.1sec., part of the cultural noise period band, it shows an increase of power during the hours of the day of 25dB due to increase of daylight working hours.

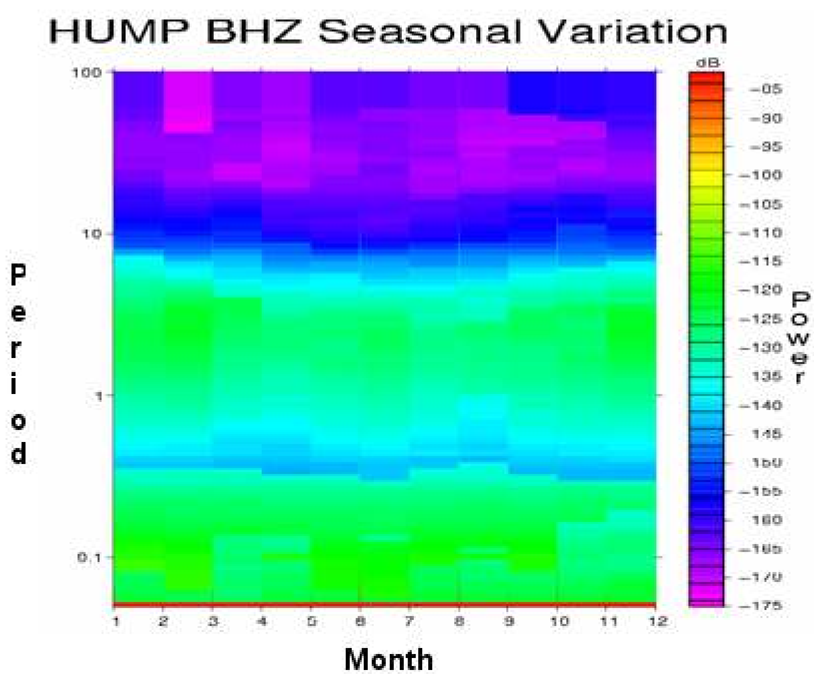


Figure 4.60 HUMP Seasonal Variation

The Figure 4.60 shows the seasonal variation for the HUMP seismic station. In the cultural noise period band (0.1-1sec) the power vary by 20-25dB. In the microseism band (4-16 sec.) the power vary by 30-35dB. In the long period band (20-100sec) the power vary by 5dB. There is no seasonal change due to the different month of the years.

**4. 8 ICM, Isla Caja de Muertos**

Figure 4.61 ICM Seismic Station

This seismic station is instrumented with a Reftek 7208 digitizer and a Guralp CMG-40T seismometer**.** The Figure 4.61 shows the house where the seismic station is installed.

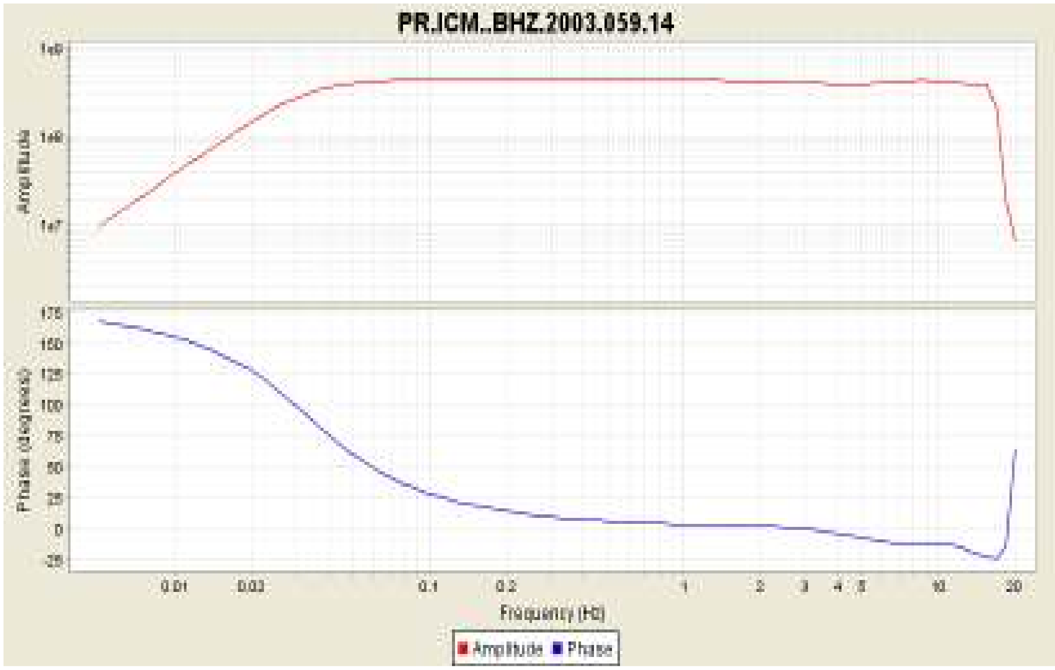

Figure 4.62 ICM Frequency Response

The Figure 4.62 shows the frequency response for the ICM seismic station. It shows a flat response from the frequency of 16 Hz until the frequency of 0.04Hz. The phase changes from 175 to -25 degrees.

Figure 4.63 ICM Poles and Zeros

The figure 4.63 shows the poles, zeros and scale factor for the frequency response for seismometer used in this station which a 20sec. The right of the plot presents the poles and zeros used to make the figure to the left. The figure to the left shows that it has a frequency response from 0.01Hz to 10Hz and also has an amplitude of 1.

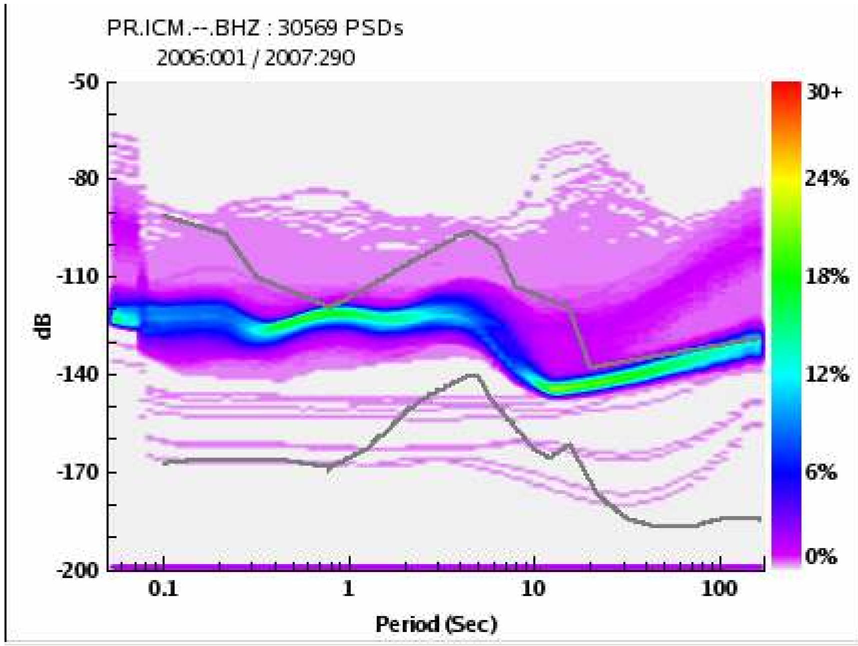


Figure 4.64 ICM PDF

The Figure 4.64 shows the ICM PDF plot. This station has a good performance in the cultural noise band(0.1- 1sec) and microseism band (4-16sec) because the blue color maintain between the grey curves which represents the NHNN and NLNM curves, but in the long period band (20-100sec) reach the NHNM curve. The right of the plot shows the probability of occurrence of each PSD in a colorbar. The figure 4.5 is taken from this PDF using the mode values. Finally this PDF is constructed with 43142 PSDs in the range shown.

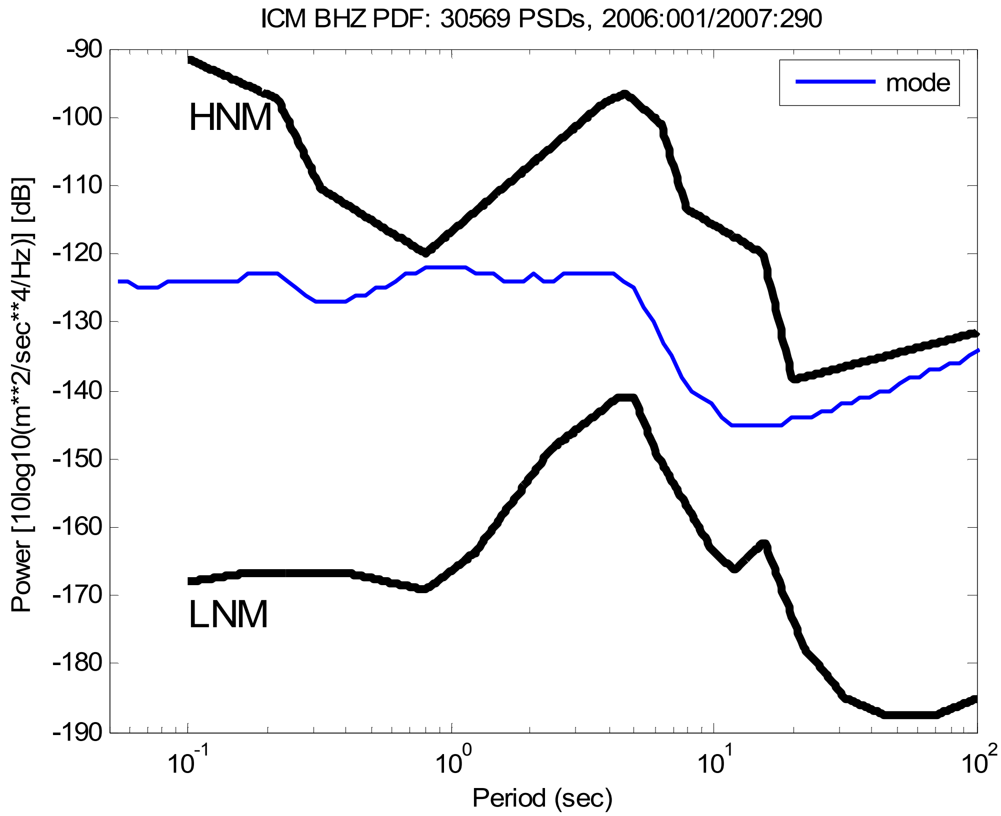


Figure 4.65 ICM PDF Mode

The Figure 4.65 shows the ICM PDF Mode. The seismic station has 45dB over the LNM curve in the cultural noise band (0.1 -1 sec), this is very good for detecting local earthquakes. In the microseism band (4-16 sec.) the noise level is 15 dB over the LNM curves in the double frequency peak (4-8sec) and 20 dB over the LNM curve in the single frequency peak band (10-16sec). For long period band it go 5dB below the HNM curve.

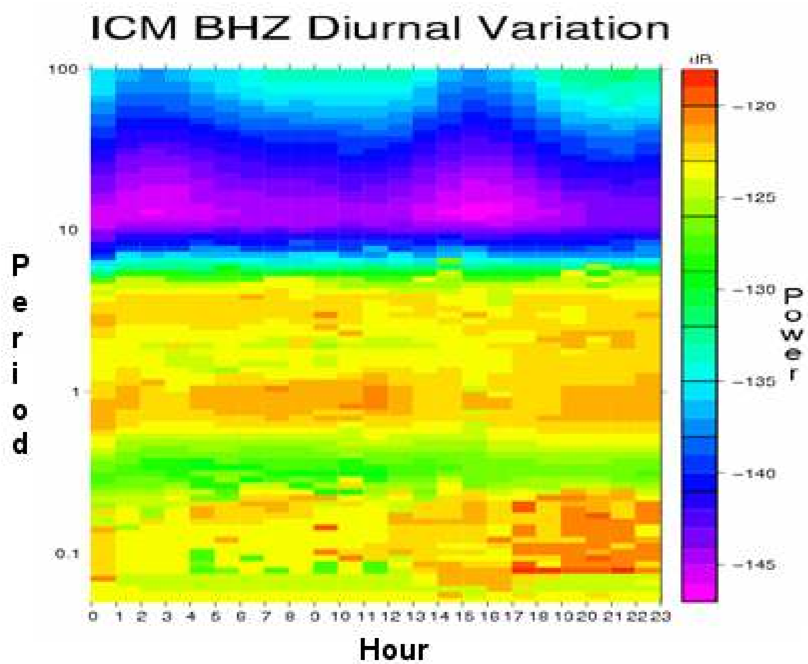


Figure 4.66 ICM Diurnal Variation

The Figure 4.66 shows the diurnal variation for the ICM seismic station. In the cultural noise period band (0.1-1sec) the power vary by 5-10dB. In the microseism band (4-16 sec.) the power vary by 20-25dB. In the long period band (20-100sec) the power vary by 10-15dB. In the period of 0.1sec., part of the cultural noise period band, it does not show an increase of power during the hours of the day due to increase of daylight working hours, this is because the island of Caja de Muertos is unpopulated.

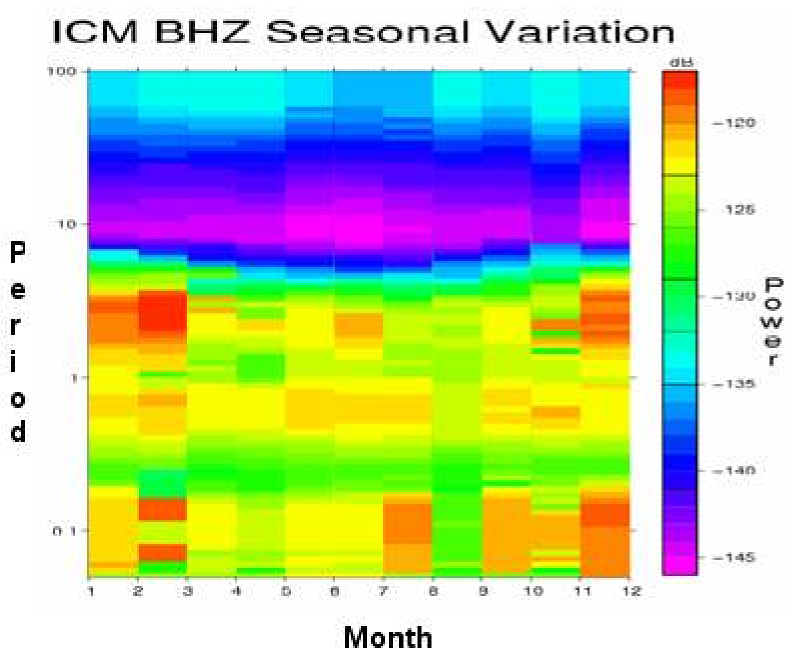


Figure 4.67 ICM Seasonal Variation

The Figure 4.67 shows the seasonal variation for the ICM seismic station. In the cultural noise period band (0.1-1sec) the power vary by 5-10dB. In the microseism band (4-16 sec.) the power vary by 20-25dB. In the long period band (20-100sec) the power vary by 5-10dB. There is no seasonal change due to the different month of the years.

**4. 9 MPR, Mayaguez**

Figure 4.68 MPR Seismic Station

This seismic station is instrumented with a Netdas digitizer and a Guralp CMG-3T seismometer**.** The Figure 4.68 shows the places where the seismometer is installed.

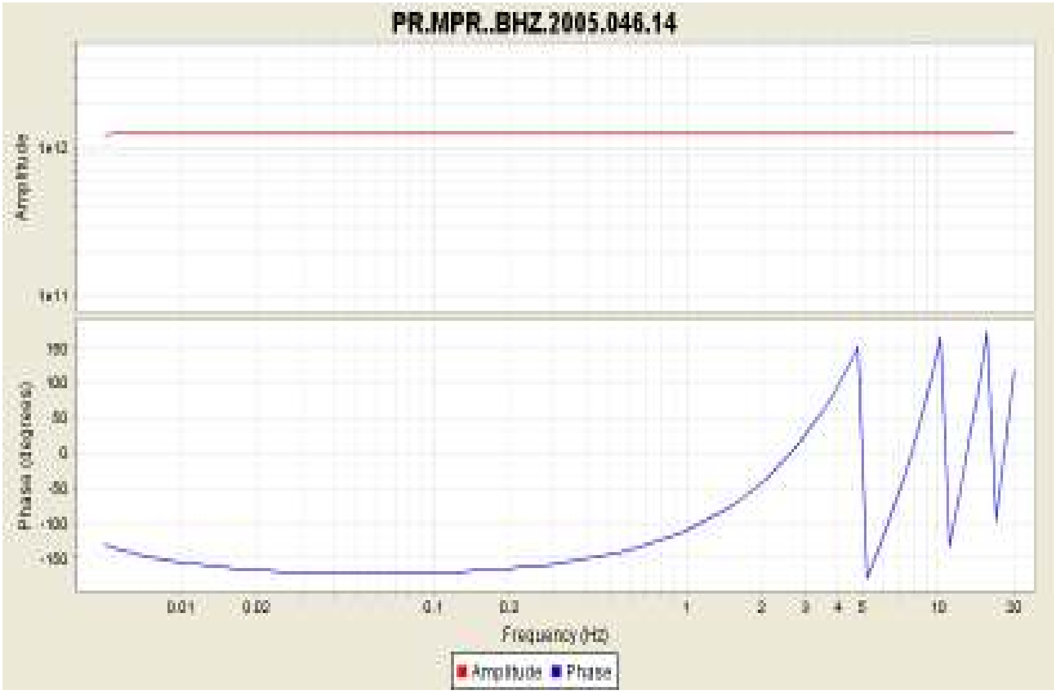

Figure 4.69 MPR Frequency Response 1

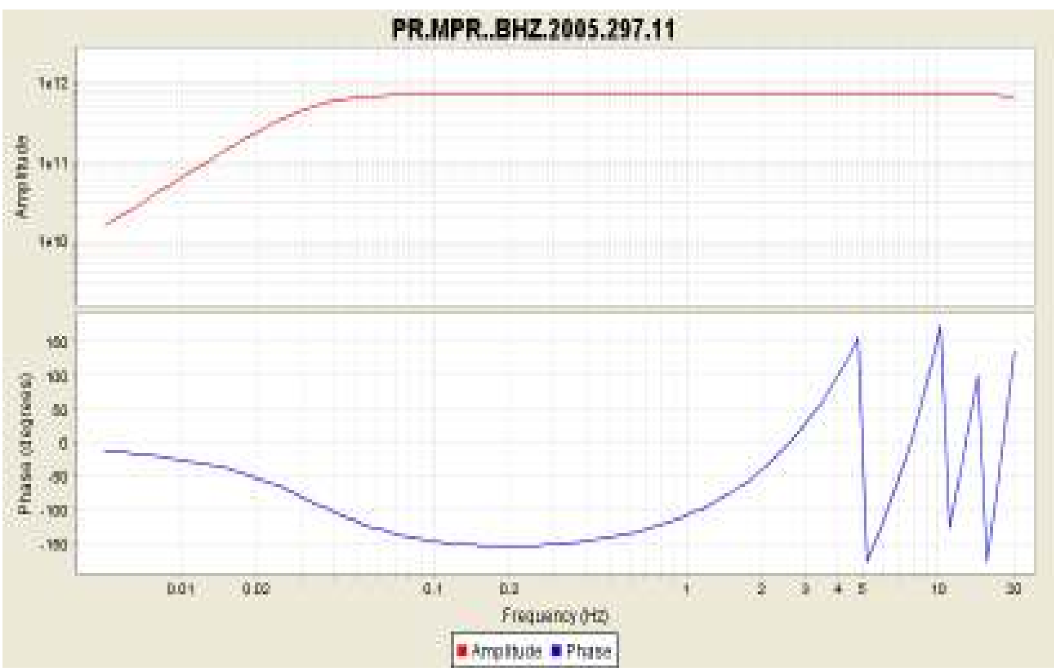

Figure 4.70 MPR Frequency Response 2

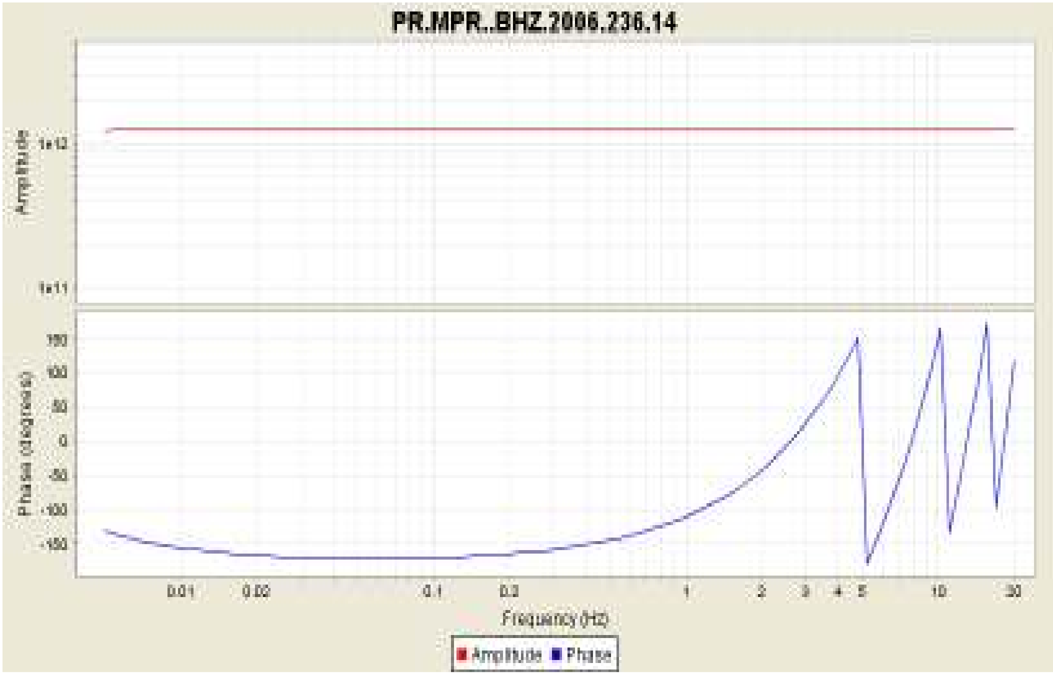

Figure 4.71 MPR Frequency Response 3

The Figure 4.69, 4.70 and 4.71 shows the different frequency responses used in the station of MPR. The figure 4.69 shows a flat response until 0.01Hz and has a change in phase from -125 to 100 degrees while the figure 4.70 does not have a flat response until the frequency of 0.01Hz and has a change in phase from 0 to 100 degrees. Also the figure 4.71 has a flat response until the frequency of 0.01Hz and has a change in phase from -125 to 100 degrees. There are three figures because of the seismometer change.

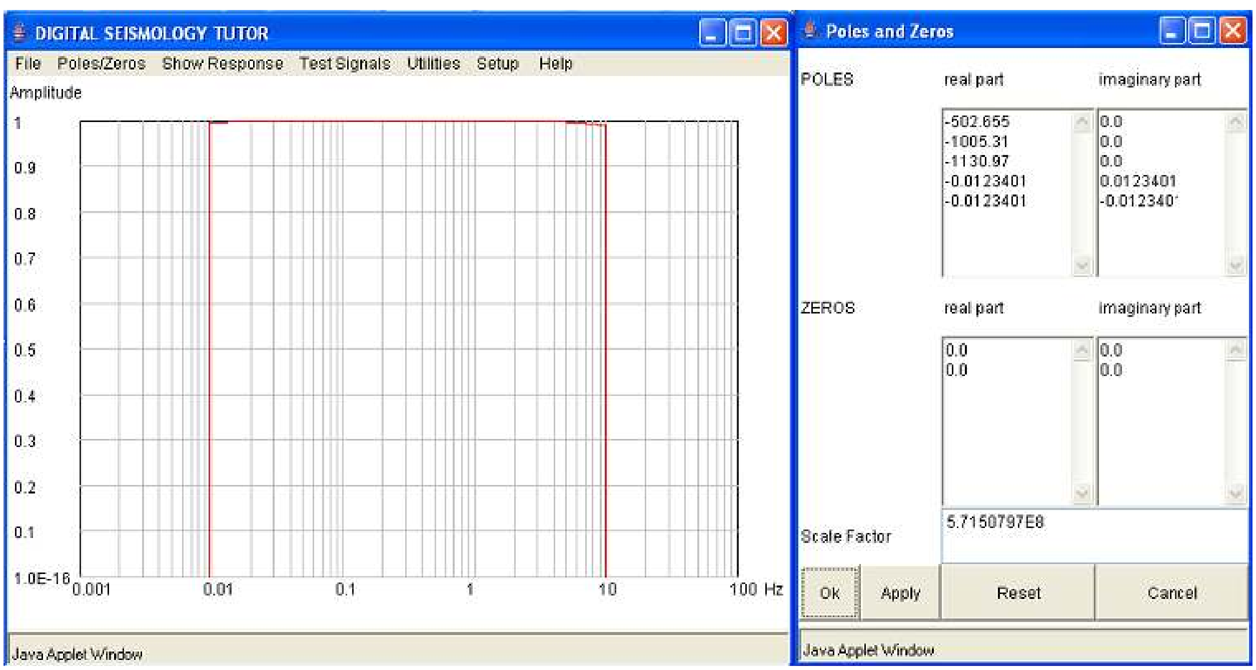

Figure 4.72 MPR Poles and Zeros

The Figure 4.72 shows the poles, zeros and scale factor for the frequency response for seismometer used in this station which a 100 sec sensor. The right of the plot presents the poles and zeros used to make the figure to the left. The figure to the left shows that it has a frequency response from 0.01Hz to 10Hz and also has normalized amplitude of 1.

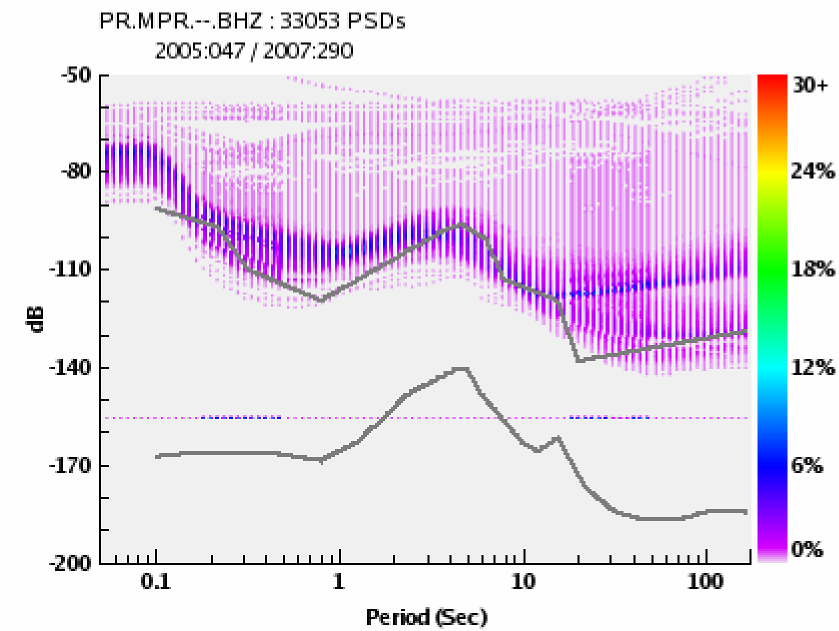


Figure 4.73 MPR PDF

The Figure 4.73shows the MPR PDF plot. This station has a bad performance because the blue color maintain over the upper grey curves which represents the NHNN. The right of the plot shows the probability of occurrence of each PSD in a colorbar. This probability of occurrence is normalized from 0% to 30%. The figure 4.65 is taken from this PDF using the mode values. Finally this PDF is constructed with 33053 PSDs in the range shown.

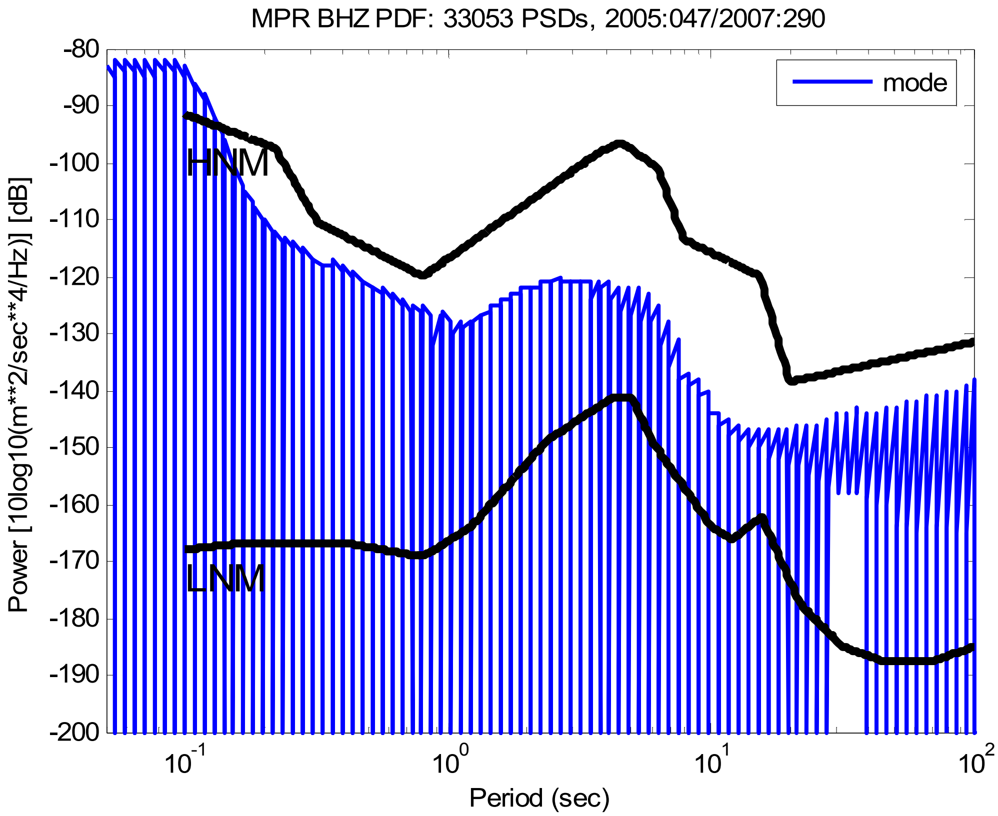


Figure 4.74 MPR PDF Mode

In the Figure 4.65 it is clear that the PDF mode has a problem, this is because this station does not have good data; the data has a problem because the sampling rate is not an integer, this is the reason we could not make diurnal and seasonal variations for this station.

### 4. 10 MTP, Isla de Vieques

Figure 4.75 MTP Seismic Station

This seismic station is instrumented with a Reftek 7208 digitizer and a Guralp CMG-3ESP seismometer**.** The Figure 4.75 shows the places where the seismic station is installed.

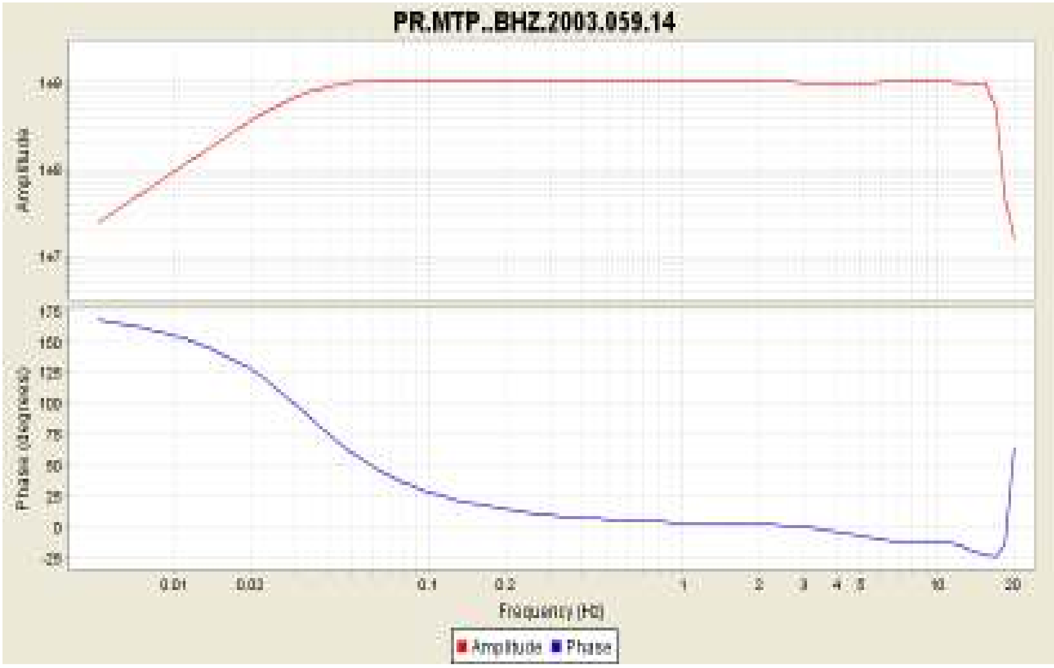


Figure 4.76 MTP Frequency Response

The Figure 4.76 shows the frequency response for the MTP seismic station. It has a flat response until the frequency of 0.04Hz and has a change in phase from 175 to -25 degrees.

Figure 4.77 MTP Poles and Zeros

The figure 4.77 shows the poles, zeros and scale factor for the frequency response for seismometer used in this station which is a 20 sec. The right of the plot presents the poles and zeros used to make the figure to the left. The figure to the left shows that it has a frequency response from 0.01Hz to 10Hz and also has normalized amplitude of 1.

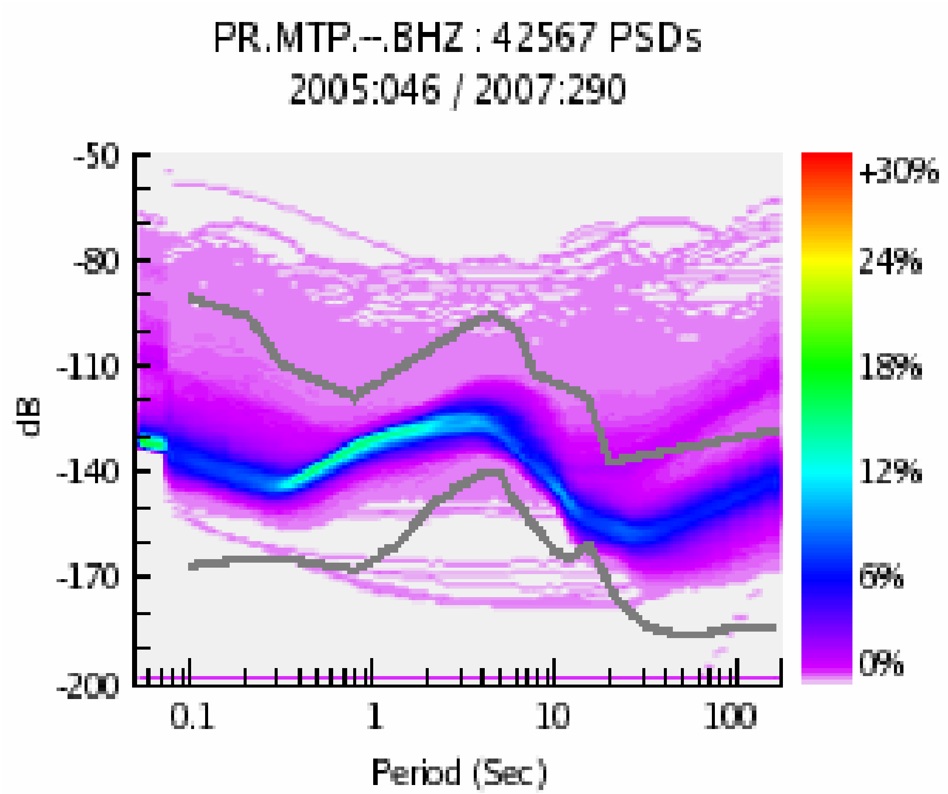


Figure 4.78 MTP PDF

The figure 4.48 shows the MTP PDF plot. This station has a good performance because the blue color maintains between the grey curves which represents the NHNN and NLNM curves. The right of the plot shows the probability of occurrence of each PSD in a colorbar. This probability of occurrence is normalized from 0% to 30%. The figure 4.79 is taken from this PDF using the mode values. Finally this PDF is constructed with 42567 PSDs in the range shown.

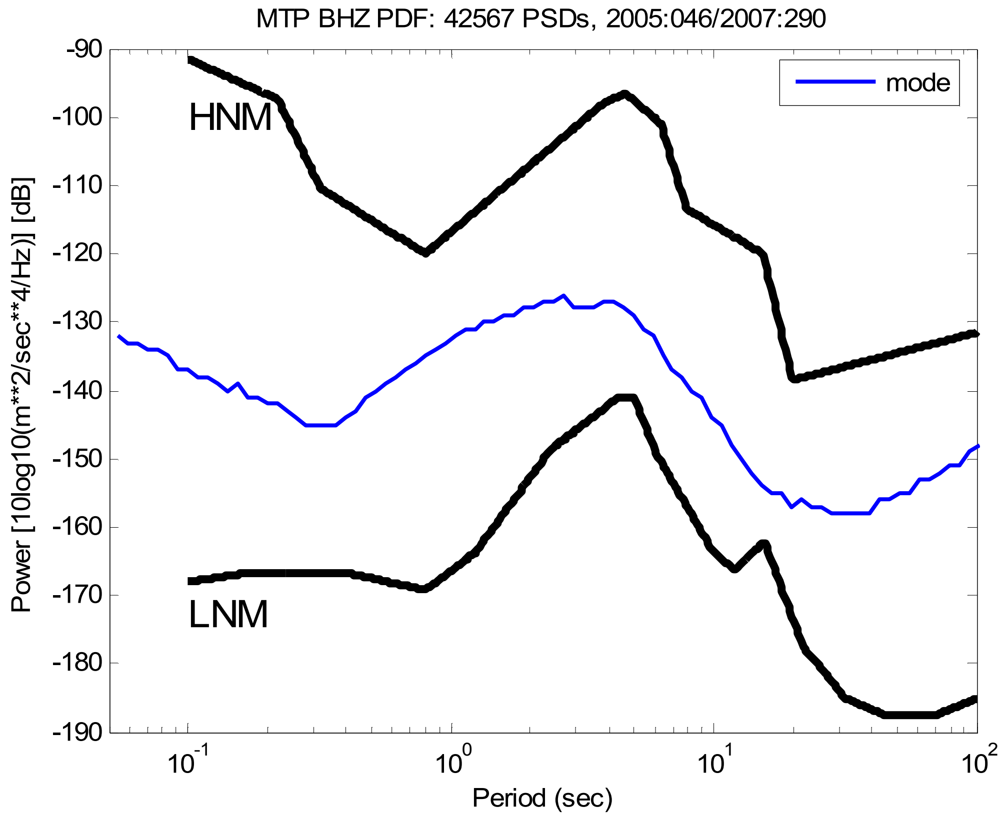


Figure 4.79 MTP PDF Mode

The Figure 4.79 shows the MTP PDF Mode. The seismic station has an average of 30dB over the LNM curve in the cultural noise band (0.1-1sec), this is very good for detectinf local earthquake. In the microseism band (4-16 sec.) the noise level is 15 dB over the LNM curves in the double frequency peak (4-8sec) and 10 dB over the LNM curve in the single frequency peak band (10-16sec). For the long period band (20-100sec) it goes 30 dB as an average over the HNM curve.

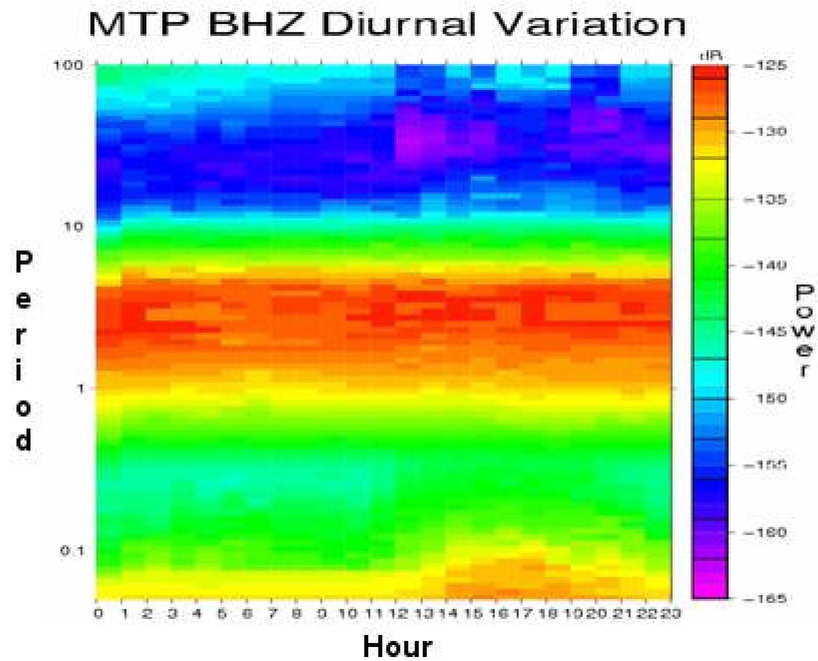

Figure 4.80 MTP Diurnal Variation

The Figure 4.80 shows the diurnal variation for the MTP seismic station. In the cultural noise period band (0.1-1sec) the power varies by 5dB. In the microseism band (4-16 sec.) the power vary by 35-40dB. In the long period band (20-100sec) the power vary by 15-20dB. In the period of 0.1sec., part of the cultural noise period band, it shows an increase of power during the hours of the day of 5dB due to increase of daylight working hours.

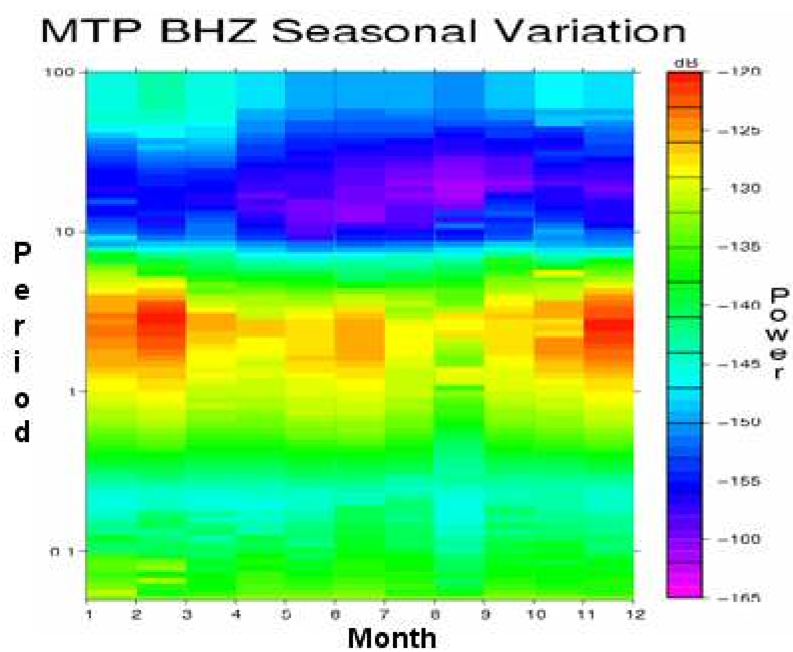

Figure 4.81 MTP Seasonal Variation

The Figure 4.81 shows the seasonal variation for the MTP seismic station. In the cultural noise period band (0.1-1sec) the power vary by 10-15dB. In the microseism band (4-16 sec.) the power vary by 40dB. In the long period band (20-100sec) the power vary by 15-20dB. There is not seasonal change due to the different month of the years.

### 4.11 OBIP, Ponce

Figure 4.82 OBIP Seismic Station

This seismic station is instrumented with a Reftek 7208 digitizer and a Guralp CMG-40T seismometer**.** The Figure 4.82 shows the places where the seismometer is installed.

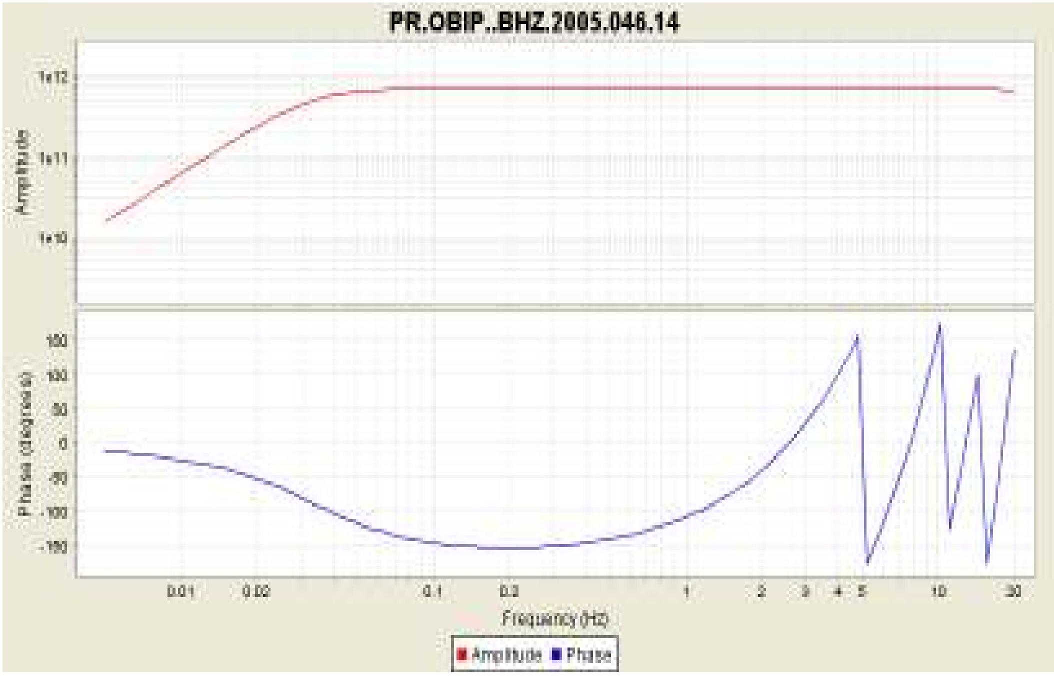

Figure 4.83 OBIP Frequency Response

In the Figure 4.83 the frequency response of the seismic station is not flat until the frequency 0.01Hz and and has a change in phase from 0 to 100 degrees.

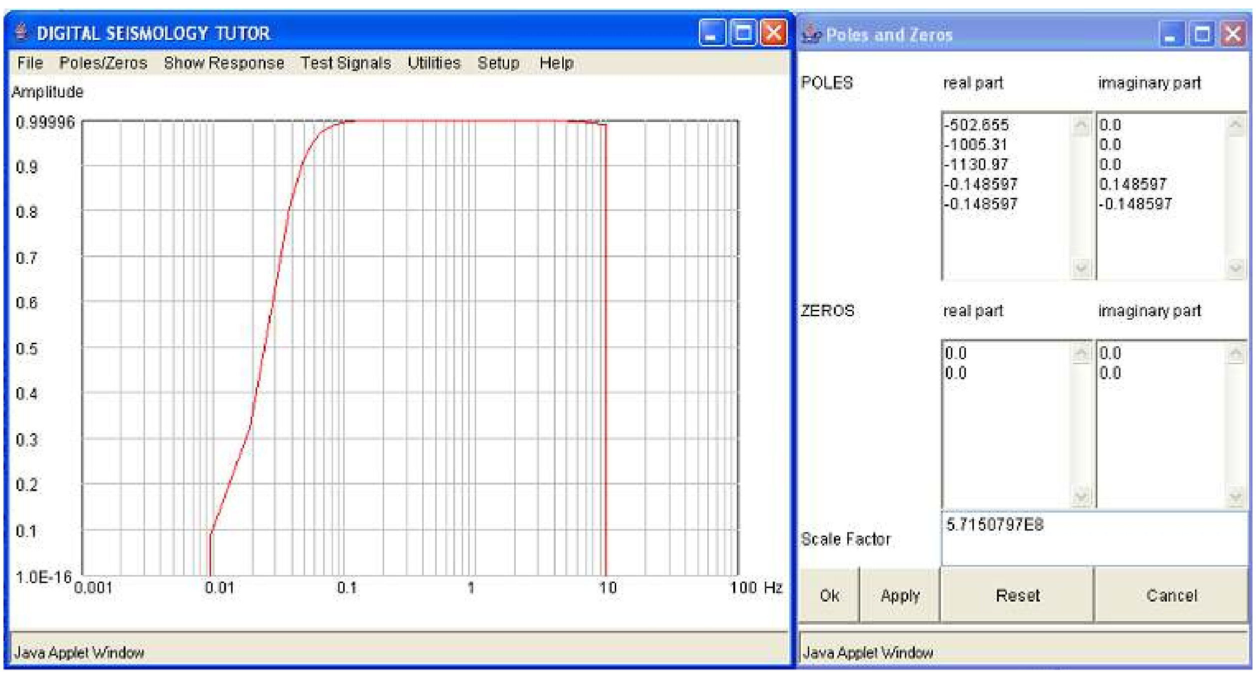

Figure 4.84 OBIP Poles and Zeros

The Figure 4.84 shows the poles, zeros and scale factor for the frequency response for seismometer used in this station which is a 30 sec. The right of the plot presents the poles and zeros used to make the figure to the left. The figure to the left shows that it has a frequency response from 0.033Hz to 10Hz and also has normalized amplitude of 1.

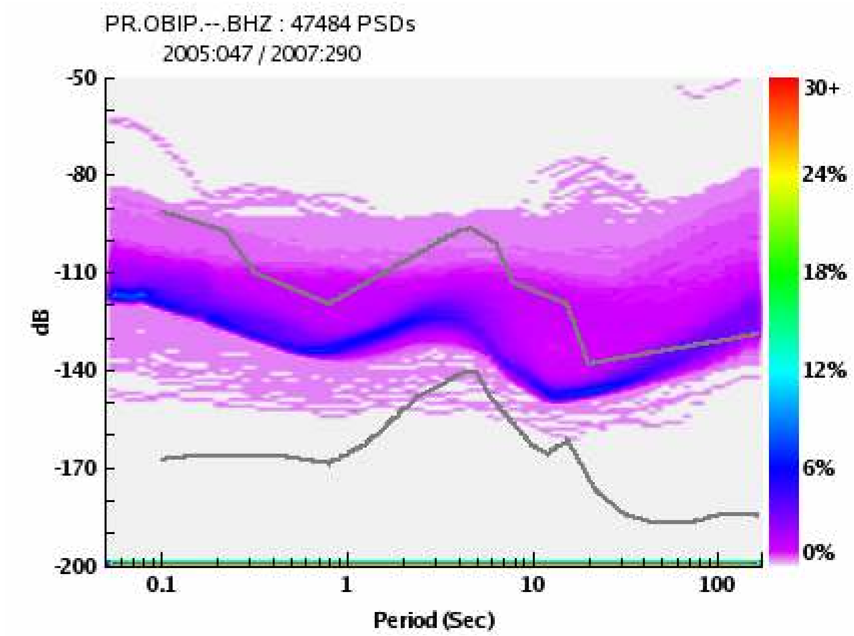

Figure 4.85 OBIP PDF

The Figure 4.4 shows the OBIP PDF plot. This station has a good performance because the blue color maintains between the grey curves which represents the NHNN and NLNM curves. The right of the plot shows the probability of occurrence of each PSD in a colorbar. This probability of occurrence is normalized from 0% to 30%. The figure 4.86 is taken from this PDF using the mode values. Finally this PDF is constructed with 47484 PSDs in the range shown.

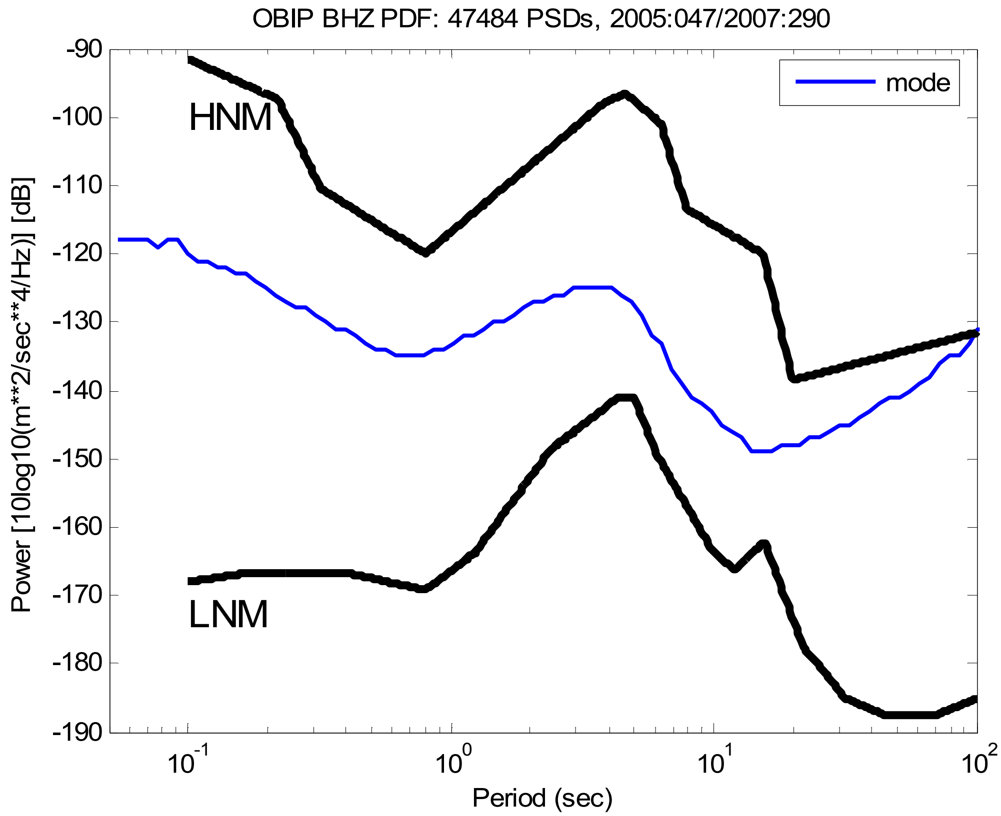


Figure 4.86 OBIP PDF Mode

The Figure 4.86 shows the OBIP PDF Mode. The seismic station has an average of 40dB over the LNM in the cultural noise period band (0.1-1sec). In the microseism band (4-16 sec.) the noise level is 15 dB over the LNM curves in the double frequency peak (4-8sec) and 15 dB over the LNM curve in the single frequency peak band (10-16sec). For the long period band (20-100 sec) it goes 45 dB over the HNM curve.

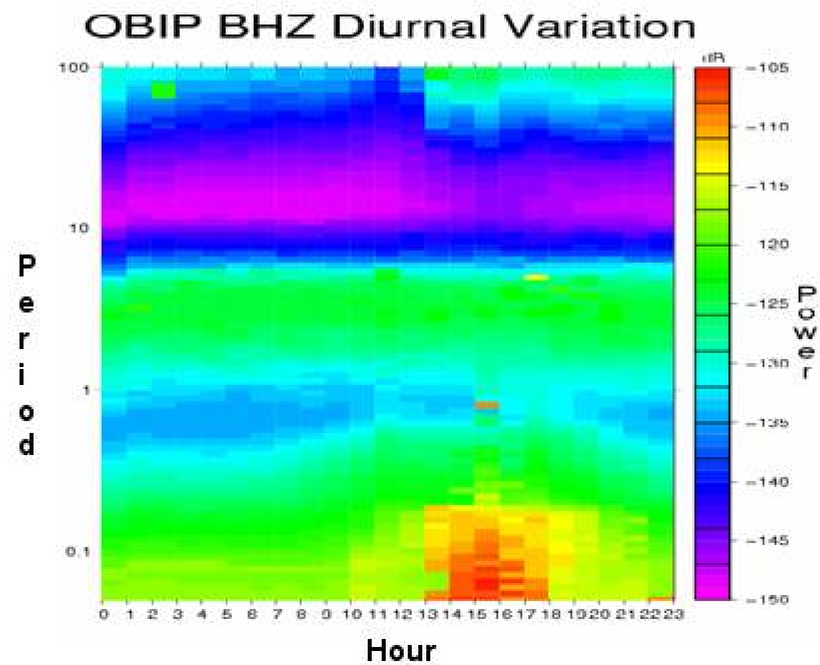


Figure 4.87 OBIP Diurnal Variation

The Figure 4.87 shows the diurnal variation for the OBIP seismic station. In the cultural noise period band (0.1-1sec) the power vary by 25-30dB. In the microseism band (4-16 sec.) the power vary by 20-25dB. In the long period band (20-100sec) the power vary by 20-30dB. In the period of 0.1sec., part of the cultural noise period band, it shows an increase of power during the hours of the day of 20dB due to increase of daylight working hours.

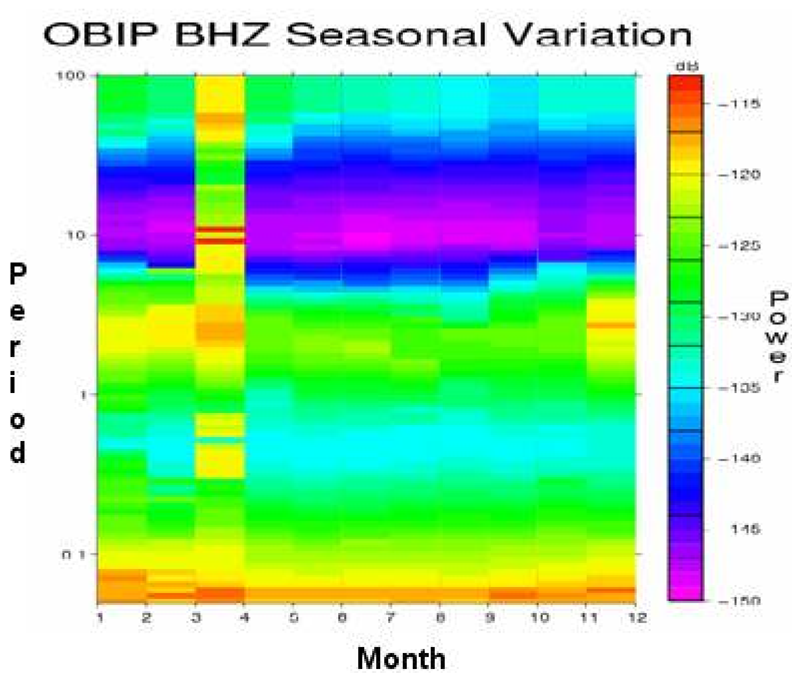


Figure 4.88 OBIP Seasonal Variation

The Figure 4.88 shows the seasonal variation for the OBIP seismic station. In the cultural noise period band (0.1-1sec) the power vary by 10-15dB. In the microseism band (4-16 sec.) the power vary by 35dB. In the long period band (20-100sec) the power vary by 30dB. There is not seasonal change due to the different month of the years.

Table 4.1 Performing in the Difference Period of the Seismic Station

| Seismic Station | Cultural Noise (0.1-1Sec) | Microseism (4-16Sec) | Long Period (>20 Sec) |
|---|---|---|---|
| SJG | GOOD | GOOD | GOOD |
| AGPR | GOOD | BAD | GOOD |
| AOPR | GOOD | GOOD | BAD |
| CBYP | GOOD | GOOD | GOOD |
| CPD | BAD | GOOD | BAD |
| CRPR | GOOD | GOOD | BAD |
| HUMP | GOOD | GOOD | GOOD |
| ICM | GOOD | GOOD | GOOD |
| MPR | BAD | GOOD | GOOD |
| MTP | GOOD | GOOD | GOOD |
| OBIP | GOOD | GOOD | GOOD |

The Table 4.1 summarizes the performing of the different seismic station. The table show that in the cultural noise band, the station of CPD and MPR are in bad condition. In the Microseism band only AGPR is in bad condition and in the long period band, AOPR, CPD and CRPR.

### 4.12 Geographical Variation of Seismic Noise

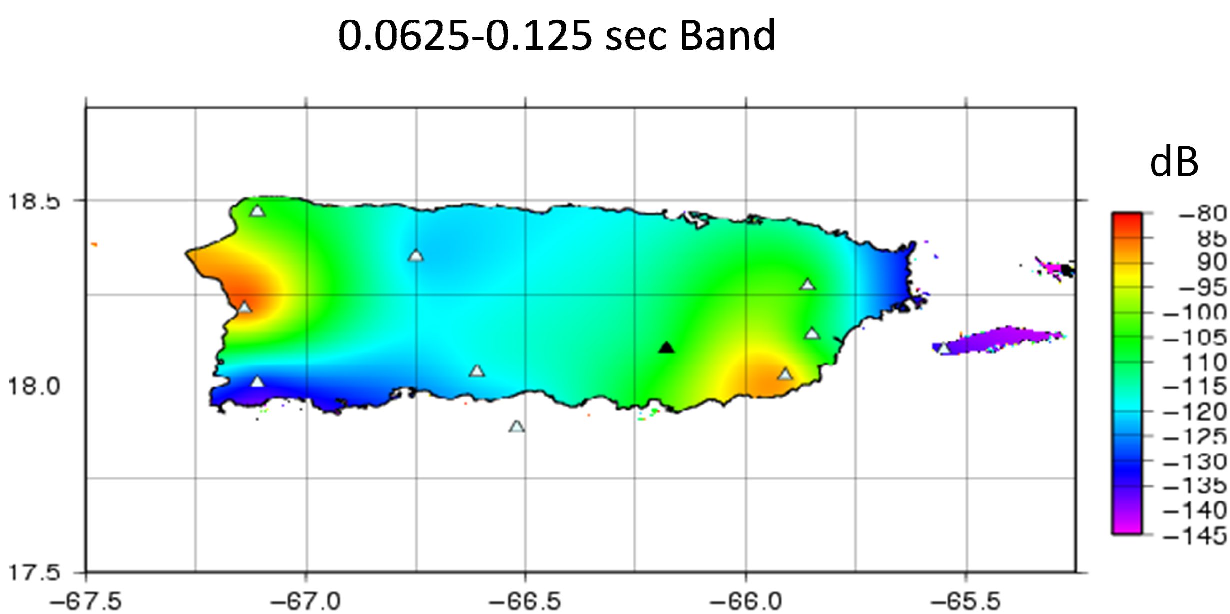


Figure 4.89 Geographical variation of cultural noise band

In the Figure 4.89 it can be observed the geographical variation of the seismic noise for the 0.0625-0.125sec. This period is part of the cultural noise band. This figure shows that the station

MPR and CPD are the noisier and the station of CRPR and MTP are the station with less noise. The colorbar to the right indicate the power in dB due to the different colors.

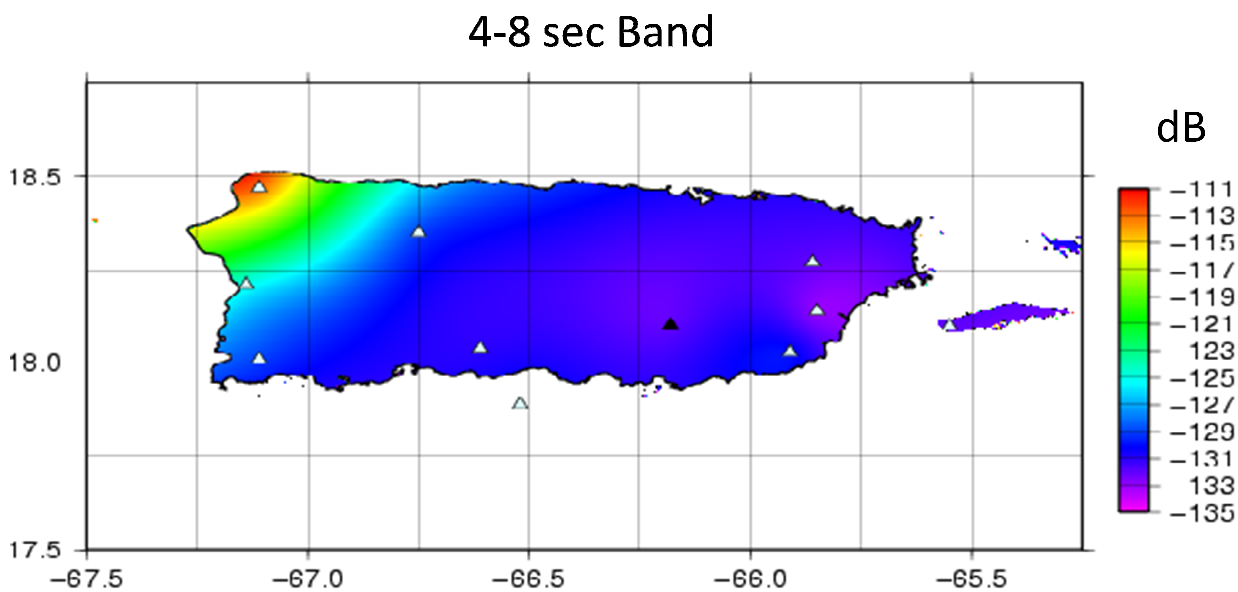


Figure 4.90 Geographical variation of microseism noise band

In the Figure 4.90 it can be observed the geographical variation of the seismic noise for the 4-8 sec period band. This period band is the double frequency peak microseism noise. In this figure only the station AGPR is affected by microseisms.

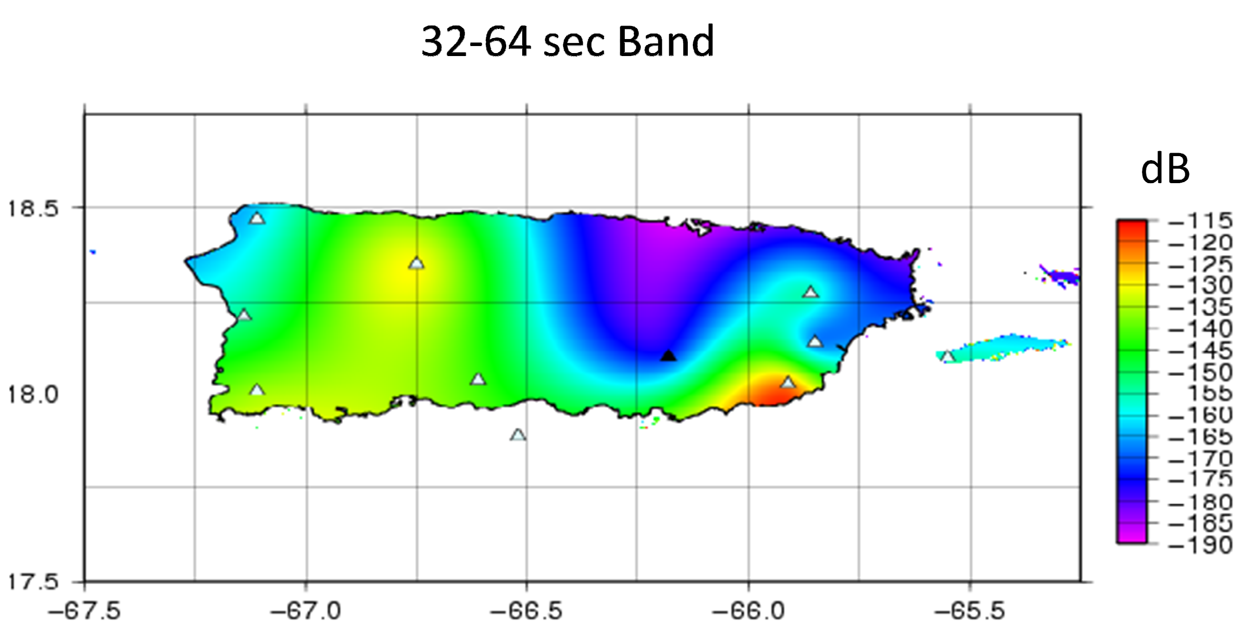


Figure 4.91 Geographical Variations of long period band

In the Figure 4.91 it can be observed the geographical variation of the seismic noise for the period 32-64 sec. This period band is part of the long period band. In this figure you observe that the noisier station in red is CPD and the less noisy are AGPR, HUMP, MTP and SJG. This is because this station can resolve long period signal.

# CHAPTER 5 CONCLUSION

## 5.3 Conclusions

This thesis describes the seismic background noise of Puerto Rico seismic stations using data of the Puerto Rico Seismic Network, the following items are the conclusion:

a) The Puerto Rico Seismic Network is a very dense seismic network which most of the seismic station showed good operation during the time. Only CPD seismic station is malfunctioning.

b) One major problem of this network is that the seismometer has to be changed very often, because failure of the seismometer causes changes in the dataless. Therefore, the dataless has to be updated all the time to prevent removal instrument removal mistakes by their data analysts and researchers.

c) The diurnal variations have significant change only in the period 0.1sec. This is the band for cultural noise. It means that the stations need to improve their installation.

d) The seasonal variation does not present any important change. The principal reason for this is that in Puerto Rico there are not large fluctuation of temperature and pressure.

e) AGPR seismic station needs to improve their site for reducing microseism noise.

## 5.4 Recommendations

To minimize the change of seismometer of different frequency response. This could be possible if there are spare for the different seismometer use in PRSN.

To improve the site for reducing cultural noise. Especially because this seismic network is interesting in local earthquake.

To implement this method as a routine procedure in the PRSN. This will be used for checking the status of the seismic station.

## 5.5 Future Work

As a recommendation for future work it is suggested to study:

a) The background noise in the horizontal channels. The same methodology will be used for this work. This study will expect more noise in the long period band.

b) The background seismic noise due to tropical storm and swell. For this work to be done it is necessary to look for the different tropical storm and swell occurred during the year 2005 and 2007, then make the PSD only for the interval of time where these happen and compare with the result of this thesis.

c) The optimal vault installation for reducing cultural noise in the island of Puerto Rico. In this topic it is necessary to research it by a geologist, an electrical engineer, a civil engineer and a seismologist to design a methodologyt and procedure for doing this work.

## REFERENCES


[1] Agnew, D. C., J. Berger, R. Buland, W. Farrell, and F. Gilbert. International deployment of accelerometers: a network for very long period seismology, EOS Trans. AM. Geophys. Union, 57, 180-188. 1978.

[2] Barzilai, A., T. V. Zandt and T. Kerry. Technique for measurement of the noise of a sensor in the presence of large background signals. Review of Scientific Instruments, 69, 2767-2772. 1998

[3] Bendat, J. S. and A. G. Piersol. Random data: analysis and measurement procedures. John Wiley and Sons, New York, 407p. 1971

[4] R. Beauduin, P. Lognonné, J. P. Montagner, S. Cacho, J. F. Karczewski, and M. Morand
The effects of the atmospheric pressure changes on seismic signals or how to improve the quality of a station, Bull. Seism. Soc. Am, 86: 1760 – 1769, 1996.

[5] Brune, J. N., and J. Oliver, The seismic noise of the Earth's surface, Bull. Seism. Soc. Am., 49, 349-353., 1959.

[6] Clinton, J. F., G. Cua, V. Huérfano, C. von Hillebrandt and J. Martínez-Cruzado, The Current State of Seismic Monitoring in Puerto Rico, Bull. Seism. Soc. Am., 77, 5, 532-543, 2006.

[7] Cooley, J. W., and J. W. Tukey, An algorithm for machine calculation of complex Fourier series, Math. Comp., 19, 297-301, 1965.

[8] Havskov, J. and g. Alguacil, Instrumentation in Earthquake Seismology, 313 p. 2002

[9] Jansma, P. E., G. S. Mattioli, A. Lopez, C. DeMets, T. H. Dixon, P. Mann, and E. Calais. Neotectonics of Puerto Rico and the Virgin Islands, northeastern Caribbean, from GPS geodesy, Tectonics 6, 1021-1037, 2000.

[10] Li, T. M. C. Lajitas quiet site noise study, Teledyne-Geotech Technical Report 81-0, Garland, Texas, 31 p. 1981

[11] McNamara, D. E. and R. P. Buland, Ambient noise levels in the continental United States, Bull. Seism. Soc. Am., 94, 4, 1517-1527, 2004.

[12] McNamara, D. E. and R. I. Boaz, Seismic Noise Analysis System Using Power Spectral Density Probability Density Functions: A Stand-Alone Software Package. *U. S. Geol. Survey Open-File Report 2005-1438, 14 pp., 2006.*

[13] McNamara, D. E., and R. I. Boaz, PQLX: A Software Tool to Evaluate Seismic Station Performance, Eos Trans. AGU, 87(52), Fall Meet. Suppl., Abstract S13B-0236, 2006.

[14] Peterson, J., Observation and modeling of seismic background noise, U. S. Geol. Surv. Tech. Rept., 93-232, 1-95, 1993.

[15] Peter M. Shearer, Introduction to Seismology, Cambridge University Press, 1999, 260 pp.

[16] Pujols, R., M. Ierkic, V. Huerfano, C. Von Hillenbrandt and D. Mcnamara. Background Seismic Noise of Puerto Rico based on data from the Puerto Rico Seismic Network. Poster Session, Caribbean Geological Conference 2008, Santo Domingo, Dom. Rep.

[17] Scherbaum, F. Of Poles and Zeros, Fundamentals of Digital Seismology, Kluwer Academic Publisher, 268 pp., 2002.

[18 Sleeman, R. and J. Vila, Toward an automated Quality Control Manager for the Virtual European Broadband Seismograph Network (VESBN), Orfeus Newsletter, 7, 1. 2007. http://www.orfeus-eu.org/newsletter/vol7no1/QCM/QCM.html

[19] Stutzmann, S. ,Geneviève Roult, and Luciana Astiz GEOSCOPE Station Noise Levels, Bull. Seism. Soc. Am., 90: 690 – 701, 2000

[20] Angelis, S. Broadband Seismic Noise Analysis of the Soufriere Hills Volcano Network, Seismological Research Letters, Vol. 79, Number 4, Jul/Aug 2008

[21] Vila, J. (1998), the broadband seismic station CAD (Túnel Del Cadí, Eastern Pyrenees): Site Characteristics and Background Noise, Bull. Seism. Soc. Am., 88, 1998.

[22] Welch, P., The use of Fast Fourier Transform for the estimation of power spectra: a method based on time averaging over short, modified periodigrams, IEEE Trans. Audio Electroacustics AU15, 70-73. , 1967.

[23] Wessel, P. and W. Smith, Free software helps display data, EOS, 72, 445-446, 1991.

[24] Wilson, D., J. Leon, R. Aster, J. Ni, J. Schlue, S. Grand, S. Semken, and S. Baldridge, Broadband seismic background noise at temporary seismic stations observed on a regional scale in the southwester United States, Bull. Seism. Soc. Am., 92, 3335-3341, 2002